Title
Chemical genetic analysis of signaling by the Saccharomyces cerevisiae mitotic kinases Cdc15, Dbf2, and Cdc5

Author
Paulson, Jennifer L

Publication Date
2006

Peer reviewed|Thesis/dissertation

Chemical genetic analysis of signaling by the Saccharomyces cerevisiae mitotic kinases Cdc15, Dbf2, and Cdc5

by

Jennifer L. Paulson

DISSERTATION

Submitted in partial satisfaction of the requirements for the degree of

DOCTOR OF PHILOSOPHY

in

Biochemistry and Molecular Biology

in the

GRADUATE DIVISION

of the

UNIVERSITY OF CALIFORNIA, SAN FRANCISCO

Acknowledgments

Through my time in graduate school, I have learned a lot about science, about being a scientist, and about myself. I have many people to thank for generously sharing with me the wisdom and support that have gotten me to this point.

I first need to thank my thesis advisor Kevan Shokat. Kevan is incredibly enthusiastic about his work, and that enthusiasm motivates and energizes everyone working for him. His advice always comes at just the right time, and he has been truly supportive of my goals. Among the many things I admire about Kevan, his creativity and kindness stand out.

My other thesis committee members, Dave Toczyski and Dave Morgan have also been endless sources of ideas and advice and have had a large influence on the direction of my project. In particular, I would like to thank for Dave Morgan for welcoming me to join in his group meetings and work closely with his lab. He and everyone in his lab always made me feel like part of their happy lab family.

Thanks also to the Tetrad program and those that keep it running smoothly, especially Sue Adams and Danny Dam. And special thanks to Valerie Ohman, who has gone out of her way on so many occasions to make the Shokat lab run smoothly, and to help me personally.

There have been many people at UCSF who I have had the pleasure of working with, including too many just in the Shokat lab to mention all of them. I just would like to especially thank Scotty for introducing me to the lab and overseeing my rotation, Kristi who generously passed her project on to me and gave me so much scientific and life advice in my first year in the lab, my bay mate Matt who patiently listened to the details

of my daily experimental battles, PJ who has given me more advice about more diverse subjects than anyone else I have ever met, and Quincey whose confidence and friendship in the lab I am already missing.

Many members of the Morgan lab have also helped me so much throughout the years. As a whole, they are as kind and generous a group as I have ever met. In particular, Jeff and Topher really gave me the advice that got me going on my project, Maria has gone out of her way to give me great advice and encouragement, I had the pleasure of working closely with Dave R. and Matt on my project, and Greg, Erika, Monica, Mary, and Liam always stopped what they were doing to answer my questions.

My classmates were also a part of what made my time at UCSF special. That everyone worked so well together to support each other during our first year classes really speaks to the great group of people they are. I especially want to thank Joyce Tung for being a terrific friend and for dragging me to dance class every week.

I also owe thanks to my family, whose encouragement throughout my life has been invaluable, especially my parents, Charles and Judy, who support me in all my efforts, and my sister, Bonnie, who has kept me laughing throughout. Last, but far from least, I thank my fiancé, Aaron, who always reminds me to focus on what is important.

Portions of this work have been published elsewhere. Chapter 2, Figures 7 and 8, as well selected text, were previously published in Nature Methods, 2005 June, volume 2, number 6, Zhang C, Sessa G, Cross JV, Templeton DJ, and Shokat KM, A second-site suppressor strategy for chemical genetic analysis of diverse protein kinases, pages 435-41. The experiments reproduced in Chapter 2, Figure 8 were performed by Jennifer L. Paulson, and the alignment in Chapter 2, Figure 7 was prepared by C Zhang.

The entirety of Chapter 4 has been submitted for publication elsewhere. MJ Sullivan performed the detailed analysis of cell cycle progression upon CMK treatment and observed the anaphase spindle migration defect (Fig. 2 c-e). DM Lowery performed the bioinformatic analysis of the yeast proteome and selected the candidate Cdc5 substrates. MS Cohen synthesized CMK and the scaffold molecule. DH Randle prepared purified Cdc5, GST-PBD, and GST-PBD* and initially developed the PBD binding assay.

The small molecules tested for inhibition of *as* kinases in Chapter 2 were synthesized by Anthony C. Bishop (compounds **1-14**), Raynard Bateman (compounds **15** and **16**) and Chao Zhang (compounds **17-22**). ATP analogs tested in Chapter 3 were synthesized by Jasmina Allen, except where commercially obtained as noted. Kristi Lieberman performed the initial analysis of analog-sensitive Cdc15 (Chapter 2 Figure 3) and Cdc5 (Chapter 2 Figure 7b) mutants.

With these exceptions, the remainder of the work was performed by Jennifer L. Paulson, under the direction and supervision of Kevan M. Shokat.

Chemical genetic analysis of signaling by the Saccharomyces cerevisiae mitotic kinases Cdc15, Dbf2, and Cdc5

by

Jennifer L. Paulson

Abstract

Protein phosphorylation is a ubiquitous regulatory mechanism for cellular signal propagation, and the complexity of signaling networks presents a challenge to protein kinase substrate identification. Chemical genetic control of kinase function provides a handle for kinase pathway analysis. Here, we apply this approach to three kinases that function in a signaling network that regulates exit from mitosis in the budding yeast, *Saccharomyces cerevisiae*. These include the mitogen-activating protein kinase, Cdc15, the nuclear Dbf2-related kinase, Dbf2, and the Polo-like kinase, Cdc5. Each kinase was successfully engineered for selective chemical inhibition *in vivo*. We found that monospecific pharmacological inhibition of Cdc5 delays anaphase nucleus migration into the bud, revealing a novel Cdc5 function. Additionally, chemical genetic, bioinformatic, and yeast proteomic tools were combined for Cdc5 substrate identification. Systematically chosen candidate Cdc5 substrates were examined for loss of phosphorylation upon cellular Cdc5 inhibition. The identified Cdc5 targets include Spc72, a spindle pole body (SPB) component and microtubule anchor required for nuclear positioning. Spc72 binds Cdc5 in a cell cycle specific manner, and *in vivo* Cdc5 inhibition prevents mitotic Spc72 phosphorylation. Studies *in vitro* demonstrate direct Spc72 phosphorylation by Cdc5. Finally, we expanded our knowledge of Cdc5 function at the SPB by examining SPB-localized proteins for presence in a Cdc5 complex. In summary, a chemical genetic approach was used to inhibit three protein kinases from diverse families, which led to a greater understanding of Cdc5 cellular function.

Table of Contents

List of Tables and Figures

CHAPTER 1

CHAPTER 2

CHAPTER 3

APPENDIX

Chapter 1

Introduction

Protein kinases

Protein phosphorylation by kinases is the primary signaling mechanism for rapid distribution of information within the cell. Consequentially, protein kinases regulate diverse processes and their disregulation is implicated in many diseases, including cancer. Protein kinases are enzymes that catalyze the transfer of the γ-phosphate from ATP to serine, threonine, and tyrosine hydroxyls in protein substrates (reviewed in (Adams, 2001)). Individual cellular phosphorylation events are regulated by activation state, localization, and sequence specificity of the kinase and together form large interlaced signaling networks. Thus, deconvolution of these networks is fundamental to understanding cell biology and controlling disease.

Protein kinases in mitosis

Proper cell division is essential for the survival of an organism and requires a carefully coordinated set of cellular events regulated by molecular mechanisms that are highly conserved among eukaryotes, from yeast to human. The genome must be faithfully replicated, then, in mitosis, duplicated chromosomes are individually segregated into mother and daughter cell, followed by cytokinesis and cell separation. The complexity of mitosis necessitates signaling pathways to coordinate, monitor, and temporally regulate this sequence of events.

Protein kinases regulate processes throughout mitosis, from mitotic entry to cytokinesis, and respond to checkpoints that ensure mitotic fidelity. Although many diverse kinases function in mitosis, several families play key conserved mitotic roles across eukaryotes. Cyclin-dependent kinases (Cdks) are master cell cycle regulators that

complex with B-type cyclins in mitosis (reviewed in (Morgan, 1997)). Cdk-cyclin B complexes promote mitotic progression, and they are inhibited by phosphorylation, binding, and proteolysis, mechanisms that restrain the activity of this complex to mitosis.

Downstream of mitotic Cdk activation are the Aurora kinases, NIMA-related kinases, nuclear Dbf2-related kinases, and Polo-like kinases. Aurora kinases function at the centrosome, spindle, kinetochore, spindle midzone, and cleavage furrow (reviewed in (Andrews, 2005)). Another important family of mitotic kinases is the NIMA-related kinases (Nrks) (reviewed in (O'Connell et al., 2003)). Like the Aurora kinases, Nrks control centrosome structure and microtubule function. Although these three families of kinases play significant roles in mitosis, our work has primarily focused on other mitotic kinases, including those from the nuclear Dbf2-related (NDR) and Polo-like (PLK) kinase families.

NDR family

Nuclear Dbf2-related (NDR) family kinases regulate mitosis, cell growth, and development (reviewed in (Hergovich et al., 2006)). Besides a conserved catalytic domain, NDR kinases are characterized by their requirement for Mps1-binding (MOB) family co-activators. Their name derives from the *S. cerevisiae* (budding yeast) kinase, Dbf2, although there are two other budding yeast NDR kinases, Dbf20 and Cbk1, and four NDR kinases in humans, NDR1, NDR2, LATS1, and LATS2. Mammalian NDR kinase family members are tumor suppressors or potential proto-oncogenes (reviewed in (Hergovich et al., 2006)).

In budding yeast, Dbf2-Mob1 is required for mitotic exit and cytokinesis (see below), and the human LATS1 tumor suppressor has been implicated in mitotic exit as well (Bothos et al., 2005). LATS1 may also function in mitotic checkpoints by inducing G2/M arrest or apoptosis (Yang et al., 2001). Consistent with its cell cycle role, animals lacking LATS1 develop tumors and are particularly sensitive to carcinogens (St John et al., 1999). Like Dbf2, LATS1 localizes to the centrosome (Hirota et al., 2000) and is activated by an upstream Ste20 family kinase (Chan et al., 2005). Notably, only one substrate of this family of kinases is known (*D. melanogater* Yki) (Huang et al., 2005).

Plk family

Polo-like kinases (Plks) are a family of serine/threonine protein kinases conserved from yeast to humans. They are characterized by a conserved kinase domain and one or more Polo-boxes. *Drosophila* Polo was the first identified member of this family, and its name reflects the monopolar spindle defect observed in *polo* mutants (Sunkel and Glover, 1988). They have emerged as an important class of cell cycle regulators that coordinate mitotic progression, with roles in mitotic entry, centrosome duplication and maturation, spindle assembly, mitotic exit, and cytokinesis (reviewed in (Barr et al., 2004)). Humans have four Polo like kinases (Plk 1-4), of which Plk1 is the best characterized. Consistent with its functions, Plk1 localizes to the centrosome and kinetochore by G2 and in anaphase relocalizes to the spindle midzone and midbody (Arnaud et al., 1998; Golsteyn et al., 1995; Lee et al., 1995; Seong et al., 2002). Budding yeast has a single Plk, Cdc5, with significant homology to Plk1 in its kinase domain and Polo-boxes (reviewed in (Lee

et al., 2005)). The expression, activity, and localization patterns of Cdc5 mirror Plk1 (reviewed in (Lee et al., 2005)).

Consistent with its positive role in cell cycle progression, elevated expression of Plk1 is observed in many tumor types and often correlates with malignancy and poor prognosis (Eckerdt et al., 2005). In culture, overexpression of Plk1 causes malignant transformation of mammalian cells, indicating that it is a cause rather than a result of tumor formation (Smith et al., 1997). Moreover, depletion of Plk1 by several means causes mitotic catastrophy in cancer cells with little effect on normal tissues, and antisense strategies directed toward Plk1 have a therapeutic effect on human tumors xenotransplanted into immunodeficient mice (Cogswell et al., 2000; Elez et al., 2000; Lane and Nigg, 1996; Spankuch-Schmitt et al., 2002; Spankuch-Schmitt et al., 2002; Spankuch et al., 2004). Despite much evidence underscoring the functional importance of Polo-like kinases, relatively little is known about the downstream effectors of Plks in their regulation of these numerous cell cycle transitions.

Presumably, important Plk substrates co-localize with Plks. A conserved C-terminal region of Plks called the Polo-box Domain (PBD) is required for their localization and function (Elia et al., 2003; Elia et al., 2003; Song et al., 2000). Recently, the PBD of several Plks has been crystalized and its binding motif characterized (Cheng et al., 2003; Elia et al., 2003; Elia et al., 2003; Leung et al., 2002). The PBD is a phospho-serine/threonine binding module that targets Plks to their substrates after prior "priming" phosphorylation of the target by an upstream kinase (Elia et al., 2003; Lowery et al., 2005). This specificity mechanism is similar to SH2 domain targeting of Src kinase to its substrates (Pawson, 2004). The optimal binding motif sequence may aid in

the identification of Plk binding partners at these cellular locations, and many of these binding partners are also likely to be substrates (Lowery et al., 2005).

The phosphorylation motif for Polo-like kinases, (D/E)-X-(pS/pT)-ϕ (X is any residue, ϕ is any hydrophobic residue, and p denotes the phosphorylated residue), has also been characterized (Nakajima et al., 2003). While this motif already contains little specificity, Plk1 phosphorylation sites identified in several substrates deviate from the motif (reviewed in (Lowery et al., 2005)). Recently the more comprehenisive motif, (S/E/D)-X_{0-2}-(N/Q)- X_{0-2}-(pS/pT)-X_3-π (π is a polar residue), was determined based on phosphorylation sites on Rec8 that were dependent on Cdc5 during meiosis (Brar et al., 2006). However, this motif alone has limited utility in identifying Cdc5 substrates, and thus additional information is necessary for furthering our understanding of Plk family signaling.

The role of the SPB in budding yeast mitosis

A common feature of the kinase families described above is their use of microtubule organizing centers (MTOCs) as key subcellular platforms for mitotic signaling. MTOCs nucleate microtubules, which form the mitotic spindle, position the nucleus, direct cell motility, and traffic cellular proteins (reviewed in (Jaspersen and Winey, 2004)). Thus, they are ideally positioned to sense and respond to cellular cues. The mammalian MTOC is the centrosome, and the budding yeast MTOC is the Spindle Pole Body (SPB).

In budding yeast, microtubules are nucleated by a complex containing γ-tubulin, which binds Spc110 on the nuclear face and Spc72 on the cytoplasmic face of the SPB to

nucleate spindle and cytoplasmic astral microtubules, respectively (Knop et al., 1997; Knop and Schiebel, 1997; Knop and Schiebel, 1998). Budding yeast have a defined axis of cell polarity along which a daughter cell bud is formed and with which the mitotic spindle aligns (reviewed in (Pruyne et al., 2004; Roegiers and Jan, 2004)). Additionally, the cell division plane at the bud neck is specified prior to spindle formation, so one set of chromosomes must be moved into the bud prior to cytokinesis. Cytoplasmic microtubules nucleated from the SPB properly position the mitotic spindle by transporting cell polarity determinants and motor proteins that provide pushing and pulling forces on the nucleus (reviewed in (Pearson and Bloom, 2004)). The SPB component Nud1 localizes a mitotic exit signaling complex to the cytoplasmic face of the SPB, where this complex monitors and responds to movement of the anaphase spindle into the daughter cell bud (Gruneberg et al., 2000).

Mitotic exit in budding yeast

Careful studies of the regulation of mitotic exit have been performed using the genetically tractable eukaryotic model organism *Saccharomyces cerevisiae*. A complex set of events have been shown to occur as cells exit mitosis and complete cell division. In late anaphase the mitotic spindle is disassembled and the nuclear machinery is returned to a premitotic (G1) state, an event triggered by destruction of mitotic cyclins and inhibition of Cdk1 (reviewed in (Morgan, 1999)). Mitotic exit occurs only after the sister chromosomes have properly segregated, but before the cell undergoes cytokinesis. Although well studied, the molecular regulation of the exit from mitosis is one aspect of

the eukaryotic cell cycle where significant questions remain unanswered. In particular, the targets of the kinases which regulate mitotic exit are largely unknown.

The mitotic exit network

In yeast, mitotic exit is governed by a complex regulatory network including a phosphatase, Cdc14; a GTPase, Tem1; a two-component GTPase activating protein, Bub2-Bfa1; a putative guanine nucleotide exchange factor, Lte1; the kinases, Cdc5, Cdc15, and Dbf2/Dbf20; a Dbf2-associated factor, Mob1; and a scaffolding protein, Nud1 (reviewed in (Bardin and Amon, 2001)). Together they have been termed the mitotic exit network (MEN) (Jaspersen et al., 1998). The output of this network results in activation of Cdc14, which subsequently dephosphorylates regulators of mitotic cyclin/cdk activity (Jaspersen et al., 1999; Visintin et al., 1998).

Cdc14 activation

Prior to anaphase, Cdc14 is inactivated by sequestration in the nucleolus by Net1 (also known as Cfi1) (Shou et al., 1999; Visintin et al., 1999). Cdc14 release from the nucleolus occurs in two phases. A group of proteins termed the FEAR (Cdc14 early anaphase release) network are required for a transient Cdc14 activation in early anaphase (Pereira et al., 2002; Stegmeier et al., 2002; Sullivan and Uhlmann, 2003; Yoshida et al., 2002). FEAR network-mediated Cdc14 release is required for proper timing of mitotic exit, and Cdc14 released in early anaphase has distinct functions (reviewed in (D'Amours and Amon, 2004)). However, it is MEN-mediated Cdc14 release in late anaphase that is

essen

detail

Activa

assemb

cascade

Tem1, i

at the bu

A

activatio

2002) and

2002), spa

bud (Adam

2005; Pere

checkpoint

through the

position ens

division pla

chromosome

essential for mitotic exit (Pereira et al., 2002; Stegmeier et al., 2002). The molecular details of how either the FEAR network or MEN leads to Cdc14 release are unclear.

Activation of the MEN

MEN components resemble a Ras-like GTPase signaling cascade that is assembled at the SPB. Tem1, Cdc15, and Dbf2 have been ordered into a linear signaling cascade (Lee et al., 2001; Visintin and Amon, 2001). Activity of the upstream GTPase, Tem1, is negatively regulated by Bub2-Bfa1 at the SPB and positively regulated by Lte1 at the bud cortex (reviewed in (Bardin and Amon, 2001)).

Although the transient activation of Cdc14 in early anaphase may promote activation of the MEN by inactivating Bub2-Bfa1 (Pereira et al., 2002; Yoshida et al., 2002) and/or dephosphorylation of Cdc15 (Jaspersen and Morgan, 2000; Stegmeier et al., 2002), spatial cues restrict MEN activation via Tem1 until one SPB has migrated into the bud (Adames et al., 2001; Bardin et al., 2000; Bloecher et al., 2000; D'Aquino et al., 2005; Pereira et al., 2000; Pereira and Schiebel, 2005). In this way, the MEN acts as a checkpoint to monitor spindle position, remaining inactive until the spindle elongates through the bud neck into the daughter bud. Coordinating mitotic exit with spindle position ensures that the separated sister chromosomes are located on each side of the cell division plane before cytokinesis occurs, thus ensuring proper segregation of chromosomes into mother and daughter cells.

MEN signaling and cytokinesis

The MEN proteins appear to have additional roles beyond signaling the release of Cdc14 from the nucleolus, including the regulation of cytokinesis. Although the myosin and septin components of the contractile ring are assembled early in the cell cycle, several late events in initiating cytokinesis have been linked to MEN protein function. In anaphase, following release from a Cdc15 temperature-sensitive arrest, actin and an IQGAP protein required for cytokinesis, Iqg1 (also known as Cyk1), co-localize to the myosin ring (Lippincott and Li, 1998; Shannon and Li, 1999). Just prior to actomyosin ring contraction, the septin rings split, and Hof1 (also known as Cyk2), relocalizes from the two septin rings to the single actomyosin ring (Lippincott and Li, 1998; Vallen et al., 2000). This is coincident with Hof1 phosphorylation, which does not occur in MEN mutants (Vallen et al., 2000).

Interestingly, Tem1 associates *in vitro* with Iqg1/Cyk1 (Shannon and Li, 1999). In addition, when Cdc14 is constitutively activated, depletion of Tem1 causes a defect in septin ring splitting, impeding cytokinesis (Lippincott et al., 2001). Lastly, MEN components are required for repolarization of the actin cytoskeleton to the bud neck following actomyosin ring contraction (Corbett et al., 2006). It is notable that an analogous pathway (septum initiation network, SIN) exists in *Schizosaccharomyces pombe* in which homologs of mitotic exit proteins have roles in cytokinesis (but not mitotic exit) (reviewed in (Bardin and Amon, 2001)).

Cdc15 and Dbf2

The MEN protein, Cdc15, belongs to the Ste20-related family of mitogen-activated protein kinase kinase kinases (MAP3Ks). Cdc15 binds to Tem1 through a region of Cdc15 also required for localization to the SPB (Asakawa et al., 2001; Bardin et al., 2003). Since neither the expression nor the kinase activity of Cdc15 is cell cycle regulated (Jaspersen et al., 1998; Jaspersen and Morgan, 2000), co-localization with Tem1 is likely critical for Cdc15 activation. Dbf2 is an NDR family kinase that also co-localizes with Cdc15 at the SPB, coincident with activation of Dbf2 kinase activity (Visintin and Amon, 2001). Dbf2 phosphorylation and activity is dependent on Cdc15 *in vitro* and *in vivo* (Mah et al., 2001), and it is not known if Cdc15 has a cellular function independent of Dbf2 activation. Thus, these three MEN proteins appear to act in a linear cascade, with Tem1 recruiting and activating Cdc15 at the SPB, followed by Cdc15 activating Dbf2 by phosphorylation, although Cdc15 may also have targets outside of this pathway. The ultimate consequence of this signaling cascade is the activation of the Cdc14 phosphatase, though the identity of Dbf2 substrates which promote Cdc14 activation is unknown.

In addition to their essential role in mitotic exit, both Cdc15 and Dbf2 may regulate cytokinesis. A cytokinesis defect is associated with a temperature-sensitive Cdc15 allele (Jiménez et al., 1998), and a C-terminal Cdc15 deletion that prevents localization to the spindle pole body also results in a cytokinesis defect, while not affecting mitotic exit (Menssen et al., 2001). This defect may specifically be in septum deposition, as *cdc15-2* cells at semi-permissive temperature constrict the actomyosin ring but do not build a septum (Hwa Lim et al., 2003).

Additionally, Cdc15 and Dbf2 localize to the bud neck, the site of constriction during cytokinesis (Frenz et al., 2000; Xu et al., 2000). Dbf2 localization to the bud neck is dependent on MEN components, Cdc5, Cdc15, and Mob1, suggesting that Dbf2 is the downstream effector in initiating cytokinesis, and Dbf2 function in cytokinesis occurs downstream of Cdc14 activation, requiring mitotic Cdk1 inactivation (Frenz et al., 2000; Hwa Lim et al., 2003). The Dbf2 binding partner, Mob1 (Komarnitsky et al., 1998), has also been implicated in cytokinesis (Luca et al., 2001). Despite this evidence, substrates of Cdc15 or Dbf2 with a function in cytokinesis have not yet been identified.

Cdc5

The Plk family kinase, Cdc5, is a component of both the FEAR and MEN and, thus, is also a critical regulator of mitotic exit. Cdc5 promotes MEN signaling in a complicated manner. Cdc5 phosphorylation of Bfa1 activates the MEN at the top of the cascade (see below for details), and Cdc5 may regulate Lte1 as this level as well (Lee et al., 2001). Additionally, Cdc5 regulates Dbf2 activity in a Bub2-independent manner (Lee et al., 2001). This can potentially be explained through Cdc5's function in FEAR network-mediated release of Cdc14, which results in activation of Cdc15 through dephosphorylation (Jaspersen and Morgan, 2000; Stegmeier et al., 2002). The molecular function of Cdc5 in the FEAR network is unknown. Cdc5 has been implicated in phosphorylation of Cdc14 and Net1 (Shou et al., 2002; Visintin et al., 2003; Yoshida and Toh-e, 2002); however, Net1 phosphorylation by Cdk1 is required for FEAR-mediated Cdc14 activiation (Azzam et al., 2004). Cdk1 is also required for Cdc5 activity *in vivo*,

and Cdc5 activation loop phosphorylation by Cdk1 activates Cdc5 *in vitro* (Mortensen et al., 2005).

Unlike other Polo kinases, the namesake monopolar spindle defect has not been associated with Cdc5, and Cdc5 is not active in S phase when bipolar spindle formation is initiated (Byers and Goetsch, 1974; Byers and Goetsch, 1975). However, Cdc5 expression, localization, and function largely parallel Plk1. Cdc5 expression peaks at G2/M with its kinase activity maximal in mitosis (Charles et al., 1998; Cheng et al., 1998; Kitada et al., 1993). Cdc5 localizes to the cytoplasmic face of the SPB, beginning after bipolar spindle formation and disappearing prior to cytokinesis (Shirayama et al., 1998; Song et al., 2000), as well as to chromosomes and the bud neck (Hornig and Uhlmann, 2004; Sakchaisri et al., 2004). Consistent with its expression and localization pattern, as well as functions of other Plks, Cdc5 has been implicated in processes throughout mitosis in addition to its essential role in mitotic exit. These include progression through G2/M phase, cohesin cleavage at anaphase entry, adaptation to the DNA damage checkpoint, and cytokinesis (reviewed in (Lee et al., 2005)). Significantly, despite the multiple mitotic functions and distinct localization pattern of this kinase, only a few of its substrates have been identified (Alexandru et al., 1999; Hu et al., 2001; Sakchaisri et al., 2004; Yoshida et al., 2006).

Known mitotic substrates of Cdc5

Bfa1

As described above, Bfa1 is a component of the Bfa1-Bub2 two-component GTPase activating protein (GAP), which negatively regulates the MEN. Bfa1-Bub2 Bfa1 is a mitotic phosphoprotein, and its phosphorylation is dependent on Cdc5 *in vivo* (Hu et al., 2001; Lee et al., 2001). Additionally, purified Cdc5 phosphorylates Bfa1 *in vitro* (Hu et al., 2001). The resultant phosphorylation sites were mapped and mutated to alanine in the *BFA-11A* strain, which was synthetically lethal with a *cdc5* allele that does not have a defect in Bfa1 phosphorylation, but not synthetically lethal with a *cdc5* allele that has a defect in Bfa1 phosphorylation. Finally, Bfa1 phosphorylation inactivates the Bfa1-Bub2 GAP activity *in vitro* and prevents association with Tem1 *in vivo* (Geymonat et al., 2003; Hu et al., 2001). Thus, Cdc5 phosphorylation of Bfa1 promotes activation of the MEN.

Mcd1

Mcd1 (also known as Scc1) is a component of a multi-subunit complex called cohesin, which holds sister chromatids together prior to the onset of anaphase. Separation of sister chromatids is initiated by Mcd1 cleavage by the separase Esp1, which is in turn activated by the proteolytic destruction of its inhibitor, Pds1, at the metaphase-to-anaphase transition (Cohen-Fix et al., 1996; Uhlmann et al., 2000). Mcd1 phosphorylation in mitosis dependent on Cdc5 *in vivo*, and purified Cdc5 phosphorylates Mcd1 *in vitro* (Alexandru et al., 2001). Cdc5 preferably phosphorylates chromatin-bound Mcd1, and chromatin-bound Mcd1 is preferably cleaved by Esp1 (Hornig and Uhlmann, 2004). Consistent with this, in the absence of Cdc5 there is a delay in, and lower

efficiency of, Mcd1 cleavage (Alexandru et al., 2001). Together, these results implicate Cdc5 in regulating the timing of anaphase onset.

Swe1

Swe1 functions as part of the morphogenesis checkpoint, which coordinates mitotic entry with cell growth. Swe1 responds to perturbations of the cytoskeleton by inactivating Cdk1 through phosphorylation and binding (Booher et al., 1993; McMillan et al., 1999). Swe1 is itself phosphorylated, leading to its degradation (Kaiser et al., 1998; Shulewitz et al., 1999; Sia et al., 1998). Localization of Cdc5 to the bud neck is required for Swe1 regulation (Park et al., 2004). Cdc5 functions upstream of Swe1 in mitotic entry by genetic epistasis, and these two proteins also physically interact (Bartholomew et al., 2001).

In all, three kinases, Cla4, Cdk1, and Cdc5, contribute to *in vivo* Swe1 phosphorylation and are required for Swe1 degradation (Asano et al., 2005; McMillan et al., 2002; Sakchaisri et al., 2004). Cla4-mediated Swe1 phosphorylation occurs in S phase (Sakchaisri et al., 2004), but Cdc5 and Cdk1 act synergistically in G2/M, with Cdk1 acting to promote Cdc5-dependent Swe1 regulation (Asano et al., 2005). Significantly, prior phosphorylation of Swe1 by Cdk1 enhances Swe1 phosphorylation by Cdc5 *in vitro* (Asano et al., 2005). This enhancement may due to the priming phosphorylation by Cdk1 generating a Cdc5 PBD binding site, since a functional PBD is required for the Cdc5-Swe1 interaction (Asano et al., 2005).

Tus1

A number of studies have linked Cdc5 to cytokinesis regulation. Cdc5 depletion results in a defect in cytokinesis in addition to the mitotic arrest (Song and Lee, 2001). In addition, overexpression of the Cdc5 Polo-box domain (PBD) results in a dominant-negative inhibition of cytokinesis (Song et al., 2000; Song and Lee, 2001) and displays genetic interactions with the cytokinesis components Cyk2/Hof1 and Myo1 (Song and Lee, 2001).

Cdc5 localizes to the bud neck (Song et al., 2000) and is required for actomyosin contractile ring formation and maintenance (Yoshida et al., 2006). The GTPase, Rho1, is essential for contractile ring assembly (Tolliday et al., 2002). In the absence of Cdc5 activity, Rho1 is not in its active GTP state nor properly localized to the bud neck (Yoshida et al., 2006). This defect can be explained by Cdc5 regulation of Tus1. Tus1 is a guanine nucleotide exchange factor (GEF) that positively regulates Rho1 (Levin, 2005). Tus1 interacts with the Cdc5 PBD, and the Cdc5 PBD is required for Tus1 localization to the bud neck (Yoshida et al., 2006). Additionally, Tus1 is phosphorylated by purified Cdc5 in a Polo-box dependent manner (Yoshida et al., 2006). Therefore, the role of Cdc5 in cytokinesis is, at least in part, mediated by phosphorylation of Tus1.

Analog-sensitive kinases

In summary, Cdc15, Dbf2, and Cdc5 have been implicated in diverse processes including mitotic exit and cytokinesis, although the full complexity of their mitotic roles is likely not yet appreciated, and their molecular effectors are largely unknown. For these reasons, we were interested in methods to further study the mitotic roles of these kinases.

The study of protein kinases such as those described above is limited by the chemical and genetic methods necessary to modulate their function during the course of an experiment. Typically, genetic alleles of kinases are used to study kinase loss of function; however, gene deletions and temperature sensitive alleles generally lead to physical absence of the kinase (rather than catalytic inactivation). This makes these genetic approaches subject to cellular compensation mechanisms, which can complicate analysis. Alternatively, chemical inhibition of protein kinases using small molecule inhibitors inactivates only the catalytic activity of the kinase. Kinases are ideal small molecule targets, as they have an inherent small molecule (ATP) binding site. However, the high degree of structural conservation among protein kinases in the ATP binding site makes it difficult for protein kinase inhibitors to be selective for a given kinase, and off target effects of chemical inhibition can also complicate analysis.

Fortunately, a chemical genetic approach has been developed to study protein kinase function, which couples chemical and genetic strategies to selectively study the function of any protein kinase (Bishop et al., 1998). The method utilizes a functionally silent mutation of a single conserved large hydrophobic residue in the kinase domain to glycine or alanine, which can be identified by sequence alignment and generalized to protein kinases from diverse families (Bishop et al., 2000). This residue has been termed the "gatekeeper", because it controls access to a hydrophobic pocket within the ATP binding site (Liu et al., 1998). Significantly, mutation of the gatekeeper residue does not alter the substrate specificity of the kinase (Witucki et al., 2002).

This mutation has two effects. First, a kinase inhibitor, PP1 (4-amino-1-*tert*-butyl-3-(*p*-methylphenyl) pyrazolo[3,4-d]pyrimidine), can be made selective for the

mutant "analog-sensitive" kinase by chemical derivatization (Bishop et al., 1998). These derivatized inhibitors are cell permeable and provide a rapid and reversible method for specifically inhibiting kinase activity; thus, circumventing the need to change temperature, as with a conditional allele, or eliminate additional functions, as with a genetic deletion. Resultantly, this technique has provided useful information about the cellular role of several budding yeast proteins (reviewed in (Knight and Shokat, 2005)), including the cell cycle regulator, Cdk1 (Bishop et al., 2000).

Second, analog-sensitive kinases can often transfer phosphate from an ATP analog containing a large group at the *N6* position, often *N6*-benzyl ATP, a molecule with low utility among wild-type kinases (Liu et al., 1998; Shah et al., 1997). This allows specific labeling with radiolabeled phosphate of direct substrates of the "analog sensitive" kinase and has been used to identify substrates of yeast kinases in the presence of a complex cellular lysate (Dephoure et al., 2005; Ubersax et al., 2003).

The analog sensitive approach is well suited to studying budding yeast kinases, due to the ease of introducing kinase "analog sensitive" allele knock-ins in this organism. We aimed to generate "analog sensitive" alleles of the mitotic exit kinases Cdc15, Dbf2, and Cdc5 to further study their function in mitosis, including their role in the MEN and cytokinesis regulation. Particularly, we were interested in identifying novel substrates of these kinases, and, since our attempts at identifying substrates with *N6*-derivatized ATP labeling was not fruitful for this set of kinases, we focused on developing and characterizing the potent and selective inhibition of these three mitotic exit kinases.

Chapter 2

Engineering analog-sensitive alleles of Cdc15, Dbf2, and Cdc5

INTRODUCTION

Proper orchestration of cell division requires a complex and highly regulated sequence of events from the initiation of DNA synthesis to sister chromatid separation to cytokinesis. Oscillations in cyclin-Cdk activity is the hallmark of the many cell cycle transitions, but complex signaling networks monitor cell cycle events and ultimately influence these critical oscillations. For instance, mitotic exit in yeast requires a network of proteins called the mitotic exit network, or MEN, which are required for destruction of mitotic cyclins following anaphase (Jaspersen et al., 1998). Many MEN proteins are also required for cytokinesis following their role in cyclin destruction (Balasubramanian et al., 2004). Despite their genetic implication in these two processes, little molecular detail is known about functions of individual MEN components. Since we began our work, progress has been made in determining the order of function of MEN components (Lee et al., 2001; Visintin and Amon, 2001); however, critical questions remain. For instance, despite the complex functional requirement for the three MEN kinases, relatively few of their downstream substrates have been identified.

The three MEN kinases are Cdc15, Dbf2, and Cdc5. Cdc15 acts upstream of Dbf2 and activates Dbf2 through phosphorylation (Mah et al., 2001). Whether Cdc15 has other targets besides Dbf2 or whether Cdc15 phosphorylation of Dbf2 mediates the role of Cdc15 in cytokinesis remain open questions. Dbf2 function has been largely unexplored, although it is known that the Dbf2 binding partner, Mob1, is required for both Dbf2 kinase activity and cellular function (Komarnitsky et al., 1998; Mah et al., 2001). No direct targets of Dbf2 have been identified, and as a downstream MEN kinase,

Dbf2 substrates are likely an important link between MEN signaling and the functional outputs of mitotic exit and cytokinesis.

In contrast, several mitotic substrates of Cdc5 have been identified, although the function of this kinase appears more diverse than that of Cdc15 and Dbf2. Cdc5 is the sole budding yeast member of the polo-like family of kinases (PLK), a family of serine/threonine protein kinases conserved from yeast to humans. Cdc5 functions in mitotic entry, adaptation to the DNA damage checkpoint, spindle checkpoint, mitotic exit and cytokinesis (Lee et al., 2005). Known Cdc5 substrates include Swe1 (at the G2/M transition), the cohesion Mcd1 (at anaphase initiation), the MEN component Bfa1 (at mitotic exit), and the Rho-GAP Tus1 (at cytokinesis) (Alexandru et al., 2001; Asano et al., 2005; Hu et al., 2001; Yoshida et al., 2006). However, by analogy to other PLK family members, Cdc5 is likely to have additional roles and substrates not yet discovered.

Despite an intensive interest in yeast mitotic exit, relatively little is known about the MEN kinases Cdc15, Dbf2, and Cdc5. We aimed to discover new functions of these kinases, explore their role in cytokinesis, and identify novel Cdc15, Dbf2, and Cdc5 substrates. To do so, we focused on a chemical inhibition approach to studying kinase function *in vivo*. This approach has successfully revealed new roles for several yeast kinases (Knight and Shokat, 2005) and thus was particularly suitable to the study of Cdc15, Dbf2, and Cdc5.

The method is founded on the introduction of a space-creating mutation within the kinase active site at a residue termed the "gatekeeper". The gatekeeper residue is so named because it controls access to a hydrophobic pocket within the ATP binding site (Liu et al., 1998). Significantly, mutation of the gatekeeper residue does not alter the

substrate specificity of the kinase (Witucki et al., 2002). Two analog sensitive, or "as", alleles encode space-creating mutations at the gatekeeper position. A glycine gatekeeper is encoded by the *as1* allele, and an alanine gatekeeper is encoded by the *as2* allele.

This approach takes advantage of striking homology between protein kinases within the ATP binding active site, and the gatekeeper position residue can be identified by a simple primary sequence alignment (Fig. 1a). Like most yeast kinases, Cdc15, Dbf2, and Cdc5 have a methionine or leucine gatekeeper position residue (Fig. 1b). Significantly, no yeast kinases have an alanine or glycine gatekeeper position residue (Fig. 2b), so mutation of this residue to alanine or glycine imparts a unique property to "as" kinases.

In particular, introduction of the "as" mutation allows access to a hydrophobic pocket in kinase active sites, which is inaccessible in wild type kinases with a larger gatekeeper residue (Liu et al., 1998). This allows binding of ATP-competitive molecules in the active site of "as" kinases that would otherwise be sterically occluded, providing a means for selective inhibition of "as" kinases (Bishop et al., 2001). As depicted in Figure 2a, both "as" and wild type kinases can bind ATP in their active sites for phosphorylation of protein substrates, but only the "as" kinase is inhibited by the bulky inhibitor (analog).

Selective inhibitors of "as" kinases have been successfully generated by derivatizing a pyrazolopyrimidine scaffold (Bishop et al., 1999; Bishop et al., 1998). The pyrazolopyrimidine PP1 (4-amino-1-*tert*-butyl-3-(*p*-methylphenyl) pyrazolo[3,4-d]pyrimidine) (Fig. 2b, **1**) was previously shown to be a general inhibitor of Src family tyrosine kinases (Hanke et al., 1996). PP1 gains selectivity for this family because they have a medium sized threonine gatekeeper residue that contacts the C-3 methyl phenyl in

PP1, and kinases with larger gatekeepers do not bind PP1 because they sterically occlude this methyl phenyl (Liu et al., 1999). If the methyl phenyl is replaced with a larger group such as napthyl (Fig. 2b, **2** NA) or napthylmethyl (Fig. 2b, **3** NM), Src family kinases are no longer inhibited; however, mutation of the gatekeeper position residue to glycine or alanine (genetic *as* alleles) restores inhibition by NA or NM (Bishop et al., 1999). This combined chemical and genetic approach to selective kinase inhibition has been successfully applied to protein kinases from diverse families (Bishop et al., 2000).

Based on this previous experience with engineering analog sensitive kinases, we predict that mutation of L99 in Cdc15, M254 in Dbf2, and L158 in Cdc5 to alanine or glycine will render these kinases sensitive to C-3 derivatized pyrazolopyrimidine inhibitors, most likely NA or NM. However, some kinases have been found to be intolerant to this approach. Intolerant kinases fall into two categories. First are a small number of kinases that are not inhibited by NA or NM despite introduction of the glycine or alanine "as" gatekeeper mutation. Our laboratory has produced many C-3 derivates of PP1, as well as derivatives of several other scaffolds in order to circumvent this problem. The entire panel of molecules tested in these studies is included in Figure 2b.

A second and more significant problem of this method is reduced catalytic activity and cellular function of the kinase upon introduction of the analog sensitive mutation. For example, introduction of a glycine residue at the gatekeeper position in yeast Cdk1 (also known as Cdc28) results in a 6-fold decrease in k_{cat} and a 20% increase in cell doubling time, indicating this kinase is not fully functional (Bishop et al., 2000). Despite this loss of function, the transcriptional profile of wild type and *cdk1-as1* cells was virtually identical, and inhibition of Cdk1-as1 with NM revealed an important new

role this kinase (Bishop et al., 2000). Although Cdk1-as1 retained enough function for its analysis, introduction of the as mutation into other kinases can result a more significant loss of function. These kinases must then be examined for residues that can be mutated to restore activity, while maintaining inhibitor sensitivity.

An approach was undertaken by Chao Zhang to identify potential second site mutations that would suppress the reduced activity of kinases intolerant to glycine at the gatekeeper position. A screen for suppressors of the non-functional APH(3')-IIIa (M90G) identified suppressor of glycine gatekeeper (*sogg*) alleles (Zhang et al., 2005). Many of these *sogg* alleles are predicted to stabilize beta sheets of the N-terminal lobe of the kinase domain. Consequently, the principle of *sogg* alleles may be extended to mutations of N-terminal beta sheet residues to residues that are predicted to increase stability or are highly conserved at that position.

Here we describe the development of analog sensitive alleles for the budding yeast protein kinases Cdc15, Dbf2, and Cdc5. These three kinases fall in three different families of protein kinases, STE20, NDR, and PLK, respectively, and thus expand the diversity of kinases to which the analog sensitive approach has been applied. We found them to differ in their tolerance to "as" mutations at the gatekeeper position and in their inhibitor sensitivity profile. Second site mutations were examined for Dbf2 and Cdc5, and a *cdc5 sogg* allele encoding C96V was found to improve Cdc5-as cellular function. Cdc15 was particularly amenable to this chemical genetic approach, and yeast strains in which *CDC15* was replaced by *cdc15-as1* were constructed and found to exhibit a telophase arrest upon inhibition with NA or NM. *cdc5-as1* strains were also successfully constructed and are further examined in Chapter 3.

RESULTS

Cdc15 analog sensitive alleles are inhibited by PP1 derivatives

We began our extension of the analog sensitive kinase approach with Cdc15 in order to study the function of this kinase. Our aim was to generate selectively inhibitable alleles of Cdc15 that could be used to temporally order late mitotic signaling events. To this end, we generated *cdc15* alleles encoding L99G and L99A mutations at the gatekeeper residue. These genes are termed *cdc15-as1* and *cdc15-as2*, respectively.

We first tested *cdc15-as1* and *cdc15-as2* in a functional assay. These two genes were assessed for their ability to functionally complement the temperature sensitive *cdc15-2* allele using a colony-forming efficiency assay (Fig. 3a). Because *cdc15-2* is nonfunctional at restrictive temperatures (37 C), viability of the yeast is dependent on Cdc15, Cdc15(L99G), or Cdc15(L99A) encoded by plasmid-borne *CDC15* alleles. At restrictive temperature, yeast transformed with vector alone did not grow; however, yeast transformed with CDC15, *cdc15-as1,* and *cdc15-as2* bearing plasmids grew equally well, indicating that *cdc15-as1* and *cdc15-as2* are functional *CDC15* alleles (Fig. 3a).

After confirming the functional competency of *cdc15-as1* and *cdc15-as2* alleles to complement *cdc15-2*, we next determined the sensitivity of *cdc15-as1* and *cdc15-as2* to PP1-based inhibitors in a halo assay. *cdc15-2* yeast bearing *cdc15-as1* or *cdc15-as2* were exposed to inhibitor-treated discs and grown at restrictive temperature. Chemical inactivation of *cdc15-as1* or *cdc15-as2* was visualized by a halo of no cell growth surrounding the disc, due to diffusion of the molecule in this region. Since the concentration of the molecule decreases the further from the disc, the size of the halo is

an approximate measure of the potency of inhibition. Yeast expressing Cdc15(L99G) (*cdc15-as1*) were inhibited by both NA and NM (molecules **2** and **3**, respectively, in Fig. 2b), and yeast expressing Cdc15(L99A) (*cdc15-as2*) were potently inhibited by NA (Fig. 3b). Treatment with another PP1 derivative (**4**) had no effect on the growth of *cdc15-as1* and *cdc15-as2* bearing cells (Fig. 3b). NA and NM were selective inhibitors of the gatekeeper-modified Cdc15 alleles, since they did not inhibit growth of the wild type CDC15 expressing strain (data not shown).

Mitotic arrest and potential cytokinesis defect of *cdc15-as1* strains

The ability of *cdc15-as1* and *cdc15-as2* to complement the *cdc15-2* strain at restrictive temperature, coupled with the selective inhibition of *cdc15-as1* and *cdc15-as2* with NA and NM in the same background, encouraged us to generate strains in which endogenous *CDC15* was replaced with *cdc15-as1* or *cdc15-as2*. Generation of these strains would allow functional assessment of Cdc15(L99G) or Cdc15(L99A) expressed at endogenous levels, as well as provide an endogenous system to study the biological effect of Cdc15(L99G) or Cdc15(L99A) inhibition.

Two-step gene replacement was used to replace the *CDC15* gene with *cdc15-as1* or *cdc15-as2*. This approach generated *cdc15-as1* and *cdc15-as2* strains. However, as opposed to our observations in the cdc15-2 strain background, colony formation assays of individual isolates of the *cdc15-as2* gene replacement showed some variability in growth visualized by colony size and number (Fig. 4a). No such effect was observed for *cdc15-as1*, indicating that *cdc15-as1* allele was better tolerated (Fig. 4a). Consistent with this,

the *cdc15-as2* strain had a temperature-sensitive reduction of growth at 37 °C relative to 30 C, whereas the *cdc15-as1* strain did not (Fig. 4b).

Furthermore, both *cdc15-as1* and *cdc15-as2* strains demonstrated synthetic interactions with weakened alleles of genes with similar functions in mitotic exit, indicating that both *cdc15-as1* and *cdc15-as2* are slightly hypomorphic alleles. We attempted the two-step gene replacement of *CDC15* with *cdc15-as1* or *cdc15-as2* in *cdc5-1* and *cdc14-1* strain backgrounds. At all times yeast were grown at 30 °C or less, which is permissive temperature for *cdc5-1* and *cdc14-1* alone. Strikingly, of more than 50 integrants screened for each strain, no viable *cdc15-as1, cdc5-1*; *cdc15-as2, cdc5*-1; or *cdc15-as2, cdc14-1* strains were obtained, suggesting that these combinations cannot be tolerated. *cdc15-as1, cdc14-1* strains were successfully constructed, once again suggesting that *cdc15-as1* retains more function than *cdc15-as2*. However, individually isolated *cdc15-as1, cdc14-1* strains showed a high degree of variability in the colony formation growth assay, indicating that *cdc15-as1, cdc14-1* strains are not fully functional.

Finally, a quantitative growth assay confirmed the qualitative observations described above. The *cdc15-as1* strain had a slight increase (9%) in doubling time relative to wild type (*CDC15*), whereas *cdc15-as2* and *cdc15-as1, cdc14-1* strains had more significant increases (68% and 82%, respectively) (Fig. 4c).

Since the *cdc15-as1* strain retained growth properties approaching wild type, we focused on this strain and proceeded to characterize the phenotype of selective *cdc15-as1* inhibition. The inhibitor sensitivity profile of analog sensitive *cdc15* strains was the same as observed in the *cdc15-2* background (Fig. 3b), with *cdc15-as1* sensitive to NA and

NM, and *cdc15-as2* sensitive to NA (data not shown). We further determined that 5 μM NA was sufficient to prevent growth of *cdc15-as1* yeast in the colony formation assay, whereas growth of wild type yeast (*CDC15*) was unaffected (Fig. 4d). Additionally, *cdc15-as1* cells bearing plasmid-borne wild type *CDC15* were not inhibited by NA, indicating that inhibition of *cdc15-as1* does not exert a dominant negative affect on colony growth (Fig. 4d).

Microscopic observation of *cdc15-as1* cells in the presence or absence of inhibitor treatment revealed a small proportion of cells interconnected in linear or branched chains of cell bodies (Fig. 4e, top panels), which were not observed in wild type cells (data not shown). This result implies a cytokinesis defect in *cdc15-as1* cells, which could explain their increased doubling time. Despite the presence of chained *cdc15-as1* cells, the majority of cells observed were phenotypically indistinguishable from wild type, and treatment with 5 μM NA resulted in uniform cell cycle arrest of *cdc15-as1* cells with large buds and separated DNA masses (Fig. 4e, bottom panels).

Inhibition and fitness of Dbf2 alleles

Encouraged by our success developing a selectively inhibitable analog sensitive *cdc15* strain, we applied the same strategy to engineering inhibitor sensitivity for the Dbf2 kinase. Similar to our initial Cdc15 experiments, we used a yeast strain with a temperature sensitive *dbf2* allele, *dbf2-2*, which does not grow at 37 C, in which to test various Dbf2 mutants. This was a critical tool for our Dbf2 studies, since *DBF2* is not generally an essential gene. Despite the unusual nature of the *dbf2-2* growth arrest,

growth of *dbf2-2* cells at restrictive temperature is fully restored by expression of HA3 tagged wild type Dbf2 (Fig. 5a).

Similarly plasmid-borne *dbf2-as1* (encoding HA3 tagged Dbf2(M254G)) and *dbf2-as2* (encoding HA3 tagged Dbf2(M254A)) alleles were examined for their ability to complement *dbf2-2* at restrictive temperature. Strikingly, Dbf2(M254G) appeared to be a non-functional kinase, since no cell growth was observed in Dbf2(M254G) expressing *dbf2-2* cells at restrictive temperature. However, Dbf2(M254A) expressing cells were able to support cell growth at restrictive temperature, though with reduced colony size and number relative to wild type Dbf2 expressing cells.

The reduction in viability of Dbf2(M254A) compared with wild type Dbf2 expressing cells was not a result of the HA3 tag on these two proteins, because the same effect was seen using constructs expressing untagged proteins (Fig. 5b). Given the apparent reduction in functionality upon introduction of the M254A gatekeeper residue mutation in Dbf2, we sought to identify second site mutations that could restore function of Dbf2(M254A) to near wild type levels. To do so, we manually inspected a primary sequence alignment of protein kinases from diverse families to identify residues in Dbf2 that differed from the majority of kinases and, in particular, from kinases that functionally tolerate gatekeeper residue mutations (data not shown). We focused on residues in the N-terminal lobe beta sheets, as this was found to be a hotspot for mutations in a selection for restored APH(3')-IIIa (M90G) activity (Zhang et al., 2005).

Three residues were identified as potential sites for suppression, C203 and L205 in sheet β3 and A253 in sheet β5. These sites were individually mutated in Dbf2(M254A) to the residue more commonly found among protein kinases at that

position, yielding Dbf2(C203V,M254A), Dbf2(L205I,M254A), and Dbf2(A253V,M254A), and expression of these proteins was tested for the ability to support *dbf2-2* cell growth at restrictive temperature in the colony formation assay. Of the three second site mutations, only L205I exhibited a minor enhancement in cell viability, and A253V or C03V led to a further reduction in viability, with no viable colonies observed in Dbf2(A253V,M254A) expressing cells (Fig. 5b).

Despite a reduced ability to support cell growth, Dbf2(M254A) expressing cells are viable, and we were able to assess their inhibitor sensitivity profile by halo assay. At restrictive temperature, treatment of *dbf2-2* yeast expressing Dbf2(M254A) with NA (**2**) and NM (**3**) resulted in halos of no cell growth surrounding the spot at which inhibitor was applied (Fig. 5c). Treatment with DMSO solvent alone (-) did not result in a halo (Fig 5c). In notable contrast to Cdc15 gatekeeper residue mutants, NM was a more potent inhibitor of Dbf2(M254A) than NA.

Inhibitor sensitivity of Cdc5 alleles

Like with Cdc15 and Dbf2, we introduced mutations of the gatekeeper residue in Cdc5 and tested the resulting proteins for selective inhibition *in vivo*. Plasmid-borne Cdc5 mutants were expressed in the temperature sensitive *cdc5-1* strain, which is inviable at restrictive temperature. Cdc5 mutants that support growth of *cdc5-1* at restrictive temperature were tested for growth inhibition by small molecules in the halo assay described above. Table 1 reports the small molecules that were assayed against *cdc5-1* cells expressing the gatekeeper mutants Cdc5(L158G), Cdc5(L158A), and these in combination with other second site mutations. Surprisingly, no *cdc5* alleles tested were

sensitive to NA or NM, molecules which potently inhibited *cdc15* and *dbf2* "*as*" alleles (Table 1). Additionally, Cdc5(L158G) and Cdc5(L158A) expressing yeast were tested for growth inhibition by many other inhibitors, including other PP1 pyrazolopyrimidine scaffold derivatives (**4-15**), purine scaffold derivatives (**17-22**), and a pyrroloprimidine scaffold derivative (**16**) (Table 1); however, these all failed to inhibit proliferation.

Fitness of Cdc5 alleles

We assessed the degree to which gatekeeper-modified Cdc5 mutants functionally complemented the temperature sensitive *cdc5-1* allele using the colony-forming efficiency assay. Growth of strains bearing *cdc5* alleles encoding the larger gatekeeper residues threonine and valine was indistinguishable from those expressing wild type Cdc5; however, strains bearing *cdc5* alleles encoding glycine, serine, and (to a lesser extent) alanine gatekeeper position residues had significantly reduced viability (Fig. 6a).

Unfortunately, our chemical genetic method exploits these small gatekeeper residues encoded by the *cdc5-as1* (L158G) and *cdc5-as2* (L158A) alleles, which had a reduced ability to support cell proliferation (Figs. 6a, 6b, 8a). Thus, we aimed to identify second site residues that when mutated would restore activity to *cdc5-as1* and *cdc5-as2*. We first examined Cdc5 for residues that are significantly conserved in other kinases but that deviated from the conserved residue in Cdc5. Cdc5 F211 is such a residue, since in most kinases this position is occupied by the smaller leucine residue. Therefore, we tested Cdc5(L158G,F211L) in the colony formation assay. Although cells expressing Cdc5(F211L) were indistinguishable from wild type, Cdc5(L158G,F211L) expressing cells grew no better than Cdc5(L158G) expressing cells. Thus, F211L did not restore

activity of Cdc5(L158G). However, we expanded our search for second site mutants based on findings by Chao Zhang. His work with APH (3')-IIIa focused our search for suppressor of glycine gatekeeper, or *sogg*, alleles of Cdc5.

Identification of *sogg* mutations for Cdc5

Ideally, identification of *sogg* mutations should be based primarily on sequence analysis, which is both general and efficient (requiring a minimum number of candidate mutations to be screened). Given that the APH(3')-IIIa selection revealed that the βsheet of the N-terminal lobe is a hotspot of *sogg* mutations, we generated a structure-based sequence alignment of both tolerant and intolerant protein kinases within this region. The two edge strands (β1 and β4) are largely exposed and frequently involved in protein-protein interactions, so they were excluded from the alignment. Twelve residues in the remaining three central βstrands were included in the alignment (Fig. 7). We examined these positions for any patterns that could distinguish intolerant kinases from tolerant kinases and tested for rescue of kinase activity.

Structure-based sequence alignment revealed that Cdc5 contains cysteine (Cys96) rather than the most commonly occurring valine at this particular position (Fig. 7), and we introduced the second-site mutation C96V into the kinase and examined its effect on the cellular function of Cdc5 using the colony-forming efficiency assay. Notably, this second-site mutation rescued the *in vivo* function of either *cdc5-as1* or *cdc5-as2* close to wild-type levels (Fig. 8a). Moreover, C96V alone did not seem to affect the viability of yeast cells (Fig. 8b), suggesting that the C96V mutation did not cause drastic perturbation to the structure and biological function of Cdc5.

cdc5-as1 and *cdc5-as2* strain viability

Although *cdc5-as1* and *cdc5-as2* could not fully restore growth of the *cdc5-1* strain at restrictive temperature, we were able to replace CDC5 at the endogenous locus with both the *cdc5-as1* and *cdc5-as2* alleles. The resulting strains were viable and surprisingly had no discernable defect in colony formation assays (data not shown). Figure 9 shows the growth of *CDC5*, *cdc5-as1* and *cdc5-as2* strains. *cdc5-as1* and *cdc5-as2* have respectively a 45% and 22% increase in doubling time relative to the wild type strain (Fig. 9). The *cdc5-as1* strain was further characterized and described in detail in Chapter 3.

DISCUSSION

A chemical genetic approach was applied to the yeast mitotic exit kinases Cdc15, Dbf2, and Cdc5. Growth of both *cdc15-as1* and *dbf2-as2* strains was successfully inhibited using selective small molecule inhibitors.

Although Cdc15 tolerated the as approach well (best of the three kinases studied here and on par with other kinases previously studied (Bishop et al., 2000)), careful examination of *cdc15-as1* cells revealed a slight functional defect in this strain, indicated by a reduction of doubling time and synthetic interactions with *cdc14-1* and *cdc5-1* alleles. This synthetic interaction was the result which most limited the utility of *cdc15-as1*. Because the order of function of mitotic exit network components was not known when our study was initiated, we had hoped to use *cdc15-as*, *cdc14-1* and *cdc15-as*, *cdc5-1* in reciprocal inactivation experiments for ordering Cdc5 and Cdc14 function in

relation to that of Cdc15. These experiments were not possible in absence of *cdc15-as*, *cdc14-1* and *cdc15-as*, *cdc5-1* strains.

However, we observed that treatment of *cdc15-as1* with NA led to cell cycle arrest with large buds and separated DNA masses, consistent with the previously observed for the *cdc15-1* temperature sensitive strain, and thus the *cdc15-as1* strain has proved to be a useful tool to arrest the cell cycle during mitotic exit. This is especially important in applications where the use of elevated temperatures for inactivation of previously available temperature-sensitive alleles would complicate interpretation of the experiment. Amon and colleagues used the *cdc15-as1* strain for a late mitotic arrest in their study of Kin4, as well as further examined the *cdc15-as1* chemical arrest phenotype (D'Aquino et al., 2005). NA-inhibited *cdc15-as1* cells exhibited a uniform first cycle anaphase arrest with hyperphosphorylated Bfa1 and Bub2, as well as Bfa1 and Tem1 localization to the SPB (D'Aquino et al., 2005). Use of this strain promoted analysis of the effects of Kin4 overexpression at a defined cell cycle point, thereby avoiding complications from the effect of Kin4 expression on cell cycle progression. As a result, they were able to determine that expression of Kin4 in the *cdc15-as1* chemical arrest prevented Bfa1 and Bub2 phosphorylation and Bub2 and Tem1 localization to the SPB (D'Aquino et al., 2005). Thus, Cdc15(L99G) inhibition by NA is a useful approach to studying the cell cycle.

Like previously engineered kinases such as Cdk1 (Bishop et al., 2000), introduction of the gatekeeper mutation in Cdc15, Dbf2, and Cdc5 led to decreased function of these kinases. This finding was most extreme in the case of Dbf2; however, although weakened, Dbf2(M254A) expressing cells were viable and selectively inhibited

by NM. For Dbf2(M254A) inhibition to be of use for the study of mitotic exit and cytokinesis, a *dbf2-as2* strain will need to be constructed in which the *DBF2* gene is replaced at the endogenous locus with *dbf2-as2*. Because Dbf2 is functionally redundant with Dbf20 (Toyn et al., 1991), the *dbf2-as2* allele may need to be introduced in a *dbf20*Δ strain background. However, this may not be necessary if inhibition of Dbf2(M254A) results in a dominant-negative cell proliferation block, a question which has yet to be addressed.

Gatekeeper residue mutations in both Dbf2 and Cdc5 reduced the ability of these proteins to support cell viability monitored by strain growth, and we attempted a rationally-chosen second site suppressor strategy to restore function of these gatekeeper residue mutants. A second site C96V mutation in Cdc5 partially suppressed the growth defect of *cdc5-as1* and *cdc5-as2* alleles; however, no *cdc5* alleles were sensitive to the variety of pyrazolopyrimidine or adenine-based inhibitors described here. Chapter 3 describes a successful approach to irreversible Cdc5 inhibition that utilizes C96. Therefore the *sogg* strategy could not be used concurrently with Cdc5 inhibition. Fortunately, when *CDC5* was replaced with *cdc5-as1* or *cdc5-as2* at the endogenous locus, the growth defect was not as pronounced (45% increase in doubling time for *cdc5-as1*).

In summary, gatekeeper residue mutations were introduced in the protein kinases Cdc15, Dbf2, and Cdc5 for the purpose of sensitizing these kinases to selective small molecule inhibitors. The gatekeeper-modified alleles were tolerated to various degrees, with either the *as1* or *as2* allele for all three kinases retaining sufficient activity to support kinase-dependent cell proliferation. Additionally, *cdc15-as1*, *cdc15-as2*, and

dbf2-as2 dependent cell proliferation was prevented by PP1 analogs that have no effect on the proliferation of wild type yeast. Thus, we have successfully applied the analog sensitive allele-based method for selective *in vivo* kinase inhibition to two kinases, Cdc15 and Dbf2. Modification of this approach for selective inhibition of *cdc5-as1* cells is described in Chapter 3.

METHODS

Plasmids. Kind gifts of DO Morgan were the plasmids containing a *CDC15* (YAR019C) genomic fragment in pRS416 (p416-CDC15, pSJ09), pRS426 (p426-CDC15, pSJ10), and C-terminally triple Hemagglutinin (HA3) tagged in pRS426 (p426-CDC15-HA3, pSJ21); a *DBF2* (YGR092W) genomic fragment N-terminally tagged with a triple Hemagglutinin (HA3) tag in pRS426 (p426-HA3-DBF2, pSJ57); and a *CDC5* (YMR001C) genomic fragment in pRS315 (p315-CDC5, p012) and pRS306 (p306-CDC5, p034).

CDC15 was subcloned into pRS306, generating p306-CDC15 (pKL205). The Cdc15(L99G) mutation was introduced into p416-CDC15, p306-CDC15, and p426-CDC15-HA3, generating p416-cdc15-as1 (pKL150), p306-cdc15-as1 (pKL214), and p426-cdc15-as1-HA3 (pJP103). Similarly, introduction of L158A generated p416-cdc15-as2 (pKL145) and p306-cdc15-as2 (pKL208).

Dbf2(M254G) and Dbf2(M254A) mutations were introduced into pSJ57 to generate pJP123 and pJP124, respectively. pSJ57, pJP123, and pJP124 were found to contain a D533G mutation not found at the wild type *DBF2* locus in W303 cells. Therefore, DBF2 was amplified from W303 genomic DNA using high fidelity PfuTurbo DNA polymerase (Stratagene) and subcloned into pRS316 to generate p316-DBF2 (pJP164). M254A was

introduced into pJP164 to generate pJP200. The mutations C203V, L205I, and A253V were introduced into pJP200 to generate pJP210, pJP209, and pJP208, respectively.

The Cdc5(L158G) mutation was introduced into p315-CDC5 and p306-CDC5, generating p315-cdc5-as1 (pKL117) and p306-cdc5-as1 (pKL121). Similarly, introduction of L158A generated p315-cdc5-as2 (pKL138) and p306-cdc5-as2 (pKL142). Introduction into p315-CDC5 of L158T generated pJP183, L158V generated pJP186, and L158S generated pJP188. F211L was introduced into p315-CDC5, p315-cdc5-as1, and p315-cdc5-as2 to generate pKL155, pKL167, and pKL171, respectively. G221A was added to pKL117 and pKL171 to generate pGA1 and p171/GA1, respectively. C96V was introduced into p315-CDC5, p315-cdc5-as1, and p315-cdc5-as2 to generate pJP184, pJP176, and pJP185, respectively. L157V and L158I were introduced into pKL117 to generate pJP126 and pJP127, respectively.

Mutations were introduced by QuikChange site-directed mutagenesis (Stratagene). Open reading frames were fully sequenced after amplification. Cdc15 and Dbf2 plasmids encoded differences from published sequence (Cdc15(R316A, P321A, N900K, G901D, C902V), Dbf2(H114Y)), which were confirmed in a W303 strain.

Yeast strains and culture methods. Standard yeast media and genetic techniques were used(Guthrie and Fink, 2002). Strains were *MAT***a** and W303. Wild type budding yeast (AFS92) and yeast strains bearing the *cdc15-2* (SLJ127), *cdc14-1* (SLJ250), *dbf2-2* (SLJ256), and *cdc5-1* (JC34) temperature sensitive alleles were gifts of DO Morgan (Jaspersen et al., 1998).

The *cdc15-as1*, *cdc15-as2*, *cdc5-as1*, and *cdc5-as2* alleles were introduced at their endogenous loci by two-step gene replacement to create the following strains: *cdc15-as1* (JLP01); *cdc15-as2* (JLP15); *cdc14-1*, *cdc15-as1* (JLP07); *cdc5-as1* (JLP32); and *cdc5-as2* (JLP38). AFS92 was the parent strain for JLP01, JLP15, JLP32, and JLP38. SLJ250 was the parent strain for JLP07.

Colony-forming efficiency assay. Saturated cultures were equalized for cell density between strains, tenfold serially diluted and spotted onto a yeast-peptone-dextrose (YPD) plate. The plates were incubated at the indicated temperatures, and images were taken on an Alpha Innotech Imager.

Inhibitors and growth inhibition halo assay. Yeast cells (5×10^5 cells / plate) were evenly spread on an agar plate containing rich yeast media (YPD). Sterile filter discs were placed onto the plate, and 1 nmol of each molecule was spotted on the filter disc. The plates were incubated at 37 °C for 2 d, and images were taken on an Alpha Innotech Imager. Inhibitors were kind gifts of AC Bishop (**1**-14), R Bateman (**15-16**), and C Zhang (**17-22**). All inhibitors were prepared as 10 mM stocks in DMSO.

Growth curves. Yeast cell growth was monitored by OD^{660} with time and converted to cell number using a standard curve. Curve fitting and doubling time calculation were performed with Prism 4 (GraphPad software).

Microscopy and image processing. Cells were fixed with 3.7% formaldehyde. DNA was stained with 1 μg/ml DAPI. Images were cropped and minimum and maximum pixel values adjusted in Photoshop.

Figure legends

Figure 1. The gatekeeper residue in yeast kinases. (**a**) Protein sequence alignment of a region of the kinase domain containing the gatekeeper residue. Yeast kinases Cdc15, Dbf2, and Cdc5 are indicated, as are the previously engineered yeast Cdk1 and human v-Src, and the gatekeeper residue is shaded in gray. (b) Distribution of residues at the gatekeeper position in budding yeast protein kinases.

a

Dbf2	...250	L	Y	L	A	M	E	F	V	P	G	G
Cdc5	...154	V	Y	I	L	L	E	I	C	P	N	G
Cdc15	...95	L	Y	I	L	L	E	Y	C	A	N	G
Cdk1	...84	L	Y	L	V	F	E	F	L	D	L	D
Src	...337	I	Y	I	V	T	E	Y	M	S	K	G

b

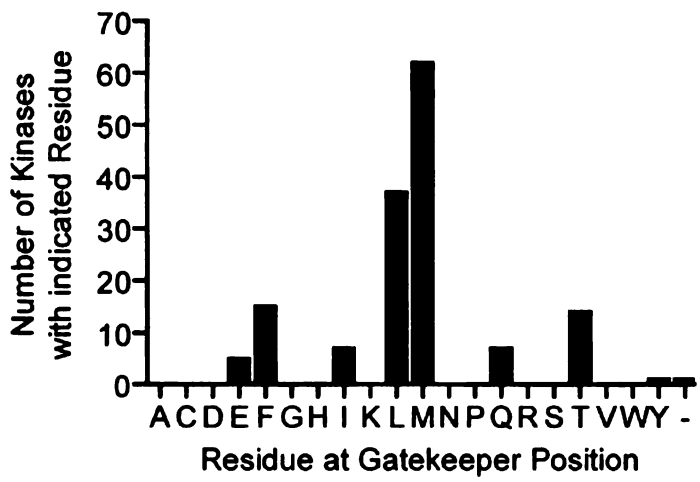

Figure 2. Inhibition of analog-sensitive kinases (**a**) Analog-sensitive kinases with a small residue at the gatekeeper position are selectively inhibited by derivatized kinase inhibitors. (**b**) Molecules used in these studies. Compounds **2-15** derive from the PP1 (**1**) pyrazolopyrimidine kinase inhibitor scaffold. NA (**2**) and NM (**3**) are particularly useful for inhibiting analog-sensitive kinases(Bishop et al., 2000). Other molecules tested include pyrrolopyrimidine (**16**) and purine derivatives (**17-22**).

a

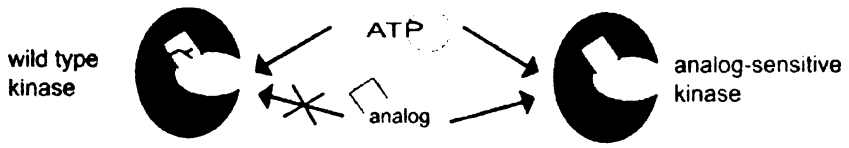
wild type
kinase
ATP
analog
analog-sensitive
kinase

b

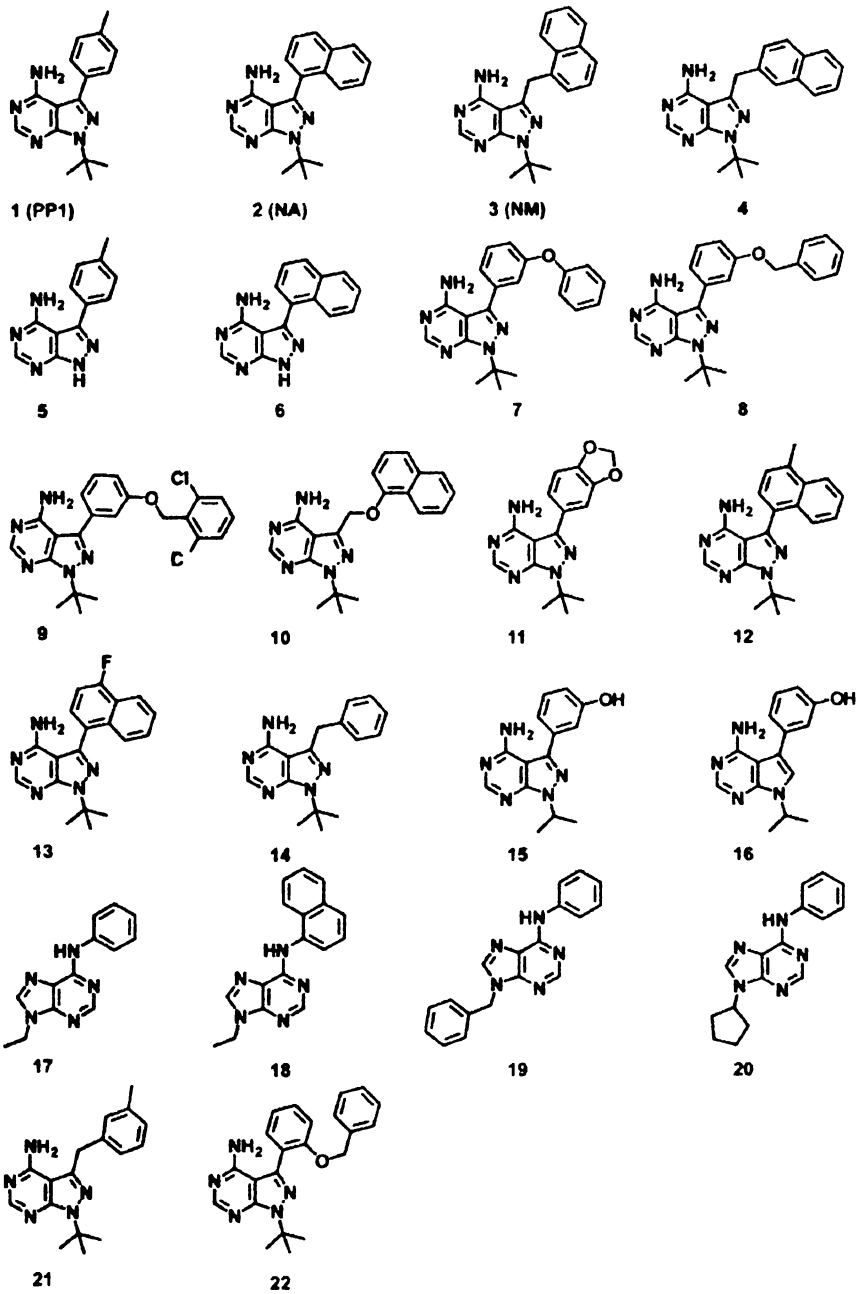
1 (PP1)
2 (NA)
3 (NM)
4
5
6
7
8
9
10
11
12
13
14
15
16
17
18
19
20
21
22

Figure 3. Viability and inhibition of analog-sensitive *cdc15* strains. (**a**) Viability of yeast strains expressing different *cdc15* alleles based on colony-forming efficiency. Temperature sensitive cdc15-2 strains expressing the indicated Cdc15 mutant were grown at permissive (23 C) or restrictive (37 C) temperature. (**b**) Cell viability halo assay. Inhibition of cell growth in the region surrounding a disc spotted with 1 nmol of the indicated molecule. *cdc15-2* cells expressing the indicated Cdc15 protein were grown at restrictive temperature (37 C). Molecule numbers refer to Figure 2. NA and NM inhibit growth of cells expressing Cdc15(L99G), and NA inhibits growth of cells expressing Cdc5(L99A).

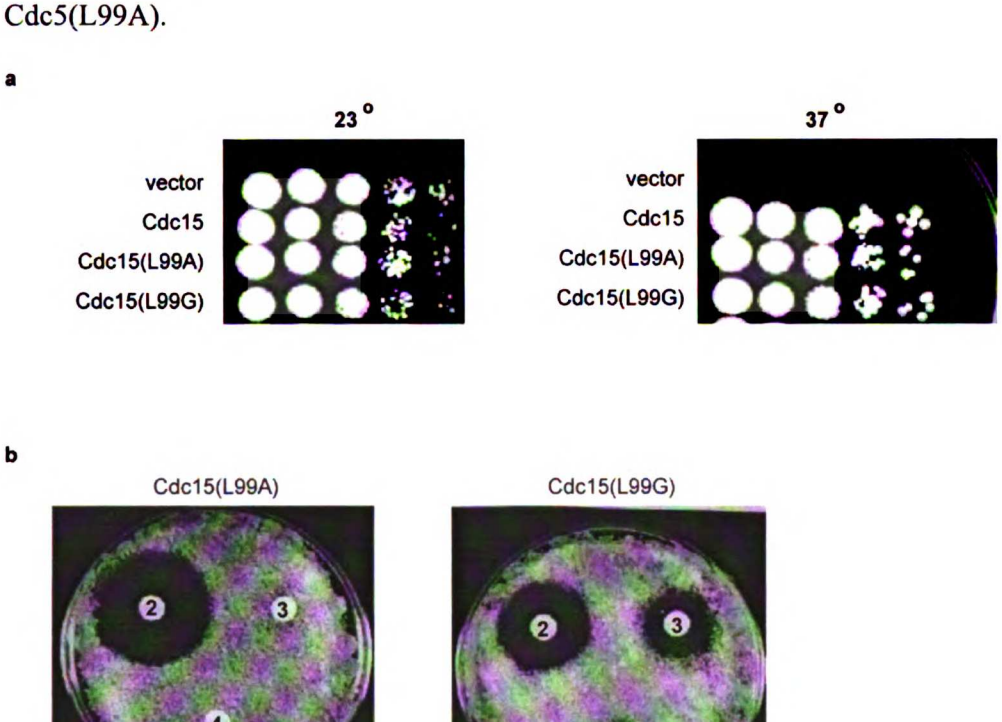

Figure 4. Phenotypic analysis of *cdc15-as* strains. (**a**) Growth variability in strains created by replacing *CDC15* with *cdc15-as* alleles at the *CDC15* endogenous locus.

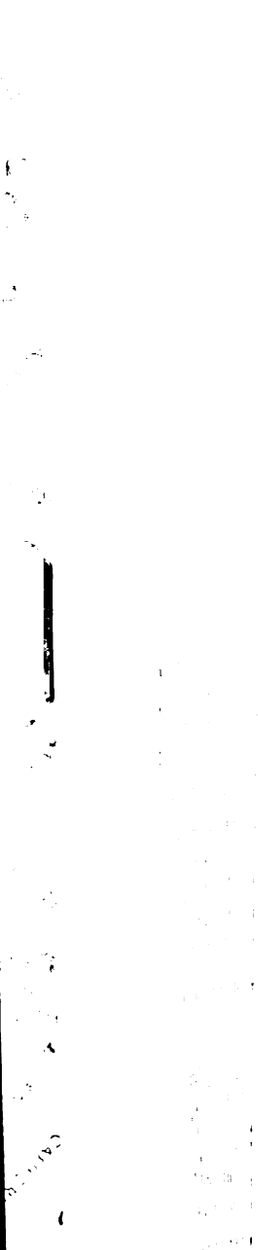

Growth of 10-fold dilutions was monitored with a colony forming efficiency assay at the indicated temperatures. Although individually isolated *cdc15-as1* strains have uniform colony forming efficiency, even at elevated temperature (37 C), *cdc15-as2* and *cdc15-as1, cdc14-1* strains show some variability in colony size. (**b**) *cdc15-as2* yeast have a sensitivity to elevated temperatures. Growth of 10-fold dilutions of the indicated strains was monitored at 30 °C and 37 °C. Only *cdc15-as2* has a reduction in colony growth at 37 C. (**c**) Doubling time of analog-sensitive *cdc15* strains. *CDC15*; *cdc15-as1*; *cdc15-as2*; and *cdc14-1, cdc15-as1* strains were grown at 23 °C and cell number determined. Doubling time (in hrs) is indicated for each strain. (**d**) *CDC15* and *cdc15-as1* yeast expressing Cdc15 (+ Cdc15), Cdc15(L99G)-HA3 (+ Cdc15(L99G)-HA3), or no additional Cdc15 (+ empty vector) from a high copy plasmid were monitored for cell growth in the colony formation assay in the presence (NA) or absence (no drug) of 5 μM NA. NA treatment of yeast containing *cdc15-as1* does not have a dominant growth inhibitory effect in the presence of wild type *CDC15*. (**e**) Cellular phenotype of Cdc15(L99G) inhibition. Images at 40x magnification of *cdc15-as1* cells treated with 5 μM NM (upper right panels) or DMSO alone (upper left panel). Both populations contain cells with linear or branched chains of 3 or more connected cell bodies (arrows). DAPI stained *cdc15-as1* cells treated before (lower left panel) and after (lower right panel) a 3 hr treatment with 10 μM NA at 30 C. An overlay of phase and DAPI stained images is shown.

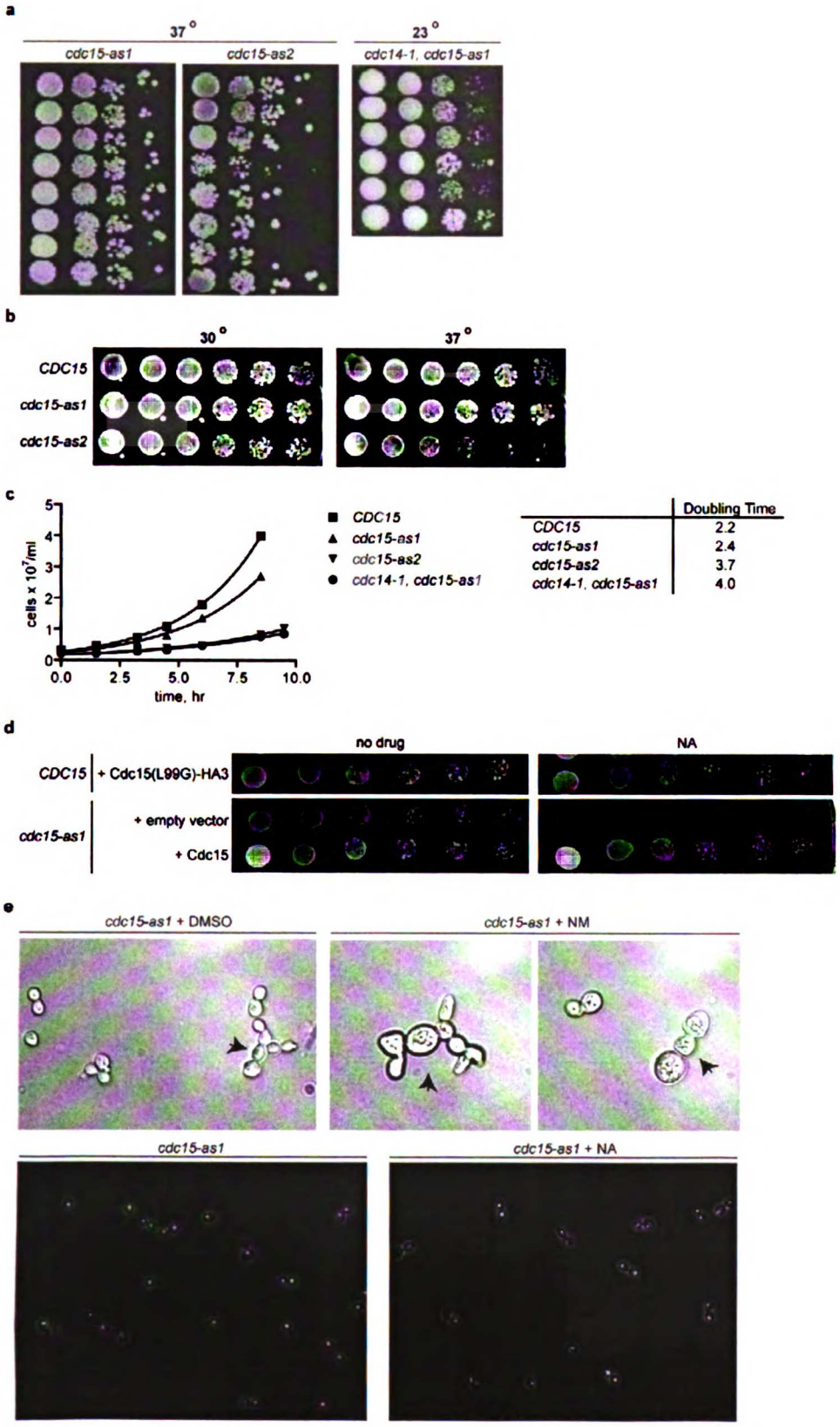
a
37°
23°
cdc15-as1
cdc15-as2
cdc14-1, cdc15-as1
b
30°
37°
CDC15
cdc15-as1
cdc15-as2
c
cells x 10^7/ml
time, hr
CDC15
cdc15-as1
cdc15-as2
cdc14-1, cdc15-as1
Doubling Time
CDC15 2.2
cdc15-as1 2.4
cdc15-as2 3.7
cdc14-1, cdc15-as1 4.0
d
no drug
NA
CDC15
+ Cdc15(L99G)-HA3
cdc15-as1
+ empty vector
+ Cdc15
e
cdc15-as1 + DMSO
cdc15-as1 + NM
cdc15-as1
cdc15-as1 + NA

Figure 5. Viability and inhibition of analog-sensitive *dbf2* strains. (**a**) Viability of yeast strains carrying different *DBF2* alleles based on colony-forming efficiency. *dbf2-2* yeast expressing HA3-Dbf2 or the indicated mutant were assayed at 10-fold cell dilution for colony formation at permissive (23 C) or restrictive (37 C) temperature, as indicated. Expression of HA3-Dbf2(M254G) could not restore growth of *dbf2-2* yeast at restrictive temperature. (**b**) Viability of yeast strains carrying different *DBF2* alleles based on colony-forming efficiency. *dbf2-2* yeast expressing Dbf2 or the indicated mutant were assayed at 10-fold cell dilution for colony formation at permissive (23 C) or restrictive (37 C) temperature, as indicated. Second site mutations did not improve the ability of Dbf2(M254A) to rescue cell growth. (**c**) Cell viability halo assay of *dbf2-2* yeast expressing wild type Dbf2 or the Dbf2(M254A) mutant allele, grown at restrictive (37 C) temperature. Inhibition of cell growth in the region surrounding a disc spotted with 1 nmol of the indicated molecule is observed only upon application of NA and NM to Dbf2(M254A) (right). Molecule numbers refer to Figure 2, and a dash indicates the DMSO carrier control.

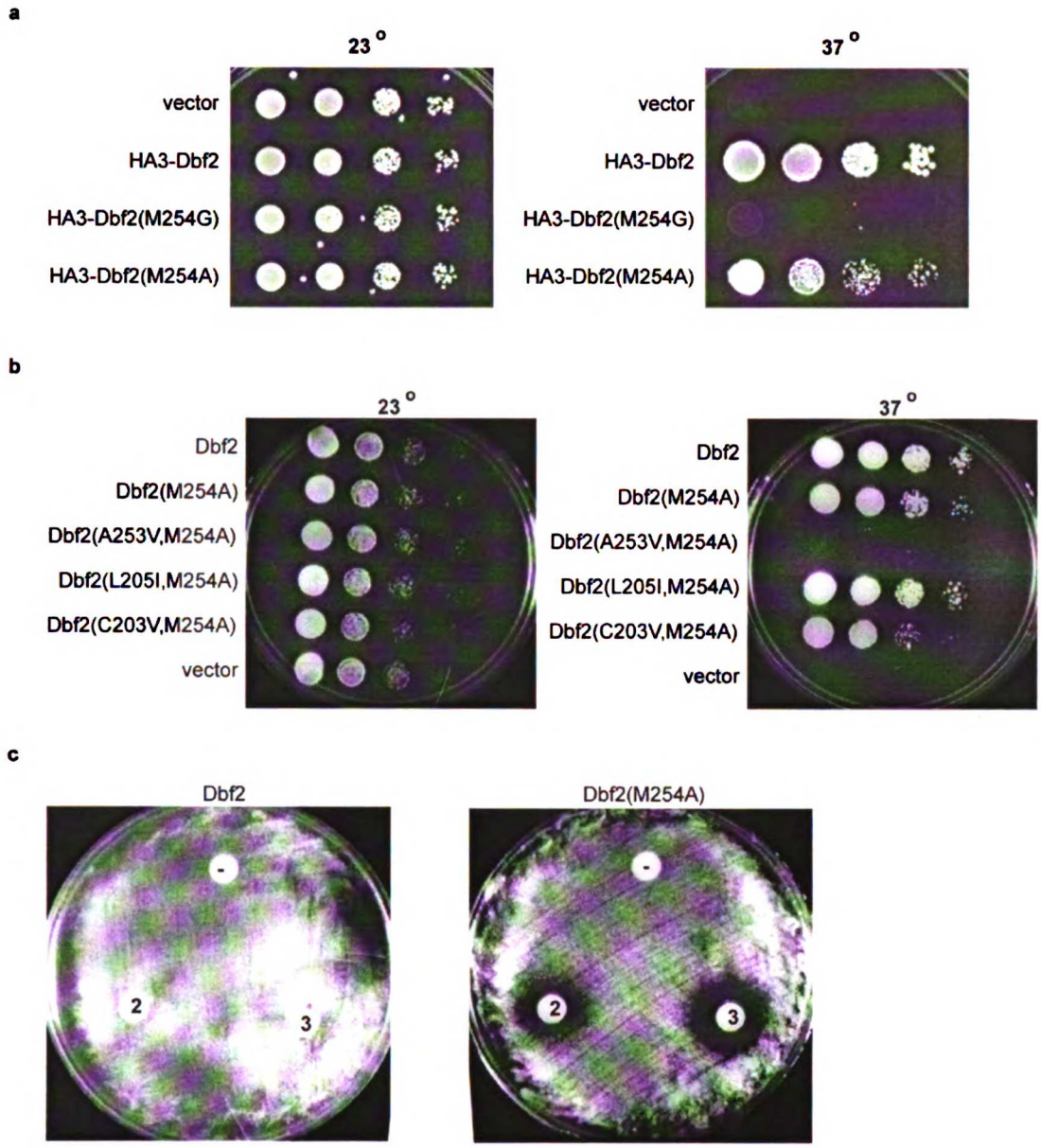

Table 1. Cdc5 mutants are not inhibited by non-electrophilic derivatives of kinase inhibitor scaffolds. *cdc5-1* strains expressing Cdc5 or the indicated mutant were tested for growth inhibition by the 1 nmol of the indicated molecules by halo assay. Molecule numbers refer to Fig. 2. Combinations indicated with a black box (■) were tested, and no

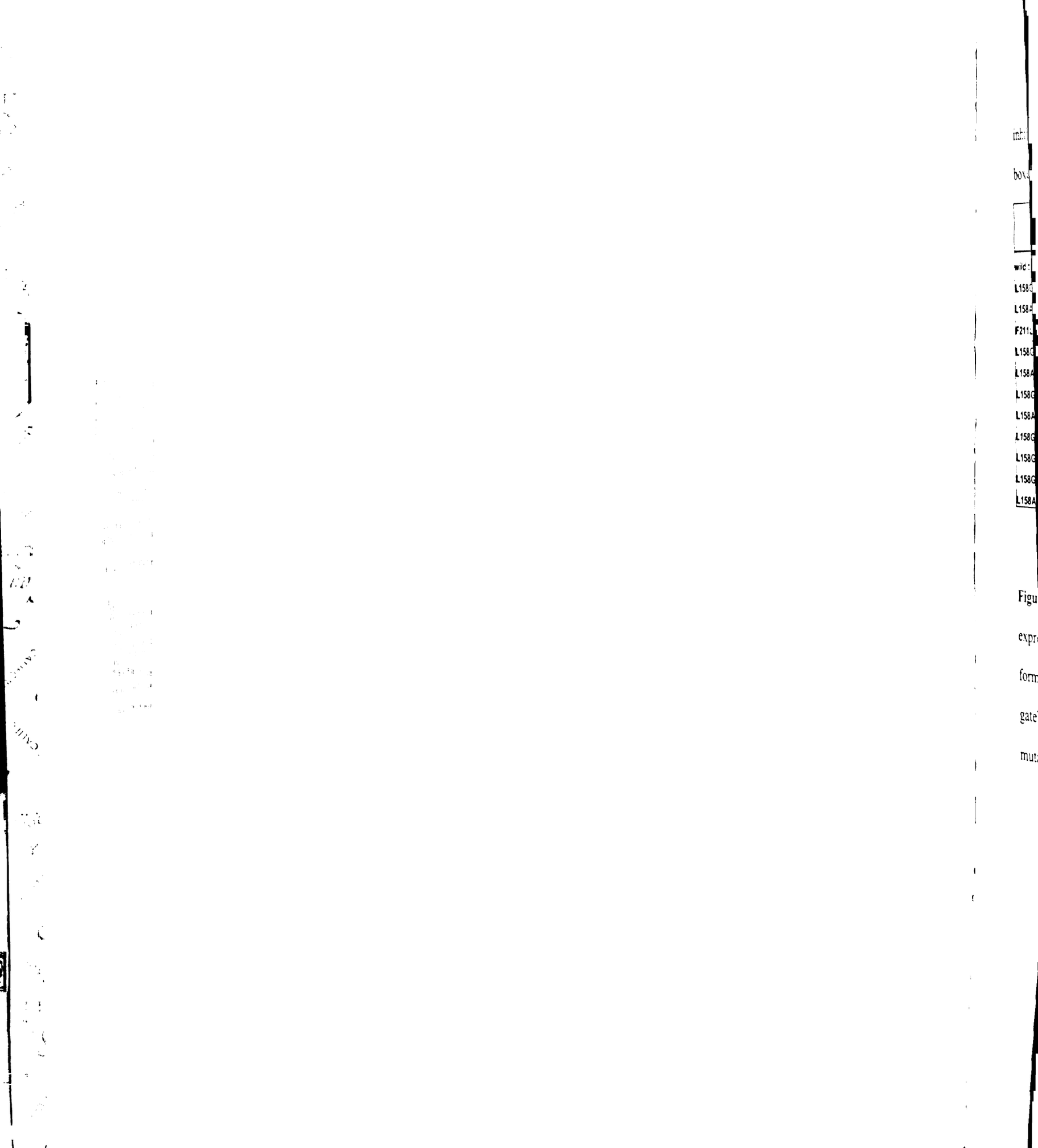

inhibition of cell growth was observed. Combinations not tested are indicated by white boxes (□).

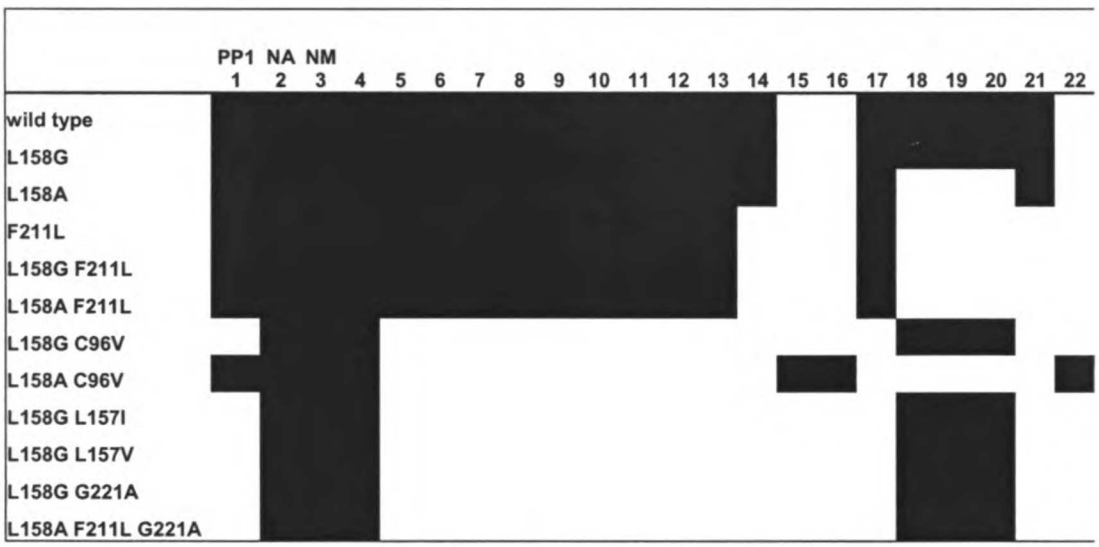

Figure 6. Fitness of Cdc5 mutants monitored by colony forming assay. *cdc5-1* yeast expressing Cdc5 or the indicated mutant were assayed at 10-fold cell dilution for colony formation at permissive (23 C) or restrictive (37 C) temperature, as indicated. (**a**) Cdc5 gatekeeper alleles demonstrate variable fitness. (**b**) An activation loop second site mutation does not rescue the reduced fitness of *cdc5* gatekeeper alleles.

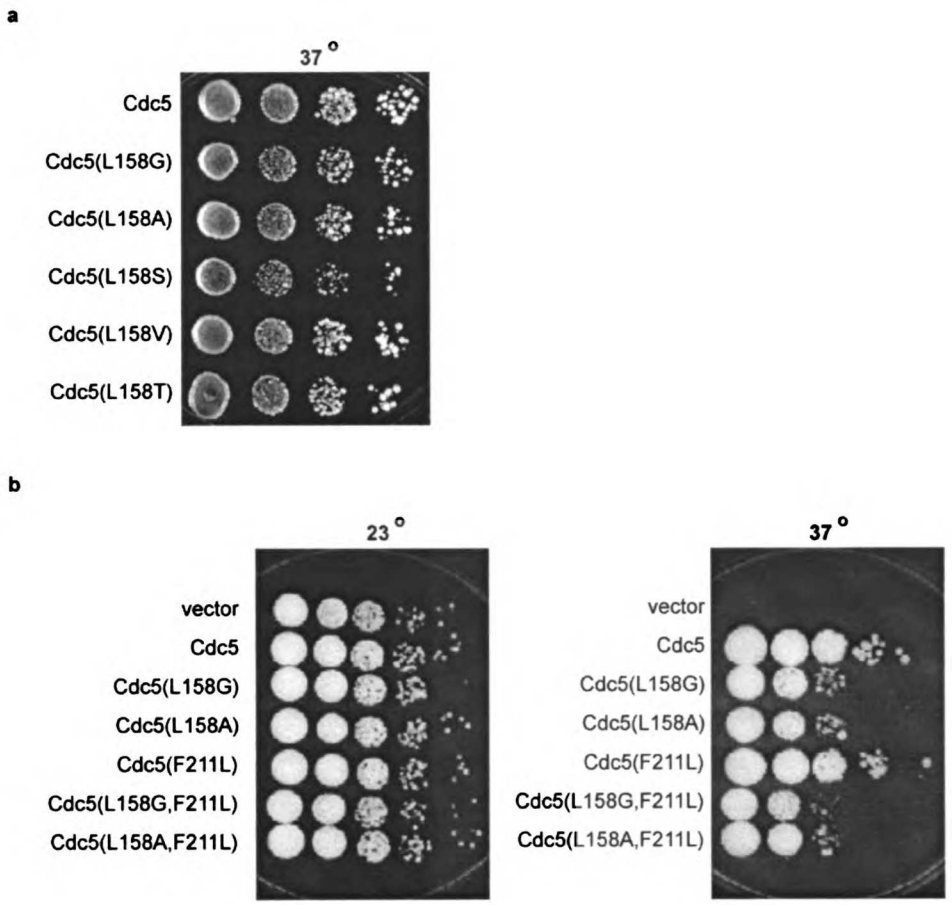

Figure 7. A structure-based sequence alignment of kinases within the β sheet in the N-terminal lobe. A structure-based sequence alignment of eight substitution-tolerant kinases and five substitution-intolerant kinases at selected positions in the three central β strands (β2, β3 and β5). Color codes for columns follow those in **a**. Residues that were mutated as potential suppressors are yellow and bold.

Secondary structure		β2			β3					β5			
Position in c-Src		283	284	285	295	296	297	298	299	338	339	340	341
Tolerant kinases	c-Src	E	V	W	V	A	I	K	T	Y	I	V	T
	Fyn	E	V	W	V	A	I	K	T	Y	I	V	T
	v-erbB	T	V	Y	V	A	I	K	E	Q	L	I	T
	CDK2	V	V	Y	V	A	L	K	K	Y	L	V	F
	Cdc28	V	V	Y	V	A	L	K	K	Y	L	V	F
	KIN28	V	V	Y	I	A	I	K	E	N	L	V	I
	CaMKIIα	V	V	R	Y	A	A	K	I	Y	L	V	F
	Fus3	V	V	C	V	A	I	K	K	Y	I	I	Q
Intolerant kinases	Cdc5	R	C	F	F	A	A	K	T	Y	I	L	L
	MEKK1	S	C	Y	M	A	V	K	Q	N	L	F	I
	GRK2	E	V	Y	Y	A	M	K	Q	S	E	I	L
	Pto	K	V	Y	V	A	L	K	R	I	L	I	Y
	APH(3')-IIIa	K	V	Y	L	A	L	K	K	N	L	L	M

Figure 8. A Cdc5 *sogg* mutation improves cellular fitness. Viability of yeast strains carrying different *CDC5* alleles based on colony-forming efficiency. (**a**) Second-site mutation C96V rescued the cellular function of Cdc5(L158G) and Cdc5(L158A). (**b**) C96V alone had little effect on the cellular function of Cdc5 based on the colony-forming efficiency assay.

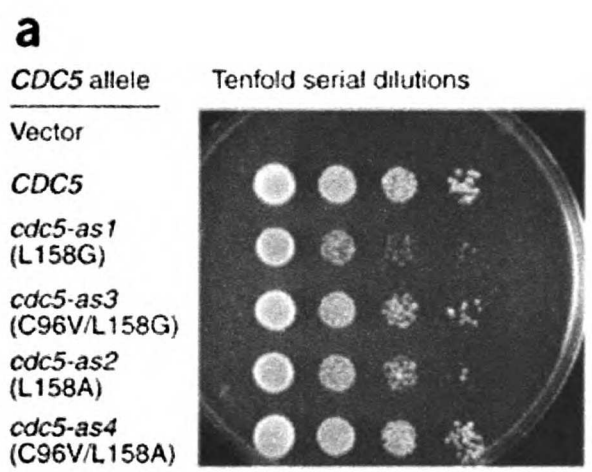

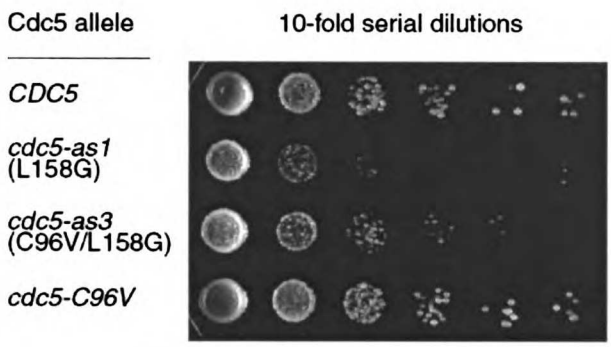

Figure 9. Doubling time of analog-sensitive *cdc5* strains. *CDC5*, *cdc5-as1*, and *cdc5-as2* strains were grown at 30 °C and cell number determined. Doubling time (in hrs) is indicated for each strain.

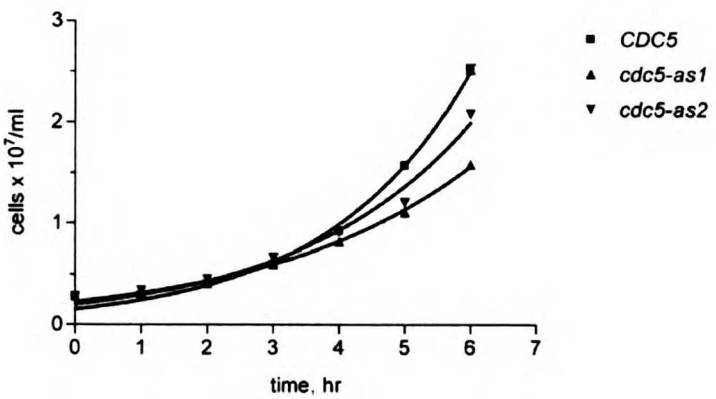

	CDC5	cdc5-as1	cdc5-as2
Doubling Time	1.499	2.179	1.827

Chapter 3

A coupled chemical genetic and bioinformatic approach to Polo-like kinase pathway exploration

A coupled chemical genetic and bioinformatic approach to Polo-like kinase pathway exploration

Paulson, J. L.[1], Sullivan, M.[2], Lowery, D. M.[3], Cohen, M. S.[1], Randle, D. H.[2], Taunton, J.[1], Yaffe, M. B.[3], Morgan, D. O.[2], and Shokat, K. M.[1,4,5]

[1]Department of Cellular and Molecular Pharmacology and [2]Department of Physiology, University of California San Francisco, San Francisco, CA 94158, USA.

[3]Center for Cancer Research, Departments of Biology and Biological Engineering, Massachusetts Institute of Technology, Cambridge, MA 02139, USA.

[4]Howard Hughes Medical Institute.

[5]Correspondence should be addressed to K.M.S. (e-mail: shokat@cmp.ucsf.edu)

Protein phosphorylation is a ubiquitous regulatory mechanism for cellular signal propagation, and the complexity of signaling networks presents a challenge to protein kinase substrate identification. Substrates of Polo-like kinases are largely unknown, despite the significant role of these kinases in coordinating mitotic cell cycle progression. Here, we combine chemical genetic, bioinformatic, and proteomic tools for yeast Polo-like kinase substrate identification. Monospecific pharmacological inhibition of budding yeast Polo-like kinase, Cdc5, delayed anaphase nuclear migration into the bud, revealing a novel Cdc5 function. Systematically chosen candidate Cdc5 substrates were examined for loss of phosphorylation upon cellular Cdc5 inhibition. The identified Cdc5 targets

included Spc72, a spindle pole body (SPB) component and microtubule anchor required for nuclear positioning. Spc72 bound to Cdc5 in a mitosis-specific manner, was directly phosphorylated by Cdc5 *in vitro*, and demonstrated a loss of mitotic phosphorylation *in vivo* upon Cdc5 inhibition. Finally, we expanded our knowledge of Cdc5 function at the SPB by examining SPB-localized proteins for their presence in a Cdc5 complex.

INTRODUCTION

Ensuring accurate chromosome segregation is fundamental to survival of a species. Temporally and spatially regulated signals are required to monitor and direct multiple cellular events during cell division. The Polo-like family of serine/threonine protein kinases (Plks) has emerged as an important class of cell cycle regulators that coordinate mitotic progression, with multiple roles from mitotic entry to cytokinesis (Barr et al., 2004). Humans have four Plks (Plk1-4), of which Plk1 is most thoroughly characterized (Barr et al., 2004). The budding yeast *S. cerevisiae* has a single Plk, Cdc5, with 49% identity to Plk1 in its kinase domain (Lee et al., 2005). Cdc5 regulates multiple cellular functions, including progression through G2/M phase, cohesin cleavage at anaphase entry, and adaptation to the DNA damage checkpoint. Cdc5 also has an essential role in promoting mitotic exit and cytokinesis as part of two signaling networks called FEAR and MEN (Lee et al., 2005).

Despite the multiple mitotic functions of Cdc5, only a few of its substrates have been conclusively identified (Alexandru et al., 1999; Hu et al., 2001; Sakchaisri et al., 2004; Yoshida et al., 2006). Cdc5 substrates are difficult to identify for several reasons.

First, cell-cycle regulators are generally low abundance proteins, and both Cdc5 and its known substrates are present at less than 1500 copies per cell (Ghaemmaghami et al., 2003). Second, characterized phosphorylation sites in Plk substrates have considerable sequence variation (Lowery et al., 2005) and are of limited utility in identifying potential substrates. Third, Cdc5 is a particularly promiscuous kinase when used in *in vitro* reactions. Fourth, different *cdc5-ts* (temperature-sensitive) alleles have given rise to differing terminal phenotypes making the study of Cdc5 function *in vivo* complex (Hu et al., 2001).

The variation in phosphorylation site preference of Cdc5 suggests that alternative specificity determinants exist, such as temporal and spatial regulation. Indeed, Cdc5 levels are tightly regulated during with maximal activity in mitosis, due to both cell-cycle transcription and APC-mediated proteolysis (Lee et al., 2005). Also, Cdc5 has a distinct localization pattern including the cytoplasmic face of the spindle pole body (SPB, the functional equivalent to the mammalian centrosome), chromosomes, and the bud neck (the future site of cytokinesis) (Hornig and Uhlmann, 2004; Sakchaisri et al., 2004; Shirayama et al., 1998; Song et al., 2000). This localization is driven by a C-terminal region of Plks, called the polo-box domain (PBD), as mutations in it severely disrupt the Cdc5 localization pattern (Song et al., 2000). The PBD is a phospho-serine/threonine binding module that targets Plks to their substrates after prior "priming" phosphorylation of the substrate by an upstream kinase (Elia et al., 2003; Lowery et al., 2005).

The importance of cellular localization for Cdc5 substrate specificity motivated us to develop an *in vivo* screen for identifying *bona fide* Cdc5 substrates. To accomplish this, we generated a mono-specific Cdc5 inhibitor using a chemical genetic approach,

which allowed for the selective and temporal inhibition of Cdc5 in cells. Using this inhibitor, we found a novel role for Cdc5 in anaphase spindle migration. Candidate Cdc5 substrates were identified by bioinformatic filtering of the proteome using Cdc5 phosphorylation and PBD binding site preferences, as well as functional criteria. The candidates were screened by chemical inhibition of Cdc5 *in vivo*. This approach identified novel Cdc5 substrates, including the SPB component Spc72. The SPB projects cytoplasmic microtubules required for movement of one set of chromosomes across the predetermined cleavage plane at the bud neck (Pearson and Bloom, 2004). Spc72 anchors cytoplasmic microtubules at the SPB and accordingly functions in nuclear position and spindle orientation, including anaphase spindle migration into the bud (Chen et al., 1998; Hoepfner et al., 2002; Knop and Schiebel, 1998; Soues and Adams, 1998). We demonstrate that Spc72 (along with other SPB components) binds the Cdc5 PBD. Thus, Cdc5 has a previously unidentified function at the SPB and in spindle migration.

RESULTS

CMK selectively inhibits an analog sensitive allele of Cdc5

To evaluate cellular roles of budding yeast Cdc5, we engineered Cdc5 to be selectively inhibited by a cell-permeable small molecule using a chemical genetic approach. This method involves introducing a space-creating mutation at the gatekeeper position coupled with a space-filling bulky derivative of the pyrazolopyrimidine (PP1) kinase inhibitor scaffold (Bishop et al., 2000). We replaced *CDC5* at its endogenous locus with the *cdc5-as1* allele (analog-sensitive) encoding the L158G gatekeeper mutation. This change conferred a modest 6-fold decrease in k_{cat}/K_m and a 47% increase

in strain doubling time; however, *cdc5-as1* cells were viable, indicating that Cdc5(L158G) is a functional kinase (data not shown). Since functional Cdc5 is required for cellular proliferation, we used growth inhibition to assess Cdc5 inactivation. Surprisingly, we were unable to obtain significant inhibition of Cdc5(L158G) using a variety of PP1 analogs despite the diverse collection of other protein kinases that have proven amenable to this approach (Bishop et al., 1999) (data not shown). Thus, the ATP binding site of Cdc5 differs enough from other kinases that a new inhibitor strategy was necessary.

Fortunately, the Cdc5 active site contains a nonconserved cysteine (Cys96) homologous to a cysteine in the mammalian p90 RSK family kinases that was recently exploited for the rational design of selective, irreversible inhibitors (Fig. 1a). These inhibitors are pyrrolopyrimidines containing either a chloromethylketone (CMK) or a fluoromethylketone (FMK) electrophile at the C-2 position, and like PP1, exploit a threonine (or smaller) gatekeeper residue (Cohen et al., 2005). We therefore hypothesized that these irreversible inhibitors would inactivate Cdc5(L158G) by virtue of the absence of a bulky gatekeeper residue and the presence of a naturally occurring Cys at position 96 (Fig. 1b). Growth of the *cdc5-as1* strain, but not the wild type strain (*CDC5*), was prevented by treatment with CMK, but not its parent pyrrolopyrimidine (scaffold), which does not contain the chloromethyl ketone electrophile (Fig. 1c). Additionally, CMK did not inhibit growth of yeast containing a Cdc5 allele with both L158G and C96V mutations (Supplementary Information, Fig. 1a). This suggests that inactivation of Cdc5(L158G) with CMK is mediated by irreversible covalent bond formation with Cys96. Notably, although a threonine gatekeeper residue is sufficient for

inhibition of RSK by CMK (Cohen et al., 2005), Cdc5 required a smaller gatekeeper residue (Supplementary Information, Fig. 1b). Together, the *cdc5-as1* strain and CMK provide a means to study cellular roles of Cdc5.

Cdc5 is required for proper timing of anaphase spindle migration

We sought to determine the nature of the growth arrest caused by CMK addition to *cdc5-as1* yeast. Wild type and *cdc5-as1* strains were released from a G1 arrest (unbudded cells) into media containing increasing concentrations of CMK, and cell cycle progression was determined by microscopic observation of budding (Fig. 2a). CMK exhibited a concentration-dependent first cell cycle mitotic arrest in the *cdc5-as1* strain with an IC_{50} of 1.1 μM (Fig. 2b). By contrast, up to 15 μM CMK had no effect on cell cycle progression in the wild type strain (Fig. 2a). We examined in precise detail the arrest phenotype at 5 μM. Notably, arrested cells were large-budded with separated DNA masses and elongated spindles. Pds1 degradation occurred with similar kinetics in both strains, indicating that anaphase onset in budding yeast is unaffected by Cdc5 inhibition (Fig. 2c). Strikingly, we also observed a high percentage of anaphase *cdc5-as1* cells (23%) in which spindle elongation occurred entirely in the mother cell, rather than through the bud neck (Fig. 2e, f). This was a rare event in anaphase wild type cells (2%) and implies a failure of the nucleus to migrate into the bud upon anaphase onset. Expression of wild type Cdc5 in the *cdc5-as1* cells rescued this defect (4% anaphase spindles in mother), while expression of Cdc5 containing a defective Polo-box domain could not (17% anaphase spindles in mother). Inhibited *cdc5-as1* cells were able to elongate their spindles to greater than 5 μm without spindle migration into the bud (Fig.

2f). The spindles eventually recovered from this defect, and the cells later arrested in telophase with high Clb2 levels (Fig. 2c) and DNA masses segregated properly into mother and daughter (Fig. 2d).

Cdc5 substrates are identified through a candidate-based *in vivo* screen

A role for Cdc5 in anaphase nuclear positioning was not previously known and cannot be easily explained by its previously identified substrates. Proper anaphase spindle migration required both Cdc5 catalytic activity and Polo-box domain function, suggesting that the critical substrates would likely contain sequences recognized by both the Polo-box domain and kinase domain (Fig. 3a). Therefore, a candidate approach to identifying substrates was designed to incorporate both of these elements (Fig. 3b).

Briefly, the roughly six thousand predicted yeast proteins were searched with the *Scansite* profile scanning algorithm (Obenauer et al., 2003; Yaffe et al., 2001) for Cdc5 binding and phosphorylation sequence motifs, generating a "Cdc5 substrate likelihood score" for each protein. The Cdc5 binding motif was determined previously by oriented library screening (Elia et al., 2003). A predicted Cdc5 phosphorylation motif was generated by combining information on Cdc5, Plk1, and Plk3 substrates (Lowery et al., 2005) with the published kinase phosphorylation motif of Plk1 (Lowery et al., 2005; Nakajima et al., 2003), since both Plk1 and Plk3 can substitute for Cdc5 function in yeast (Lee et al., 2005). The distribution of scores is represented in Figure 3c, with high scores representing likely substrates. Notably, the group of best-scoring potential Cdc5 substrates was enriched in low abundance proteins relative to the entire proteome, requiring a sensitive test of candidate phosphorylation (Fig. 3d). Cdc5 substrate

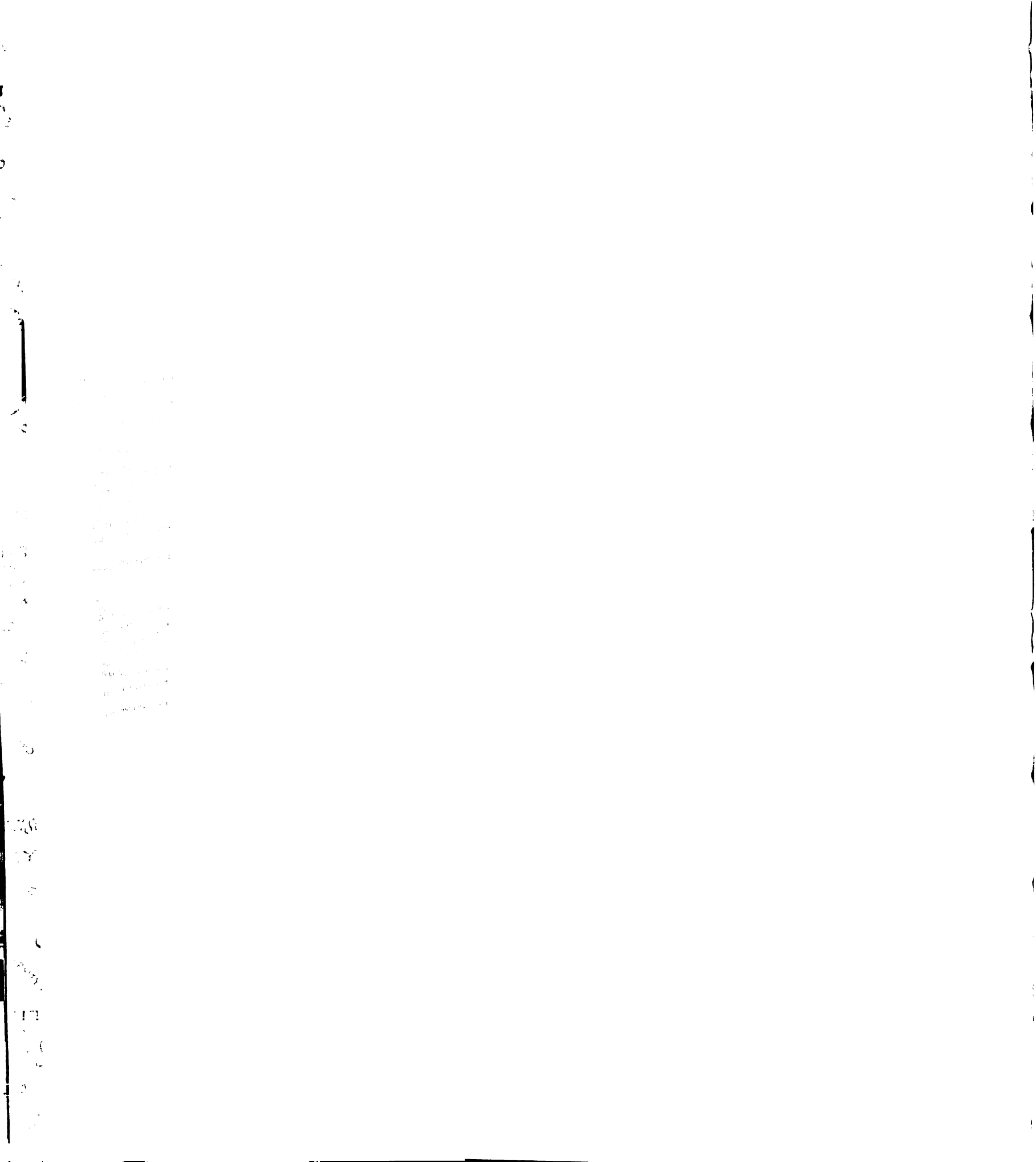

likelihood scores combined with functional criteria led us to choose 192 total candidate substrates (Supplemental Information, Table 1). Among the proteins identified by this approach were the known Cdc5 substrates Mcd1, Bfa1, and Swe1 (Alexandru et al., 2001; Hu et al., 2001; Sakchaisri et al., 2004). Swe1 is the only of the three previously shown to directly bind the PBD (Asano et al., 2005) and was ranked 12th highest overall (Supplemental Information, Table 1).

To test these candidate substrates for Cdc5-dependent phosphorylation *in vivo*, we used a library of strains each encoding a candidate substrate, at its endogenous locus, fused to a tandem affinity purification (TAP) tag, which provided an ultra-sensitive handle for immunological detection (Ghaemmaghami et al., 2003). The phosphorylation state of the TAP-tagged candidates was monitored by gel shift, a straightforward and well-established method for determining the phosphorylation state of many proteins *in vivo* (Ubersax et al., 2003). We focused on the candidates that exhibited a gel shift in a mitotic arrest, when Cdc5 is active, but not in a G1 arrest, when Cdc5 is inactive (Cheng et al., 1998) (Fig. 3b). Mitotically arrested cells were treated for 20 minutes with 10 μM CMK or DMSO (control). To avoid false positive phosphorylation, *cdc5-as1* was the sole source of Cdc5, and CMK was added for only 20 minutes to limit indirect effects of Cdc5 inhibition.

Of the 74 proteins that displayed a gel mobility shift when isolated from mitotic cells, five exhibited reproducible Cdc5-dependent changes in gel mobility (Fig. 3e and Supplemental Table 1). Significantly, of the three known Cdc5 substrates included in our screen, Bfa1 and Mcd1 (Alexandru et al., 2001; Hu et al., 2001) downshifted upon Cdc5 inhibition. Similarly, Spc72 and Ulp2 also downshifted upon Cdc5 inhibition. Spc72 is a

previously described phosphoprotein, but the upstream kinase had not been identified (Gruneberg et al., 2000). Intriguingly, Cdc5 inhibition resulted in an upshift of Mih1. The chemical nature of this shift is unclear, since it is unusual for loss of phosphorylation to result is a slower migrating form.

The SPB component Spc72 is a Cdc5 substrate and binding partner in mitosis

Spc72 has several hallmarks of a Cdc5 substrate important for the regulation of anaphase nuclear positioning. It contains both Cdc5 PBD-binding and phosphorylation motifs, exhibits Cdc5-dependent phosphorylation, and is a SPB component with a previously known function in nuclear positioning (Chen et al., 1998; Hoepfner et al., 2002; Knop and Schiebel, 1998; Soues and Adams, 1998). Spc72 phosphorylation was examined through the cell cycle to further explore this connection. In wild type cells, Spc72 phosphorylation peaked in late mitosis, just as Clb2 levels begin to decrease (Fig. 3f). This Spc72 mobility shift was prevented when Cdc5 was inhibited by treating *cdc5-as1* cells with CMK (Fig. 3f). Finally, purified 6xHis-tagged Cdc5 directly phosphorylated immunoprecipitated TAP-tagged Spc72 *in vitro* (Fig. 3g), suggesting that Spc72 is a direct substrate of Cdc5.

Spc72 was previously reported to bind to Cdc5 (Ho et al., 2002; Park et al., 2004), and we investigated the nature of this interaction. To determine whether binding could be mediated by phospho-dependent interactions between Spc72 and the Cdc5 Polo-box domain, we performed pulldown experiments for Spc72 in mitotic extracts using either the wild-type Cdc5 PBD, or a PBD variant (PBD*) in which we introduced mutations corresponding to conserved residues in Plk1 required for phosphospecific binding (Elia et

al., 2003) (Fig. 4a). Spc72 efficiently bound to the PBD, relative to a 5% input control, but failed to bind to PBD*, indicating that prior Spc72 phosphorylation by a priming kinase creates a Cdc5 binding site (Fig. 4b). Consistent with this, the interaction was also regulated by cell cycle stage, since Spc72 bound the PBD less well in a G1 extract than in a mitotic extract (Fig. 4c). Spc72 contains several minimal PBD binding sites and a site at S232 with the 74th best *Scansite* score out of 6833 matches to the PBD binding site in the yeast proteome. Mutation of S231 and S232 at this site significantly reduced binding to the PBD (Fig. 4e), suggesting that Spc72 and Cdc5 bind directly. Residual binding to this Spc72 mutant may reflect contributions from other sites in Spc72 or Cdc5 PBD interactions with Spc72 binding partners.

To identify other mediators of Cdc5 binding at the SPB, we tested the ability of the Cdc5 PBD to bind 90 proteins that were either annotated as SPB-localized or identified as SPB-localized in a proteomic study (Huh et al., 2003). Notably, PBD binders at the SPB may include Cdc5 substrates involved in anaphase spindle migration, since the PBD is required for both Cdc5 localization to the SPB (Song et al., 2000) and proper anaphase spindle migration. SPB-localized proteins were examined for PBD binding in extracts of mitotically arrested cells (Supplemental Information, Table 2). Components of the SPB cytoplasmic face, Spc72, Cnm67, and Nud1, bound to the PBD, as did known Spc72-binding proteins, Spc97, Stu2, and Kar1 (Supplementary Information, Table 2). The most efficient PBD binders, determined by the ratio of input and PBD-bound protein levels, are shown in Figure 4f. These included mitotic exit signaling network components, Cdc14 and Bub2, kinetochore proteins, Cse4 and Tid3, and the SPB component, Spc110 (Fig. 4f). Significantly, Spc72 was among the most

efficient binders, implying both that it directly interacts with the PBD and is a major site of Cdc5 binding at the SPB (Fig. 4f).

DISCUSSION

Here we report a chemical genetic and bioinformatic approach to investigate the cellular roles of the yeast Plk, Cdc5. Specific chemical inhibition of Cdc5 by CMK both revealed a new role for Cdc5 in anaphase spindle migration and facilitated identification of Spc72 as a Cdc5 substrate. Analysis of Spc72 regulation supports a model in which a kinase primes Spc72 for binding to Cdc5 at the SPB in mitosis, resulting in direct Spc72 phosphorylation by Cdc5. Interestingly, the phenotype resulting from loss of Spc72 is consistent with it being a Cdc5 effector in nuclear migration (Chen et al., 1998; Hoepfner et al., 2002; Knop and Schiebel, 1998; Soues and Adams, 1998).

Chemical genetic engineering of Cdc5 posed a significant challenge, as Cdc5 was unexpectedly incompatible with our previously extensively validated approach. Unlike other engineered kinases, Cdc5 was not inhibited by PP1 analogs. Although no Plk kinase domain structure is available, our results indicate that access to the hydrophobic pocket in Cdc5 is reduced relative to other protein kinases we have studied. Similar to RSKs, Plks have a nonconserved active site cysteine, which provided a handle for potent irreversible Cdc5 inhibition. Consistent with Plk1 inhibition by unconventional protein kinase inhibitors, such as wortmannin (Liu et al., 2005), our results suggest that Plk active sites have distinctive features, which could potentially be exploited in wild type Plk inhibitor development. Moreover, since the cysteine is conserved across the family,

the chemical genetic inhibition strategy should be applicable to studying any Plk family member.

Small molecule addition rapidly inhibits only the catalytic activity of the kinase, both avoiding compensatory mechanisms occurring in the absence of the kinase and allowing for study of temporally resolved processes, and has often revealed new aspects of kinase function missed by genetic approaches (Knight and Shokat, 2005). As well as blocking mitotic exit and cytokinesis, inhibition of Cdc5 by CMK resulted in aberrant anaphase spindle elongation without migration into the bud. The defect was corrected eventually, and the spindle moved into the neck, either due to redundant activities or by forces generated by the elongating spindle itself. Previous studies with *cdc5-ts* alleles revealed only the essential Cdc5 functions, as they are more conducive to endpoint assays. Also, elevated temperatures required for inactivating *ts* alleles accelerate the cell cycle, potentially masking transient effects such as a role in spindle positioning. Thus, this novel Cdc5 function was revealed only by the pharmocologic modulation of Cdc5 activity.

Our substrate screen combined several recent technological advances to meet the stringent requirement of low abundance Cdc5 substrate identification *in vivo*. Identification of direct Cdc5 targets necessitated selective and rapid Cdc5 inactivation for a brief period, and chemical genetics ideally suited this purpose. Unlike mass spectrometry approaches, which suffer from limited dynamic range (Ghaemmaghami et al., 2003), utilization of the TAP-tag proteomic library facilitated the visualization of even low abundance phosphoproteins by gel shift. Phosphorylation reactions occurred only in a cellular context, and, crucially, both analog-sensitive Cdc5 and the candidates

were at endogenous levels. A candidate approach made this screen feasible, and while the Cdc5 binding and phosphorylation motifs are degenerate, a useful set of candidates was obtained by utilizing the extra information contained in weighting amino acids at each position based on their preference by Cdc5. Functional criteria are a useful filter for substrate sets (Dephoure et al., 2005) and were also incorporated into the selection process. However, we were limited by the proportion of phosphoproteins that demonstrated significant phosphorylation shifts. Further advances in mass spectrometric approaches that quantitatively detect differences in low stoichiometry phosphopeptides in a complex mixture are necessary to improve this approach (Morandell et al., 2006).

Although the screen was not limited to these proteins, we were interested in finding substrates consistent with the Cdc5 spindle migration phenotype, such as molecular motors required to generate budward force, cortical determinants that interact with cytoplasmic microtubules penetrating the bud, or proteins that stabilize or nucleate cytoplasmic microtubules (Pearson and Bloom, 2004). Of the Cdc5 substrates identified, only Spc72 has a known role in nuclear position. Loss of Spc72 causes reduced cytoplasmic microtubules, as well as defects in microtubule-dependent processes, such as nuclear position and spindle orientation, and a delay in mitotic exit due to anaphase spindles that have not properly migrated into the bud (Chen et al., 1998; Hoepfner et al., 2002; Knop and Schiebel, 1998; Soues and Adams, 1998). Several lines of evidence indicate that Spc72 is a *bona fide* Cdc5 substrate. Cdc5 phosphorylated Spc72 *in vitro*, Cdc5 activity was required for the phosphorylation shift of Spc72 *in vivo*, and the Cdc5 PBD bound Spc72 in a cellular extract. Further, the binding of Spc72 to Cdc5 was dependent on phosphoselectivity elements in the PBD, cell cycle stage, and a binding site

at S232 in Spc72. These results are consistent with a model in which a kinase primes Spc72 for binding and subsequent phosphorylation by Cdc5. The unidentified kinase would likely localize to the SPB and be active in mitosis but not G1, and the sequence surrounding S232 indicates phosphorylation by a proline-directed kinase, such as cyclin-dependent kinases or mitogen activated protein kinases.

The multitude of potential Cdc5 phosphorylation sites in Spc72 (Fig. 4d) and low endogenous levels of these proteins, coupled with residual binding to Spc72(S231A,S232A), presented a technical challenge to studying the downstream effect of Cdc5 regulation of Spc72. Cell cycle regulated Spc72 phosphorylation has been implicated in shuttling of the γ-tubulin complex between distinct substructures of the SPB, and it is tempting to speculate that Cdc5 is the kinase responsible (Gruneberg et al., 2000; Pereira et al., 1999). If so, Cdc5 inhibition will provide a system to further study this event. However, regulation of Spc72 binding to other interactors, such as Stu2 (Chen et al., 1998) is also consistent with the Cdc5 inhibition phenotype. Additionally, we found the Cdc5 PBD to interact with several SPB components, indicating the potential for modulation of Cdc5 function at the SPB by a number of redundant mechanisms. More generally, our chemical genetic approach to Cdc5 inhibition provides a tool to probe the molecular mechanisms coordinating nuclear movement with the cell cycle. In yeast, movement of the anaphase spindle into the bud is required for proper chromosome segregation due to a predetermined cleavage plane. In higher organisms, spindle position is critical for developmental cell fate decisions (Pearson and Bloom, 2004).

We identified Ulp2 and Mih1 as novel Cdc5 substrates, and both are involved in Cdc5-related functions. Mih1 is the yeast homolog of Cdc25, which is phosphorylated

by Plks during mitotic entry (Lee et al., 2005). Ulp2 is a desumoylase with roles in centromeric cohesion and recovery from checkpoint arrest (Bachant et al., 2002; Li and Hochstrasser, 2000). Advantageously, many kinetochore proteins were incorrectly annotated as SPB-localized and included in the PBD binding screen. Of these, Cse4 and Tid1 bound the PBD, potentially reflecting a role for Cdc5 at the yeast kinetochore, consistent with other Plks (Barr et al., 2004). At the SPB, we find that Cdc5 binds to Spc110, the nuclear equivalent of Spc72 (Jaspersen and Winey, 2004), and therefore may regulate spindle dynamics. Likewise, Plk1 spindle functions include centrosome maturation by phosphorylation of Nlp, which (like Spc72 and Spc110) nucleates microtubules by binding to the γ-tubulin ring complex (Barr et al., 2004).

The low abundance and importance of Cdc5 localization for substrate specificity demanded assays that preserved cellular context and endogenous expression levels. Consequentially, like Cdc5 itself, many of its interactors identified here, including Spc72, are present at less than 1500 molecules per cell. Furthermore, the *in vivo* method for identifying kinase-dependent phosphoproteins can potentially be extended to additional kinases functioning in this pathway or in other dynamic cell processes.

METHODS

Plasmids, strains, and yeast methods. A *CDC5* (YMR001C) genomic fragment in pRS315 (p315-CDC5) and pRS306 (p306-CDC5) were gifts of J. Charles. The L158G mutation was introduced into p315-CDC5 and p306-CDC5, generating p315-cdc5-as1 and p306-cdc5-as1. The PBD from p315-CDC5 was cloned into pGEX-3X (GE Healthcare) to produce pGST-PBD, and W517F,H641A,K643M mutations were

introduced to make pGST-PBD*. The PBD mutations were cloned into p315-CDC5 from pGST-PBD*. *CDC5* was cloned into pFastBacHT-A (Invitrogen) to produce pFastBac-CDC5. *SPC72* (YAL047C) was amplified from W303 genomic DNA and recombined with a URA3-marked 2 μm plasmid bearing the GAL1 promoter and TAP tag (E.K. O'Shea, Harvard University) to produce pSPC72. The S231A,S232A mutations were introduced into pSPC72 to produce pSPC72-AA. Mutations were introduced by QuikChange site-directed mutagenesis (Stratagene). Open reading frames were fully sequenced after amplification. SPC72 plasmids encoded an I302N difference from published sequence, which was confirmed in a W303 strain.

Standard yeast media and genetic techniques were used(Guthrie and Fink, 2002), except as specifically described. Strains were *MAT***a** and W303 (Figs. 1 and 2, and Supplemental Information, Fig. 1) or S288C (isogenic with EY1274, all other Figs.) strain background. *cdc5-as1* was introduced at the *CDC5* locus by two-step gene replacement, except as follows. A *MAT*α strain derived from EY1274 carrying a *can1*Δ::*MFA1p-LEU2* selectable marker (E.K. O'Shea, Harvard University) was transformed with a marker fusion PCR product generated by amplification of *cdc5-as1* and *K.lactis URA3* genes. The entire *cdc5-as1* gene was sequenced in the resultant integrated strain, which was then crossed to selected *MAT***a** *HIS3* marked TAP-tagged library strains (Ghaemmaghami et al., 2003) (Open Biosystems) using a manual 96-pinning tool (V&P Scientific). After sporulation, TAP-tagged *MAT***a** haploids were selected on synthetic media lacking histidine, arginine, leucine, and uracil and containing 50 μg/ml canavanine (Sigma).

Cell cycle synchronization was obtained by G1 arrest with alpha factor for 3 hours, followed by washing to release (0 min time point). Alpha factor was readded at 70-80 minutes when arresting in the following G1. Alpha factor was used at 1 μg/ml for bar- cells (Fig. 2) and 20 μg/ml for bar+ cells (all other experiments). Mitotic arrests were obtained by nocodazole treatment at 15 μg/ml for 3 hours.

Protein expression and purification. 6xHis-Cdc5 was prepared as follows. Bacmid was produced from pFastBac-CDC5 and transfected into Sf9 insect cells using the Bac-to-Bac Baculovirus expression system (Invitrogen). Sf9 cells were harvested after a 2 day infection with Pass 3 baculovirus at $2x10^6$ cells/ml, and cell extract prepared by douncing in Cdc5 lysis buffer (CLB: 2 5 mM HEPES pH 7.4, 300 mM NaCl, 10% glycerol, 50 mM NaF, 50 mM beta-glycerophosphate, 35 nM okadaic acid) with protease inhibitors (1 mM PMSF, 1 μg/ml leupeptin, 1 μg/ml aprotinin, 1 μg/ml pepstatin). The cleared extract was applied to a HiTrap Chelating HP column (Amersham) chelated with $CoCl_2$. After washing, peak 6xHis-Cdc5 containing fractions eluted with CLB containing an imidazole gradient were combined.

GST-PBD and GST-PBD* were expressed from pGST-PBD and pGST-PBD* in BL21-CodonPlus(DE3)-RIL cells (Stratagene). Cleared extracts prepared in GST lysis buffer (GLB: 50 mM Tris, pH 8.0, 1 M NaCl, 1% NP40, 1mM PMSF, 1 μg/ml aprotinin, 10 nM DTT) were loaded onto a glutathione agarose (Sigma) column. After washing, GST fusion proteins were eluted in 50 mM Tris, pH 8.0, 250 mM KCl, 5 mM reduced glutathione. Glutathione was subsequently removed using a PD-10 desalting column (GE Healthcare).

Kinase assays. For Cdc5 kinase assays, Spc72-TAP was isolated from cell extract by pulldown with IgG sepharose (GE Healthcare) or rabbit IgG (Sigma) coupled to M-270 epoxy dynabeads (Dynal) and incubated in kinase buffer (25 mM HEPES, pH 8.0, 60 mM KCl, 15 mM $MnCl_2$, 100 μg/ml BSA, 80 nM microcystin, 1mM DTT, 100 μM 200 μCi/ml [γ-^{32}P]ATP) in the absence or presence of 100 ng purified baculovirus expressed 6xHis-Cdc5. ^{32}P incorporation was visualized on a Typhoon PhosphorImager (GE Healthcare), and images were processed using ImageQuant software (GE Healthcare).

Western blotting and pulldowns. Blots were probed with anti-TAP (Open Biosystems), anti-Clb2 (kind gift D. Kellogg), and anti-HA (16B12, Covance) primary antibodies and anti-rabbit (Amersham) and anti-mouse (Pierce) HRP-conjugated secondary antibodies. Total protein was stained using Ponceau S (Sigma).

For phosphorylation gel shifts, cell extracts were prepared in urea lysis buffer as described(Ubersax et al., 2003), and 5 μg was loaded on 5%, 7.5%, or 10% Criterion gels (Biorad) for western blotting.

For PBD binding assays, extracts from TAP-tagged library strains were prepared in TAP lysis buffer (TLB: 20 mM HEPES, pH 8.0, 150 mM NaCl, 2 mM EDTA, 0.2% NP40, 50 mM NaF, 50mM beta-glycerophosphate, 100 μM Na_3VO_4, 20 nM microcystin, Complete EDTA-free protease inhibitors (Roche), 1 μg/ml pepstatin) with 1 mM DTT. Cleared extracts were incubated with purified recombinant GST-PBD or GST-PBD* and

glutathione agarose (Sigma) in TLB with 10 mM DTT for 1 hour at 4 degrees. Bead bound complexes were washed and analyzed by western blot for presence of the TAP-tagged protein. For Figure 4e, TAP-tagged Spc72 and Spc72(S231A,S232A) were expressed from pSPC72 and pSPC72-AA in an untagged strain. Expression was induced for 1 hour in mitotically arrested cells with 2% galactose, resulting in tagged protein levels lower than that of endogenously tagged Spc72 (data not shown).

Microscopy and image processing. Cells were fixed with 3.7% formaldehyde overnight at 4 degrees. DNA was stained with 1μg/ml DAPI. Tubulin was stained with YOL 1/34 (Abcam) and Cy3-conjugated anti-Rat secondary (Jackson Laboratories). Images were acquired at 63x magnification on a Zeiss Axiovert 200 M microscope using Axiovision software. Images were cropped and minimum and maximum pixel values adjusted in Photoshop.

Bioinformatic and statistical analysis. Candidate Cdc5 substrates were initially selected based on information available in September 2003 as follows. First, proteins involved in Cdc5-dependent processes were identified by Gene Ontology (GO) term searches and selected if they contained a minimal phosphorylation or PBD motif. Second, yeast proteins in SWIS-PROT were evaluated with the *Scansite* algorithm, which assigns final scores (Sf) reflecting how well the query sequence matches a position-specific scoring matrix representing the optimal Cdc5 PBD or kinase motif, normalized to all proteins in the database(Obenauer et al., 2003; Yaffe et al., 2001). These range

from 0 (perfect match) to 1 (complete lack of even a minimal binding or phosphorylation motif). The Cdc5 substrate likelihood score was defined as 1-[0.5 (Sf_{PBD}+Sf_{Kin})], where Sf_{PBD} and Sf_{Kin} were the final *Scansite* scores for the individual PBD and kinase motifs, respectively. Highest scoring proteins were selected and the remaining proteins considered in turn by score, selecting those with cell cycle function and nuclear or cytoplasmic localization. Supplementary Information, Table 1 contains updated scoring and functional information from October 2006.

Annotations used for identifying SPB-localized proteins are from SGD (Hong, E.L., et al. "Saccharomyces Genome Database", http://www.yeastgenome.org, July 2005).

Curve fitting, regression analysis, and statistical tests were performed with Prism 4 (GraphPad software).

ACKNOWLEGMENTS

We thank EK O'Shea and J Weissman for sharing of reagents prior to publication and AN Snead for comments on the manuscript.

This work was supported by National Institute of General Medical Sciences grant GM53270 to DOM, NIH grant GM60594 and a Burroughs-Wellcome Career Development Award to MBY, NIH grant GM71434 to JT, NCI training grant 5T32CA09270 and a NSF pre-doctoral fellowship to JLP, a HHMI pre-doctoral fellowship to DML, and NIH grants EB001987 and AI44009 to KMS.

Figure legends

Figure 1 Analog-sensitive Cdc5 is inhibited by CMK. (**a**) Sequence alignment of kinase domain regions spanning the gatekeeper residue and the reactive cysteine. The Cdc5 sequence is in bold, and the specificity filters critical for RSK2 inhibition by CMK(Cohen et al., 2005) are highlighted in gray. (**b**) Chemical structure of CMK. CMK (in gray), with features of the kinase active site depicted, including a cysteine to react with the electrophilic chloromethyl ketone and a gatekeeper residue that controls access to a hydrophobic binding pocket. A predicted steric clash between the Cdc5 leucine gatekeeper residue and CMK is illustrated. (**c**) Cell viability halo assay of wild type (*CDC5*) and *cdc5-as1* yeast. Inhibition of cell growth in the region surrounding a disc spotted with 1 nmol CMK or scaffold molecule is observed only upon CMK application to *cdc5-as*1 (center), indicating a requirement for both the gatekeeper mutation and the electrophilic reactivity of CMK.

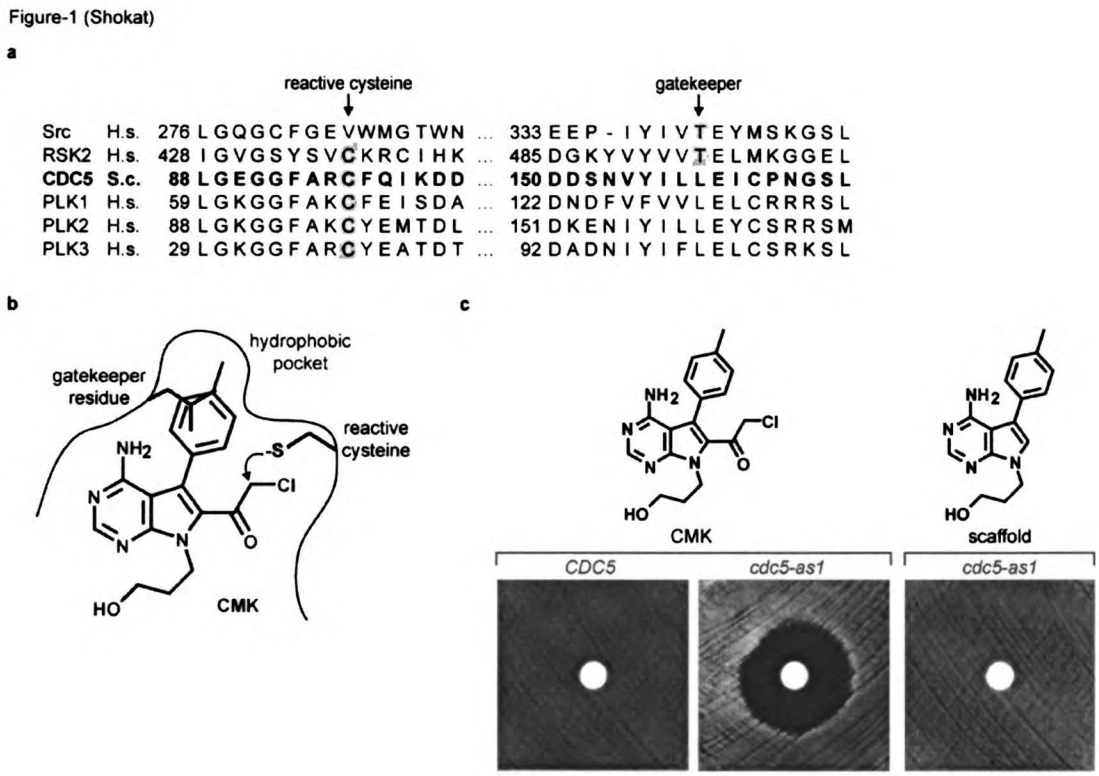

Figure 2 CMK inhibition of Cdc5(L158G) leads to a first cell cycle anaphase arrest and delay in anaphase spindle migration. (**a**) CMK treatment causes of a first cell cycle arrest of *cdc5-as1*, but not wild type, cells in a dose-dependent manner. Time course of cell cycle synchronized *CDC5* and *cdc5-as1* cultures released from G1 arrest (unbudded) into the indicated concentrations of CMK (n = 200 cells for each point) is plotted. The y-axis represents the percentage of cells in S/G2 and M phases, as judged by the presence of a medium- to large-sized bud. A second cell cycle was prevented by re-arrest in the subsequent G1. (**b**) *cdc5-as1* cells arrest with an extracellular 50% inhibitory CMK concentration of 1.1 μM (dotted line, 95% confidence interval from 0.9 to 1.2 μM). The percent *cdc5-as1* cells in S/G2 and M cell cycle phases at 180 min is shown for CMK-treated cultures prepared as in **a**. Error bars represent standard errors of the mean for

three experiments (n = 200 cells for each), and the data were fit to a sigmoidal dose response curve ($R^2 = 0.97$). (**c**) CMK-treated *cdc5-as1* cells degrade Pds1 with wild type kinetics but maintain stabilized Clb2. Cell extracts from *CDC5* and *cdc5-as1* strains expressing Pds1-HA3 released from G1 into 5 μM CMK and re-arrested in the subsequent G1 were blotted for HA (Pds1) and Clb2. (**d**) CMK-treated *cdc5-as1* cells arrest as budded cells with segregated chromosomes. Budded cells and budded cells with DNA masses separated into mother cell and bud (binucleate) were quantified for the experiment shown in **c** (n = 100 cells per point). (**e**) Mother cell localized anaphase spindles are transiently observed in CMK-treated *cdc5-as1* cells. The percentage anaphase spindles with localization depicted (n = 100 cells) in CMK-treated *cdc5-as1* and *CDC5* cells at 105 min in the experiment shown in **c** and **d**. (**f**) Examples of cells with anaphase spindles (tubulin) observed at 90 min in the experiment shown in **c-e**. The images show aberrant (*cdc5-as1*) and wild type (*CDC5*) anaphase spindle localization, but are not representative of all cells in the population. The scale bar represents 5 μm.

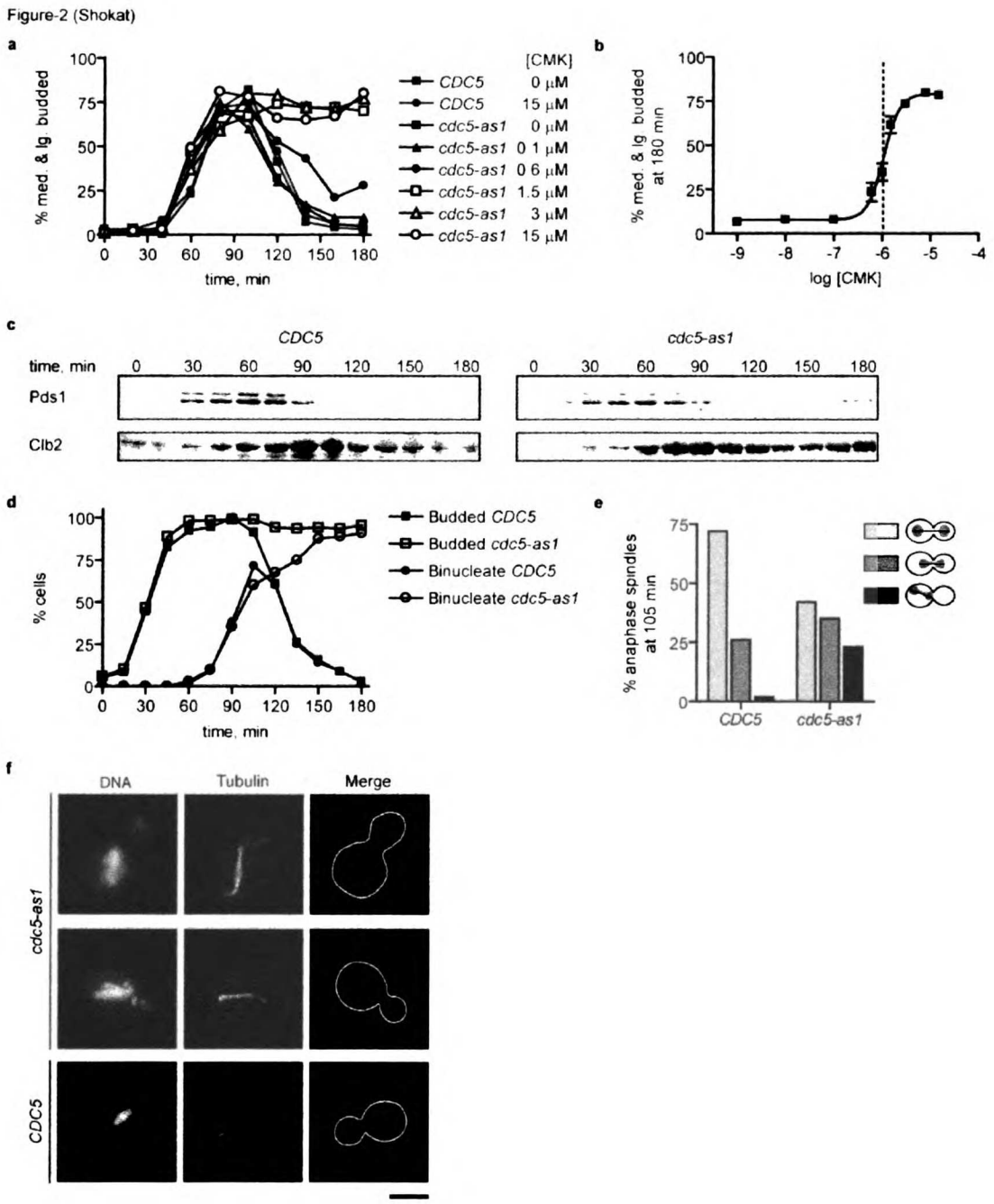

Figure 3 A candidate-based *in vivo* screen identifies Spc72 as a Cdc5 substrate. (**a**) Schematic representation of substrate recognition by Cdc5. The substrate is depicted to contain a Cdc5 phosphorylation motif, (D/E/N)X(S/T)(Brar et al., 2006) and a binding

motif, S(pS/pT)(P/X), which binds the Cdc5 Polo-boxes (PB1 and PB2)(Elia et al., 2003). X represents any amino acid, p represents phosphorylation. (**b**) Approach to screening for substrates phosphorylated by Cdc5 *in vivo*. (**c**) Bioinformatic mining of the yeast proteome for candidate Cdc5 substrates. The distribution of assigned Cdc5 substrate likelihood scores is shown for 192 Cdc5 candidate substrates compared with the proteome, with low scores reflecting likely candidates. (**d**) Cdc5 candidate substrates are enriched in low abundance proteins. Normalized distribution of protein abundance (Ghaemmaghami et al., 2003) comparing candidate Cdc5 substrates to the entire proteome. The data set means were statistically different (P=0.0003) by unpaired t-test. Proteins without abundance values (Ghaemmaghami et al., 2003) were excluded from the analysis. (**e**) Result of the screen. The gel mobility of five TAP-tagged candidate substrates is altered upon Cdc5 inhibition with 10 μM CMK (+) as compared with a DMSO control treatment (-). (**f**) Inhibition of Cdc5 with CMK eliminates the mitotic Spc72 upshift observed in a synchronized cell cycle. Cell cycle progression of *CDC5* or *cdc5-as1* cells expressing Spc72-TAP released from G1 into 10 μM CMK is indicated by budding index and Clb2 western blot. Spc72 is visualized by anti-TAP western blot (Spc72). (**g**) *In vitro* phosphorylation of Spc72 by Cdc5. Immunopurified TAP-tagged Spc72 was incubated with [γ-^{32}P]ATP, with and without purified Cdc5 (left panels). Phosphorylation (32P) and Spc72 western blot (α-TAP) are observed. No Spc72 phosphorylation is seen when Cdc5 is added to a mock pulldown reaction (untagged Spc72, - Spc72-TAP, right panels).

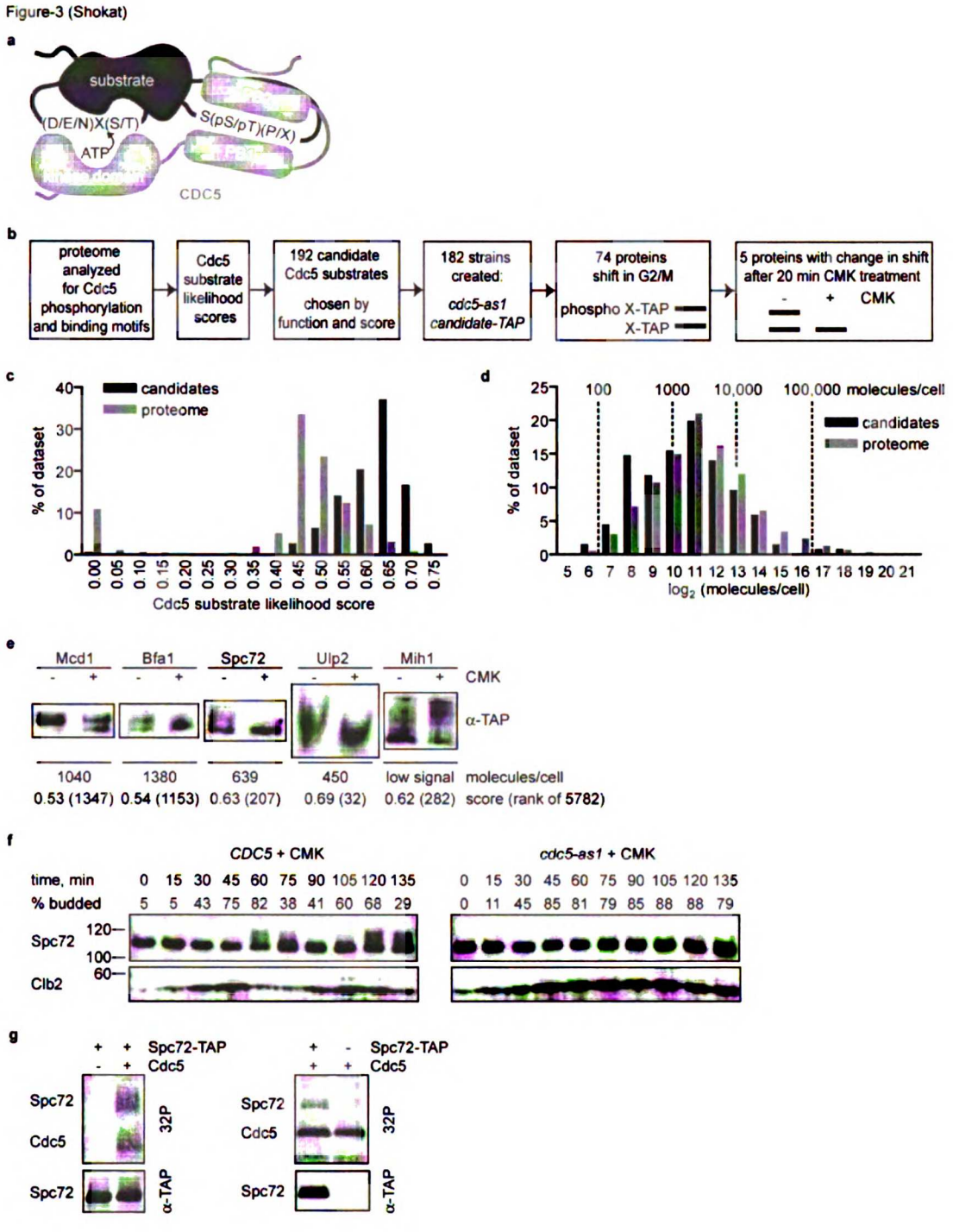

Figure 4 Spc72 binds to the Cdc5 Polo-box domain in a cell cycle and phosphospecific manner. (**a**) Cdc5 domain structure indicating the kinase domain and Polo-box domain

(PBD), and sequence alignment showing three conserved PBD residues required for phosphopeptide binding by Plk1 (highlighted in gray). The PBD* mutant contains mutations of the highlighted Cdc5 residues to the amino acids indicated for elimination of phospho-specific motif binding. (**b**) Spc72 is bound by the Cdc5 PBD, and PBD* has reduced Spc72 binding. Anti-TAP (Spc72) western blot indicates Spc72 present in the input mitotic cell extract (I) or pulled down (P) with GST-PBD (PBD) or GST-PBD* (PBD*). Total protein staining indicates the amount of GST-fusion protein in pulldown lanes (P). I = 5% input, P = pulldown. (**c**) Cdc5 preferentially binds mitotic Spc72. Wild type PBD pulldowns from mitotic cell extracts (as in **b**) or G1 phase cell extracts were probed for Spc72. (**d**) Domain structure of Spc72 including coiled-coils predicted by COILS (Lupas et al., 1991) and sites matching Cdc5 phosphorylation, (D/E/N)X(S/T), (Brar et al., 2006) and PBD binding, S(S/T), (Elia et al., 2003) minimal motifs. The best scoring PBD binding motif in Spc72 is indicated (*). (**e**) Mutation of consensus Cdc5 binding residues in Spc72 reduces binding to the PBD. PBD binding to Spc72 or Spc72(S231A,S232A) as in **b**. (**f**) SPB proteins efficiently bound to the Cdc5 PBD. Anti-TAP western blot indicates tagged SPB proteins present in the input mitotic cell extract (5%, I) or pulled down (P) with GST-PBD. Selected SPB proteins efficiently detected in the pulldown are shown, along with functional information and protein abundance (Ghaemmaghami et al., 2003).

Figure-4 (Shokat)

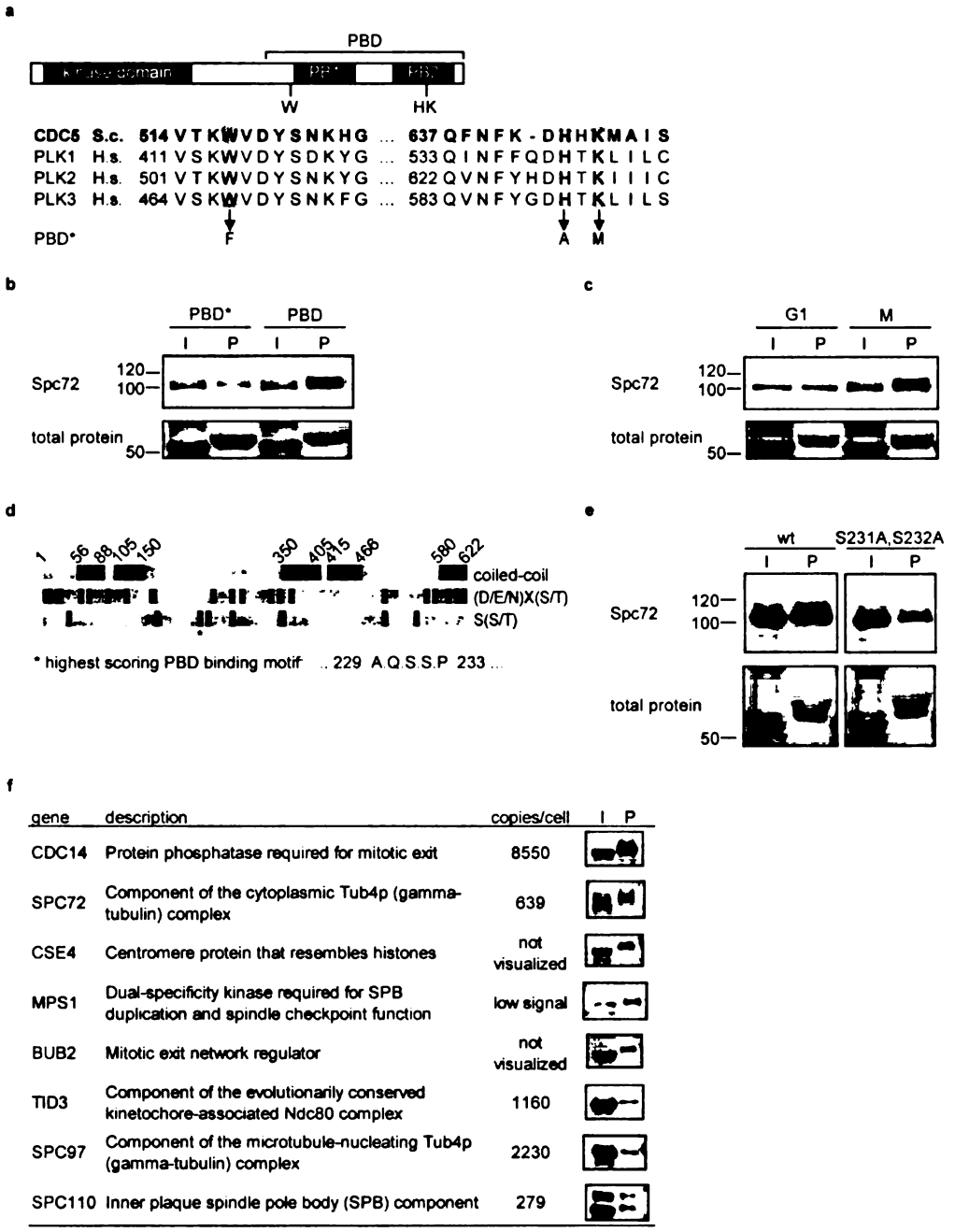

gene	description	copies/cell	I P
CDC14	Protein phosphatase required for mitotic exit	8550	
SPC72	Component of the cytoplasmic Tub4p (gamma-tubulin) complex	639	
CSE4	Centromere protein that resembles histones	not visualized	
MPS1	Dual-specificity kinase required for SPB duplication and spindle checkpoint function	low signal	
BUB2	Mitotic exit network regulator	not visualized	
TID3	Component of the evolutionarily conserved kinetochore-associated Ndc80 complex	1160	
SPC97	Component of the microtubule-nucleating Tub4p (gamma-tubulin) complex	2230	
SPC110	Inner plaque spindle pole body (SPB) component	279	

Supplementary Information, Figure 1 Additional analysis of Cdc5 sequence requirements for inhibition by CMK (**a**) Cell viability of strains grown on 10 mM CMK. Growth of strains requiring the indicated plasmid-borne CDC5 alleles for survival,

showing that both the space creating L158A mutation and a cysteine at position 96 are required in combination for inhibition by CMK. (**b**) CMK inhibition of Cdc5 alleles. cdc5-1 ts strains bearing a plasmid expressing Cdc5 or the mutant indicated was plated and 10 nmol scaffold molecule (left) or CMK (right) applied to the filter disc. CMK dependent growth inhibition of only the cdc5-L158G and cdc5-L158A cells was apparent after 3 days at restrictive temperature (37 degrees).

a

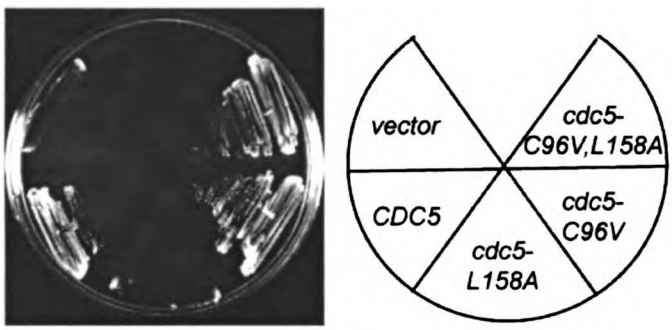

b

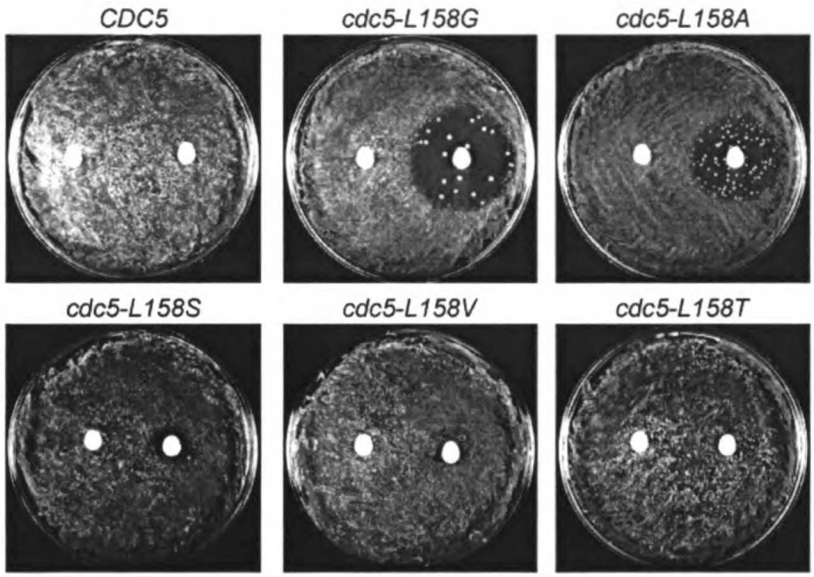

Supplementary Information, Table 1 Candidates included in the Cdc5 substrate screen. Cdc5 substrate likelihood score is shown, along with western blots. All strains constructed were examined in asynchronous, G1 arrested, and G2/M arrested cultures (asyn.,G1,G2/M). Those with a shift in G2/M were repeated without or with CMK (-,+ CMK). Gene annotations are from Saccharomyces Genome Database (1) except where otherwise referenced.

References

(1) Hong E L *et al* "Saccharomyces Genome Database" http://www.yeastgenome.org, October 2006

(2) Ghaemmaghami S *et al* Global analysis of protein expression in yeast *Nature* 425 737-741 (2003)

(3) Huh, W K *et al* Global analysis of protein localization in budding yeast *Nature* 425 686-691 (2003)

(4) Periodic genes of the yeast *Saccharomyces cerevisiae* A combined analysis of five cell cycle data sets http://www.fhcrc.org/science/labs/breeden/cellcycle/

Systematic Name	Standard Name	Cdc5 Substrate Likelihood Score	Score Rank (of 5782)	# Potential Cdc5 Phosphorylation Sites	# Potential Cdc5 PBD Binding Sites	Protein Abundance (2) (Molecules/Cell)	Molecular Weight (Da)	Description	GO Term - Biological Process	GO Term - Molecular Function	GO Term - Cellular Component	GFP localization (3)	Peak Expression (4) (0-100 from M/G1)	asyn.,G1,M	+,+ CMK
YAL012W	CYS3	0.6713	61	3	4	38,301	42,542	Cystathionine sulfur amin	cystathionine	cytoplasm		cytoplasm	36		-
YAL024C	LTE1	0.53	1262	11	36	304	163,149	Putative GDI regulation of guanyl-nuc	bud			cytoplasm	29		
YAL031C	GIP4	0.6887	33	7	18	227	86,635	Cytoplasmic chromoson	protein pho		cytoplasm	cytoplasm	61		
YAL047C	SPC72	0.6302	207	6	8	639	72,104	Component of mitotic spin	structural c	outer plaque		SPB	26		
YAR019C	CDC15	0.6519	117	11	19	238	110,283	Protein kinas	protein ami	protein kina	bud neck*	SPB	84		
YBL007C	SLA1	0.6153	291	7	18	952	135,847	Cytoskeletal	cell wall org	protein bind	actin cortical	cytoplasm/ac	36	asynch. missing	-
YBL034C	STU1	0.5617	920	14	26	521	174,176	Component of microtubule	structural c		spindle pole I	SPB	N/A		
YBL055C		0.6636	78	5	7	1,456	47,390	Hypothetical	biological p	molecular f	cytoplasm	cytoplasm	20		-
YBL066C	SEF1	0.6268	221	12	21	no strain	118,134	Putative tran	biological p	molecular f	cellular comp	none	22	strain missing	-
YBR045C	GIP1	0.5551	867	5	14	no strain	65,837	Meiosis-spec	spore wall a	protein pho	prospore mem	none	5	not seen	-
YBR059C	AKL1	0.711	14	6	31	3,005	123,989	Ser-Thr prote	actin cytosk	protein kina	cytoplasm*	budneck/cyto	14		
YBR107C	IML3	0.6291	214	2	2	125	28,086	Protein with a	sporulation	molecular f	outer kinetoc	nucleus	66	not seen	-
YBR108W		0.6536	109	7	22	no strain	92,762	Protein interv	biological p	molecular f	lipid raft	none	10		
YBR132C	AGP2	0.6995	23	2	7	no strain	67,261	High affinity p	telomere m	amino acid	endoplasmic	ER	19	not seen	-
YBR140C	IRA1	0.6424	142	27	51	no strain	350,978	GTPase-activ	sporulation	Ras GTPase	mitochondrio	cytoplasm	90	not seen	-
YBR156C	SLI15	0.5263	1329	6	15	319	79,185	Subunit of th	telomere m	protein kina	spindle micro	nucleus/mic	75	not seen	-
YBR200W	BEM1	0.5926	456	7	9	6,489	61,605	Protein conta	establishme	protein bind	bud neck*	budneck/cell	37		
YBR212W	NGR1	0.61	324	9	16	1,536	75,023	RNA binding	mitochondri	RNA bindin	cytoplasm*	cytoplasm	65		
YBR228W	SLX1	0.6219	249	1	2	no strain	35,856	Subunit of a	response to	5'-flap endo	nucleus	none	6	not seen	-
YBR274W	CHK1	0.4442	3637	2	2	2,526	60,016	DNA damage	protein ami	protein kina	nucleus	cytoplasm	43		-
YCL039W	GID7	0.7742	1	5	13	1,198	84,516	Protein of un	negative re	molecular f	cytoplasm*	cytoplasm/nu	79		-
YCR089W	CPR4	0.6479	125	2	3	low signal	35,780	Peptidyl-prol	biological p	peptidyl-pro	membrane	vacuole	70		
YDL003W	MCD1	0.5252	1347	7	4	1,041	63,290	Essential pro	mitotic sist	molecular f	nucleus*	cytoplasm/nu	55		
YDL015C	TSC13	0.5153	1534	2	4	23,597	58,320	Enoyl reducta	very-long-c	oxidoreduc	mitochondrio	cytoplasm/nu	46		
YDL101C	DUN1	0.5649	743	3	9	3,476	58,632	Cell-cycle ch	telomere m	protein kina	nucleus	nucleus	43		-
YDL178W	DLD2	0.6113	318	5	4	11,368	59,268	D-lactate deh	lactate met	actin bindi	mitochondria	mitochondric	29		

YDL194W	SNF3	0.6583	92	2	23	no strain	96.718	Plasma mem signal trans receptor ac plasma mem	none	81	not seen
YDL220C	CDC13	0.6085	334	6	19	319	104.903	Single stranc telomere m single-strar nuclear telor	cytoplasm/nu	88	
YDR004W	RAD57	0.5339	1190	6	9	238	52.247	Protein that i telomere m protein bine nucleus	cytoplasm/nu	N/A	
YDR028C	REG1	0.6222	247	13	29	2,560	112,615	Regulatory s negative re protein pho cytoplasm*	cytoplasm	21	
YDR118W	APC4	0.4442	3733	6	9	1,332	75.255	Subunit of th mitotic assi protein bine anaphase-pr	cytoplasm/nu	97	
YDR127W	ARO1	0.6781	44	12	16	6.419	174.754	Pentafunctior aromatic ar 3-dehydroc	cytoplasm	47	
YDR144C	MKC7	0.6708	62	10	27	538	64.269	GPI-anchore proteolysis aspartic-typ cell wall (sen	vacuole	N/A	
YDR146C	SWI5	0.5393	1102	6	10	688	79.774	Transcription G1-specific transcriptio	cytoplasm/nu	27	
YDR150W	NUM1	0.631	201	22	29	low signal	313,030	Protein requi nuclear mig tubulin bine	mitochondrio	punctate	58
YDR170C	SEC7	0.6364	189	18	40	3.671	226.884	Guanine nuc ER to Golg ARF guany	cytosol*	late golgi	39
YDR180W	SCC2	0.6771	45	15	29	3,313	171,100	Subunit of cc mitotic assi molecular f	nuclear cohe	nucleus	33
YDR192C	NUP42	0.7033	18	4	12	no strain	42.778	Subunit of th mRNA exp structural n	nuclear pore	none	64
YDR217C	RAD9	0.6462	131	7	20	400	148,396	DNA damage DNA repair protein bine	nucleus	cytoplasm/nu	45
YDR254W	CHL4	0.6096	328	3	2	606	52.671	Outer kinetoc chromoson DNA bindir	outer kinetoc	microtubule	63
YDR277C	MTH1	0.7218	10	4	15	low signal	49.080	Negative reg signal trans molecular f	cellular comp	none	42
YDR389C	XRS2	0.6318	194	11	19	358	98.364	Protein requi telomere m protein bine	nucleus*	cytoplasm/nu	3
YDR424C	DYN2	0	5317	0	1	1.309	10,441	Cytoplasmic microtubule microtubule	cytoplasmic r	ER	70
YDR498C	SEC20	0.5905	486	1	7	4.910	43.882	Membrane g vesicle fusi v-SNARE e	endoplasmic	ER	1
YEL007W		0.7043	17	6	21	1,708	72,533	Putative prot biological p molecular f	cytoplasm*	cytoplasm/nu	N/A
YEL042W	GDA1	0.6641	77	6	6	6.682	56.821	Guanosine d protein ami guanosine-	Golgi appara	golgi	65
YEL061C	CIN8	0.6194	261	9	21	238	117,998	Kinesin moto mitotic assi microtubule	mitochondrio	SPB/microtu	71
YER032W	FIR1	0.6333	187	16	22	low signal	98.811	Protein involv mRNA poly molecular f	bud neck	budneck	50
YER095W	RAD51	0.531	1244	2	3	6.964	42.963	Strand exche meiotic rec recombinas	nuclear chror	cytoplasm/nu	N/A
YER105C	NUP157	0.6453	134	7	20	4.422	156.647	Abundant su mRNA exp structural n	nuclear pore	nuclear peripl	39
YER106W	MAM1	0.5147	1541	3	3	no strain	35.752	Monopolin, k meiotic chr molecular f	condensed n	none	52
YER125W	RSP5	0.6208	256	10	16	no strain	91.816	Ubiquitin-pro endocytosis ubiquitin-pr	cytoplasm*	nucleus	N/A
YER130C		0.6543	107	2	11	no strain	50,319	Hypothetical biological p molecular f	cellular comp	none	35
YER132C	PMD1	0.7069	16	17	50	815	195,381	Protein with i sporulation molecular f	cytoplasm	cytoplasm	59
YER155C	BEM2	0.6231	237	20	50	1.233	245.428	Rho GTPase cell wall orig signal trans	mitochondrio	budneck/cyto	12

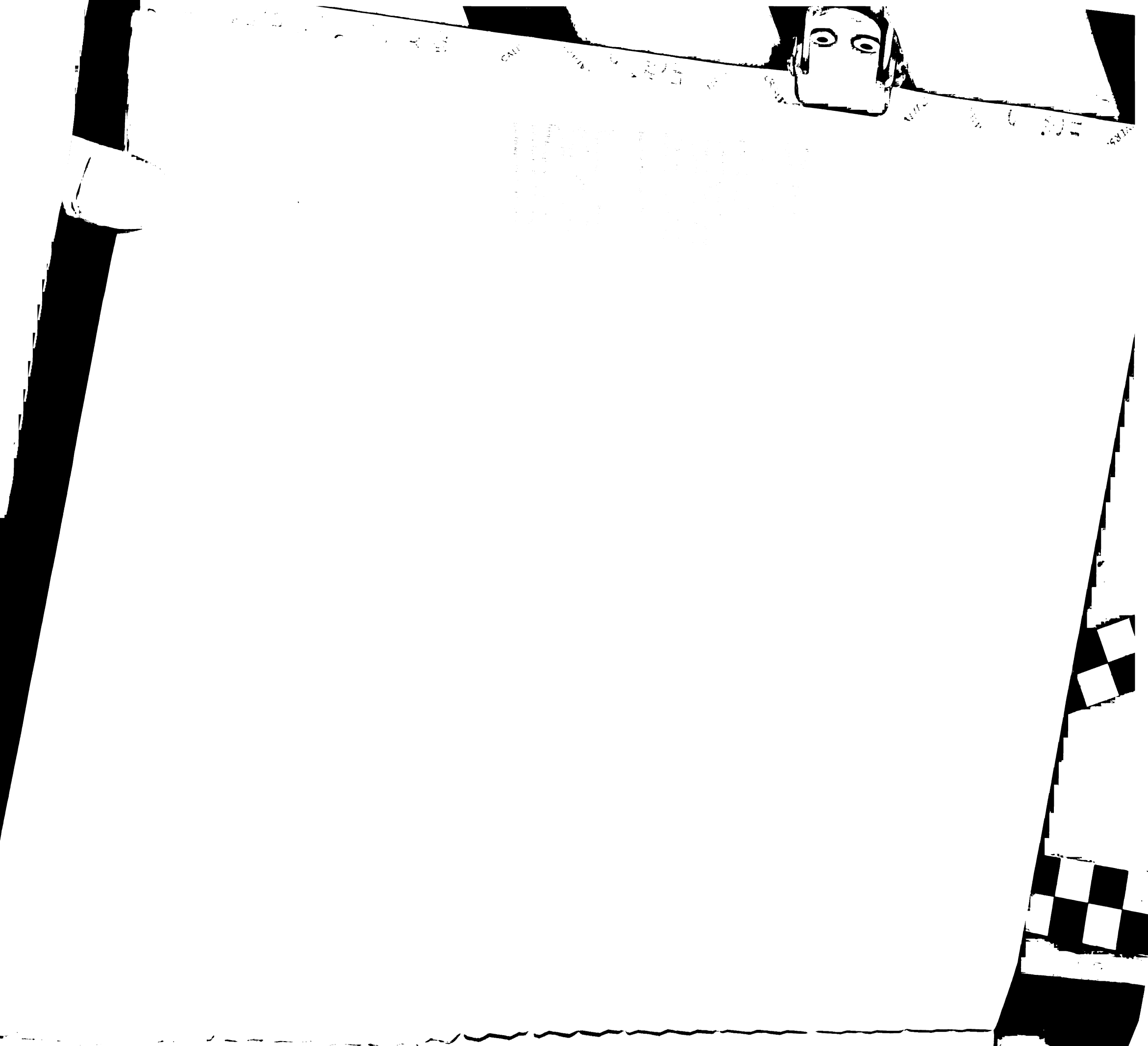

YER165W	PAB1	0.4442	3852	3	4	197.890	64.344	Poly(A) binds regulation c poly(A) bin	cytoplasm*	cytoplasm	16
YER173W	RAD24	0.6726	58	10	15	752	75,726	Checkpoint p meiotic rec DNA clamp	nucleus*	cytoplasm/nu	26
YFL024C	EPL1	0.669	65	8	15	1,112	96.737	Component c regulation t histone ace	histone acety	nucleus	70
YFL033C	RIM15	0.5865	524	14	30	low signal	196.529	Glucose-repr protein ami protein kina	cytoplasm*	cytoplasm	74
YFR022W	ROG3	0.7583	4	4	21	no strain	79.706	Protein that t biological p molecular f	cellular comp	none	17
YFR030W	MET10	0.7119	13	9	8	1.578	114.827	Subunit alph sulfate assi	sulfite redu	cytoplasm*	cytoplasm 62
YGL003C	CDH1	0.5469	995	4	14	no strain	62.821	Cell-cycle reg telomere m	enzyme ac	cytoplasm*	none N/A
YGL066W	MAD1	0.492	2465	3	6	656	87.651	Coiled-coil pr mitotic spin	molecular f	nucleus*	nucleus/perip 37
YGL092W	NUP145	0.6439	140	15	33	4.633	145,660	Essential nuc mRNA exp	structural n	nuclear pore	nucleus/perip 86
YGL094C	PAN2	0.6316	197	13	13	1.512	127.038	Essential sub poslreplica	poly(A)-spe	cytoplasm*	cytoplasm 39
YGL114W		0.5679	706	2	11	no strain	80.008	Putative mer transport	oligopeptid	membrane	none 86
YGL116W	CDC20	0.6347	176	5	11	no strain	67.359	Cell-cycle reg mitotic ass	enzyme ac	anaphase-pro	cytoplasm/nu 87
YGL137W	SEC27	0.6813	39	13	7	129.074	99.444	Essential bet ER to Golg	molecular f	COPI vesicle	golgi/ear/ygo N/A
YGL180W	ATG1	0.6964	25	8	11	1.069	101,716	Protein serin autophagy'	protein ser	cytosol	punctate 53
YGL190C	CDC55	0.5508	940	3	8	8.604	59.662	Non-essentia protein biol	protein pho	nucleus*	cytoplasm N/A
YGL201C	MCM6	0.5967	408	6	20	13.436	112.951	Protein involv DNA replic	chromatin b	cytoplasm*	cytoplasm/nu 11
YGL216W	KIP3	0.5935	451	10	14	736	91,090	Kinesin-relat mitotic spin	microtubule	cytoplasmic r	microtubule 60
YGR014W	MSB2	0.655	104	8	106	1.323	133.113	Mucin family establishm	osmosensic	integral to pla	vacuole 59
YGR056W	RSC1	0.5891	499	7	18	259	106,668	One of 15 su chromatin r	molecular f	RSC complex	cytoplasm/pu 47
YGR070W	ROM1	0.6572	95	8	24	no strain	131.391	GDP/GTP ex cell wall org	signal trans	intracellular	none 53
YGR097W	ASK10	0.6603	86	9	33	low signal	126,883	Component c response to	transcriptio	cytoplasm*	cytoplasm N/A
YGR098C	ESP1	0.519	1462	23	25	low signal	187,445	Separase wit mitotic ass	cysteine-typ	cytoplasm*	cytoplasm/nu 50
YGR143W	SKN1	0.6671	69	9	16	468	86.240	Protein involv cell wall org	glucosidase	integral to me	none 20
YGR188C	BUB1	0.5152	1536	3	17	414	117.867	Protein kinas protein ami	protein bind	nucleus*	nucleus/SPB N/A
YGR218W	CRM1	0.6604	84	9	9	7,085	124,103	Major karyop mRNA exp	protein carr	nucleus	nucleus 59
YHL007C	STE20	0.6396	150	7	23	259	102,361	Signal transc protein ami	protein ser	incipient bud	cytoplasm N/A
YHL022C	SPO11	0.5159	1523	4	2	no strain	45,412	Meiosis-spec meiotic DN	endodeoxy	nuclear chror	none N/A
YHL029C	OCA5	0.6885	34	10	18	12.532	77.756	Cytoplasmic	metabolism	molecular f	cytoplasm 30
YHL030W	ECM29	0.6917	29	16	34	2.949	210.429	Major compo protein cata	protein bind	cytoplasm*	cytoplasm/nu 78

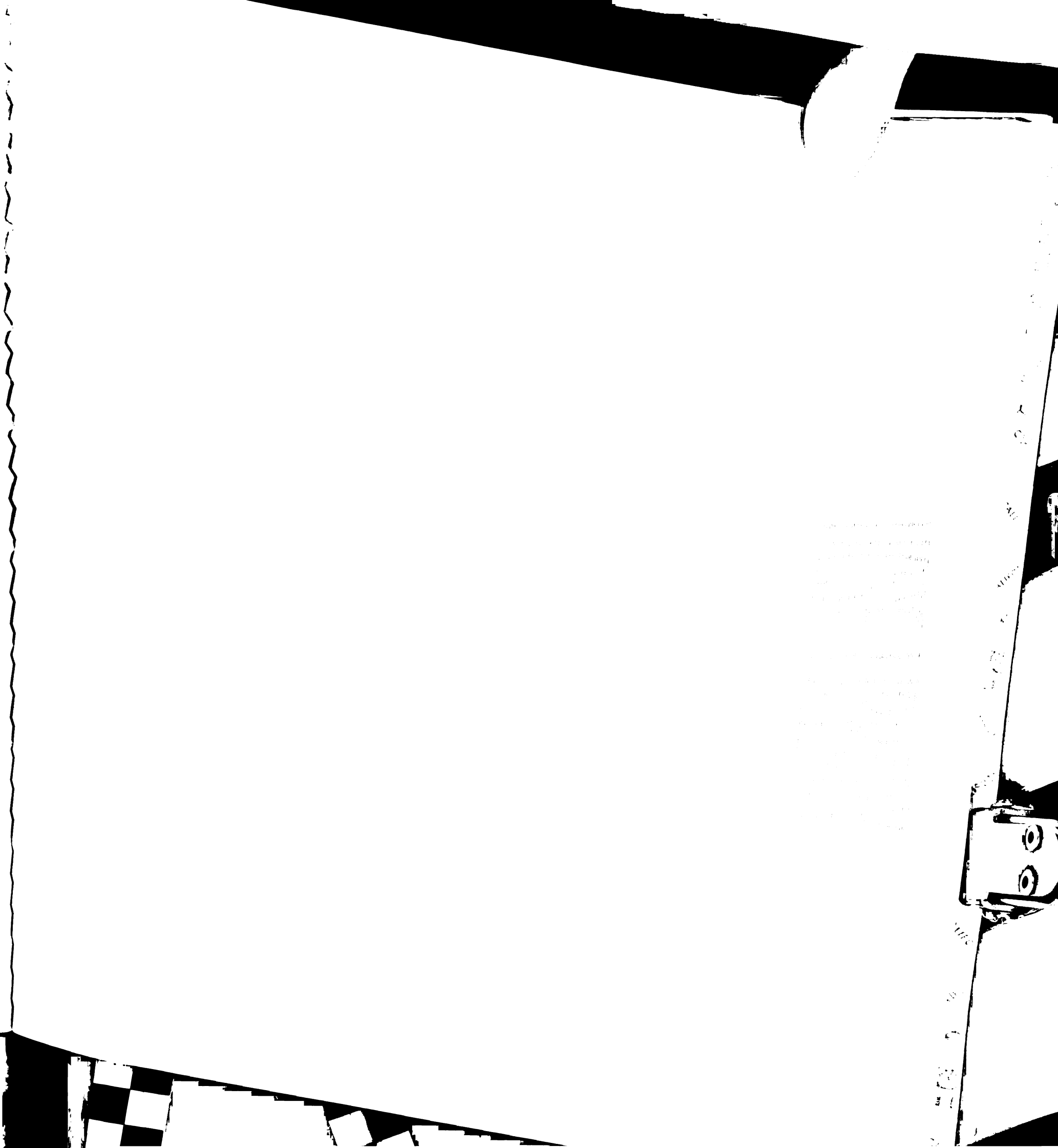

YHR014W	SPO13	0.5477	987	4	5	no strain	33.294	Meiosis-spec positive reg protein bind	nucleus*	none	60
YHR098C	SFB3	0.6663	71	10	17	12.188	103.949	Member of th ER to Golg molecular f	endoplasmic	ER to golgi	92
YHR102W	KIC1	0.6318	195	7	32	1.040	117.080	Protein kinas cell wall org kinase activ	cytoplasm*	cytoplasm	66
YHR119W	SET1	0.6303	205	7	22	172	123.911	Histone meth telomere m histone lysi	COMPASS c	nucleus	87
YHR124W	NDT80	0.5852	539	8	15	no strain	71.479	Meiosis-spec meiosis*	transcriptio nuclear chror	none	22
YHR154W	RTT107	0.6524	113	10	13	1.377	123.016	Protein impli double-stra molecular f	nucleus	nucleus	63
YHR158C	KEL1	0.6257	227	13	20	1.350	131.093	Protein requ cellular mo molecular f	cytoplasm*	bud neck/cell	76
YIL030C	SSM4	0.6655	102	8	11	technical pro	151.453	Ubiquitin-pro ER-associa ubiquitin-pr	nuclear enve	ER	25
YIL031W	ULP2	0.689	32	9	31	450	116.881	Peptidase thi mitotic spin cysteine-ty	nucleus	mitochondric	59
YIL036C	NOT3	0.6699	63	8	16	2.491	94.402	Subunit of th regulation c 3'-5'-exorib	cytoplasm*	cytoplasm	31
YIL066C	RNR3	0.4804	2625	5	9	1.364	97.514	Ribonucleotid DNA replic ribonucleot	cytoplasm*	cytoplasm	88
YIL123W	SIM1	0.6322	191	2	29	1.797	48.070	Protein of the microtubule molecular f	cell wall (sen	vacuole	20
YIL125W	KGD1	0.6587	88	10	16	14.328	114.416	Component c tricarboxyli oxoglutarat	mitochondrial	mitochondric	N/A
YIL140W	AXL2	0.6766	47	16	24	396	90.782	Integral plasi bud site se molecular f	bud neck*	bud neck/cell	56
YIL143C	SSL2	0.6966	26	8	11	825	95.340	Component c transcriptio general RN	transcription	nucleus	72
YIL153W	RRD1	0.6156	286	3	7	4.590	45.082	Activator of tl DNA repair protein pho	cytoplasm*	cytoplasm/nu	29
YJL013C	MAD3	0.457	3441	3	6	3.171	59.521	Component c mitotic spin molecular f	nucleus	cytoplasm/nu	71
YJL019W	MPS3	0.6813	40	3	10	no strain	79.174	Essential inte mitotic sista molecular f	integral to me	none	44
YJL076W	NET1	0.5923	485	12	38	1.581	128.530	Core subunit regulation c rDNA bindi	nucleolus*	nucleolus	24
YJL084C	ALY2	0.6727	57	16	28	49	117.215	Cytoplasmic biological p cyclin bindi	cytoplasm	cytoplasm	31
YJL095W	BCK1	0.645	136	19	52	112	164.194	Mitogen-activ protein ami MAP kinase	intracellular	cytoplasm	50
YJL132W		0.6636	74	4	10	no strain	84.486	Putative prot biological p molecular f	membrane fr	none	55
YJL187C	SWE1	0.7198	12	7	23	no strain	92.467	Protein kinas regulation c protein kina	nucleus*	none	N/A
YJR021C	REC107	0.5614	783	4	6	no strain	35.683	Protein involv meiotic rec molecular f	cellular comp	none	43
YJR033C	RAV1	0.7741	2	16	12	149	154.932	Subunit of th vacuolar ac molecular f	cytoplasm*	none	N/A
YJR035W	RAD26	0.6487	123	6	10	low signal	124.527	Protein involv nucleotide- DNA-depen	nucleus	cytoplasm/nu	51
YJR043C	POL32	0.6341	184	2	6	2.406	40.309	Third subunit telomere m delta DNA	nucleus*	cytoplasm/nu	N/A
YJR053W	BFA1	0.5362	1153	6	12	1.377	66.086	Component c regulation c GTPase ac	spindle pole b	SPB	48
YJR060W	CBF1	0.5771	617	3	6	6.892	39.387	Helix-loop-he chromosom DNA bindir	nucleus*	nucleus	50

YJR086W	TOR1	0.6586	90	15	27	589	261,137	PIK-related p meiosis*	protein bind plasma mem	none	71	
YJR092W	BUD4	0.5487	965	19	25	1,604	150,909	Protein invol bud site se	GTP bindin	bud neck con	budneck	18
YJR125C	ENT3	0.6764	49	4	12	no strain	45,091	Protein conta endocytosis	protein bind	actin cortical	none	36
YJR151C	DAN4	0.6669	70	9	119	no strain	118,358	Cell wall mar	biological p	molecular f	cell wall (sen	none	7
YKL052C	ASK1	0.5821	564	5	8	2,836	32,056	Essential sub	mitotic spin	structural c	condensed n	SPB	52
YKL068W	NUP100	0.6127	305	9	31	358	99,988	Subunit of th	mRNA exp	structural n	nuclear pore	nuclearpenp	57
YKL079W	SMY1	0.5525	911	11	16	1,923	73,799	Protein that i	exocytosis	motor activ	bud neck*	cytoplasm/nu	75
YKL185W	ASH1	0.6855	38	7	18	1,797	85,684	Zinc-finger in	pseudohyp	specific tra	nucleus*	nucleus	N/A
YKL195W	MIA40	0.6366	167	1	9	5,040	47,416	Essential pro	protein targ	molecular f	mitochondrio	mitochondric	89
YKL198C	PTK1	0.598	412	2	16	no strain	72,081	Putative ser/t	polyamine	protein kina	cellular comp	none	N/A
YKR054C	DYN1	0.6768	48	34	40	195	471,343	Cytoplasmic	mitotic spin	motor activ	cytoplasmic r	cytoplasm	4
YKR092C	SRP40	0.6541	108	1	56	12,938	41,015	Nucleolar se	nucleocytop	unfolded pr	nucleolus	nucleolus	8
YLR045C	STU2	0.6209	258	9	20	1,656	100,917	Microtubule-r	mitotic spin	structural c	spindle pole	SPB	81
YLR079W	SIC1	0.4642	3375	1	4	788	32,223	Inhibitor of C	G1/S transi	protein bind	cytoplasm*	cytoplasm/nu	7
YLR120C	YPS1	0.7204	11	10	19	5,436	60,009	Aspartic prot	protein pro	aspartic-typ	cell wall (sen	ER	38
YLR175W	CBF5	0.6343	182	2	7	33,649	54,704	Pseudouridir	35S primar	pseudouridi	small nucleol	nucleolus	89
YLR256W	HAP1	0.6789	46	18	40	no strain	166,106	Zinc finger tr	aerobic res	specific RN	nucleus	none	95
YLR273C	PIG1	0.5374	1132	10	11	no strain	74,145	Putative targ	regulation o	protein pho	protein phosp	none	30
YLR303W	MET17	0.6694	64	1	2	no strain	48,671	O-acetyl hom	methionine	cysteine sy	cytoplasm	none	N/A
YLR310C	CDC25	0.5986	410	16	44	319	179,090	Membrane b	regulation o	Ras guanyl	cytoplasm*	cytoplasm	90
YLR319C	BUD6	0.6586	91	13	9	2,607	88,816	Actin- and fo	actin filame	cytoskelete	actin cap*	budneck/cyt	N/A
YLR353W	BUD8	0.579	594	5	22	no strain	66,268	Protein invol	pseudohyp	molecular f	bud tip*	budneck/cell	44
YLR357W	RSC2	0.7005	22	7	10	2,325	102,299	One of 15 su	telomere m	molecular f	RSC complex	nucleus	58
YLR383W	SMC6	0.6076	340	7	9	339	128,007	Protein invol	DNA repair	molecular f	nucleus*	cytoplasm/nu	53
YML010W	SPT5	0.5782	626	5	23	2,343	115,649	Protein that f	regulation o	RNA polym	nucleus*	cytoplasm	89
YMR001C	CDC5	0.5418	1086	6	9	1,484	81,030	Polo-like kina	protein ami	protein kina	nucleus*	budneck/nuc	78
YMR032W	HOF1	0.5857	533	5	17	195	76,206	Bud neck-loc	cytokinesis	cytoskelete	bud neck con	budneck	39
YMR036C	MIH1	0.6162	282	3	17	low signal	63,357	Protein tyros	G2/M trans	protein tyro	cytoplasm*	cytoplasm/nu	71
YMR168C	CEP3	0.5152	1537	2	6	1,903	71,357	Essential kin	mitotic spin	DNA bindi	condensed n	microtubule	33

YMR190C	SGS1	0.6403	148	10	29	no strain	163,836	Nucleolar DN response ki ATP-deper nucleolus*	cytoplasm/nu	91	not seen	-
YMR198W	CIK1	0.6001	399	3	5	99	69,069	Kinesin-asso meiosis*	microtubule spindle pole f microtubule	35		
YMR261C	TPS3	0.6561	97	10	26	13,465	118,834	Regulatory s response ki enzyme req alpha,alpha-t	cytoplasm	81		
YMR273C	ZDS1	0.666	72	8	16	279	103,358	Protein that i mRNA exp protein bine	cytoplasm*	cytoplasm	N/A	-
YMR277W	FCP1	0.7075	15	5	4	6,545	83,440	Carboxy-terr transcriptio phosphopr	nucleus	nucleus	76	-
YMR301C	ATM1	0.7014	21	8	5	3,247	77,521	Mitochondria iron ion hor ATPase ac	mitochondria	mitochondric	80	-
YNL007C	SIS1	0.6304	204	1	4	20,306	37,590	Type II HSP4 protein fold unfolded pr	cytosolic ams	cytoplasm/nu	41	-
YNL012W	SPO1	0.666	73	4	10	no strain	72,186	Meiosis-spec meiosis	phospholip	nucleus	none	42
YNL048W	ALG11	0.5921	466	2	8	3,138	63,143	Alpha-1,2-ma protein ami	alpha-1,2-r	endoplasmic	ER	24
YNL056C		0.6377	159	2	12	low signal	35,046	Putative prot biological p	molecular f	vacuole (sen	vacuole	58
YNL101W	AVT4	0.5543	881	0	17	low signal	80,025	Vacuolar trar amino acid	transporter	vacuolar mer	none	N/A
YNL126W	SPC98	0.5705	681	8	10	57	98,226	Component c	mitotic spin	structural c	outer plaque	SPB/punctat 48
YNL138W	SRV2	0.7344	8	4	9	8,759	57,521	CAP (cyclase	pseudohyp	cytoskeleta	actin cortical	actin 7
YNL152W		0.6355	172	2	9	technical prc	46,225	Protein requ	biological p	phospholip	cytoplasm	cytoplasm 24
YNL154C	YCK2	0.5	2267	6	5	6,162	62,079	Palmitoylatec	protein ami	casein kina	plasma mem	cytoplasm/nu 77
YNL164C	IBD2	0.5432	1043	3	3	no strain	40,016	Component c	mitotic spin	molecular f	nucleus	cytoplasm 24
YNL166C	BNI5	0.5447	1020	2	7	no strain	49,694	Protein invol	cytokinesis	molecular f	bud neck*	budneck/cyk 91
YNL172W	APC1	0.5737	653	9	31	178	196,142	Largest subu	mitotic sele	protein bine	anaphase-pr	cytoplasm/nu 85
YNL180C	RHO5	0.6561	98	2	7	2,181	36,818	Non-essentia	Rho protei	GTPase ac	cytoplasm*	cytoplasm/nu 97
YNL188W	KAR1	0.5745	648	5	7	no strain	50,653	Essential pro	spindle pol	protein bine	half bridge of	none 79
YNL197C	WHI3	0.5688	507	7	27	5,728	71,253	RNA binding	pseudohyp	RNA bindir	cytoplasm	cytoplasm 12
YNL236W	SIN4	0.7585	3	10	14	1,720	111,296	Subunit of th	transcriptio	RNA polym	mediator com	nucleus 97
YNL267W	PIK1	0.8132	301	10	21	1,604	119,922	Phosphatidyl	sporulation	1-phosphat	nucleus*	cytoplasm N/A
YNL297C	MON2	0.6739	52	19	31	2,408	186,834	Peripheral m	endocytosis	guanyl-nuc	cytosol*	punctate/ear 51
YNR031C	BSK2	0.6462	132	12	30	217	180,526	MAP kinase	protein ami	MAP kinase	cytosol*	cytoplasm 6
YOL004W	SIN3	0.6152	292	12	21	1,662	174,838	Component c	telomere m	transcriptio	histone deac	mitochondric 14
YOL051W	GAL11	0.6462	133	4	17	606	120,308	Component c	telomere m	RNA polym	mediator com	nucleus 45
YOL081W	IRA2	0.6794	41	31	61	technical prc	351,665	GTPase-activ	Ras protei	Ras GTPas	cytoplasm*	cytoplasm 41
YOL113W	SKM1	0.638	157	4	5	238	75,331	Member of th	protein ami	protein seri	plasma mem	none 96

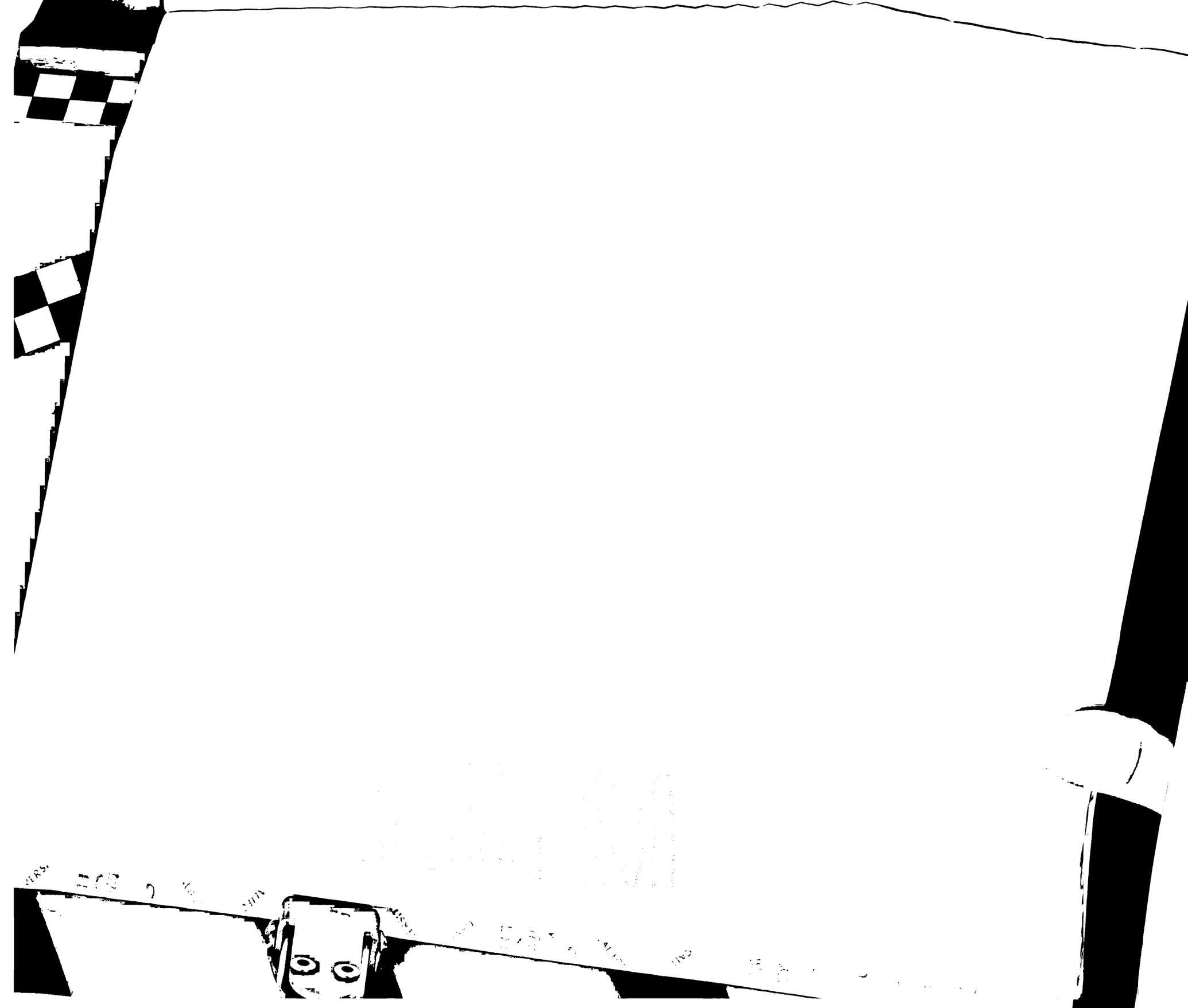

YOL148C	SPT20	0.6733	54	4	10	4.154	67.796	Subunit of th histone ace transcriptio SAGA compl	nucleus	22		
YOR008C	SLG1	0.6451	135	2	28	664	39.270	Sensor-trans cell wall org transmemb plasma mem	budneck/cyt	44		
YOR014W	RTS1	0.5937	449	3	26	300	85.334	B-type regul protein bios protein pho	cytoplasm*	cytoplasm/nu	47	
YOR026W	BUB3	0.5	2303	5	4	1.431	38.444	Kinetochore mitotic spin molecular f	condensed n	cytoplasm/nu	8	-
YOR058C	ASE1	0.4879	2528	9	18	556	101.623	Member of a mitotic spin microtubule spindle micro	microtubule	N/A		
YOR113W	AZF1	0.6861	37	11	26	556	101.169	Zinc-finger tr regulation c DNA bindir	nucleus	nucleus	77	
YOR178C	GAC1	0.5486	970	12	27	no strain	88.532	Regulatory s meiosis*	structural n protein phos	none	N/A	not seen -
YOR204W	DED1	0.6525	111	3	7	no strain	65.552	ATP-depend translational RNA helica	cytoplasm	none	24	not seen -
YOR329C	SCD5	0.6444	139	5	16	704	97.305	Protein requi endocytosis protein bin	actin cortical	none	59	
YOR348C	PUT4	0.6549	105	3	8	no strain	68.787	Proline perm proline cata	L-proline pi	plasma mem	none	97 not seen -
YPL115C	BEM3	0.675	50	17	36	752	124.912	Rho GTPase pseudohyp signal trans	intracellular	budneck/cyt	98	strain not created -
YPL153C	RAD53	0.6072	343	7	9	6.898	91.962	Protein kinas DNA repair DNA replic	nucleus	nucleus	N/A	
YPL155C	KIP2	0.5993	403	8	15	656	78.377	Kinesin-relat nuclear mig microtubule	mitochondrio	SPB/microtu	68	
YPL179W	PPQ1	0.602	380	1	17	319	61.420	Putative prot protein ami protein seri	cytoplasm	cytoplasm	23	-
YPR019W	CDC54	0.6993	24	4	18	8.803	105.002	Essential hel DNA replic chromatin b	cytoplasm*	cytoplasm/nu	83	-
YPR024W	YME1	0.6306	203	5	9	20.139	81.771	Subunit, with mitochondr ATP-depen	mitochondrio	mitochondric	74	-
YPR054W	BMK1	0.6501	119	2	5	no strain	44.300	Middle sporu protein ami MAP kinas	mitochondrio	none	22	not seen -
YPR065W	ROX1	0.6267	223	1	14	238	41.838	Heme-depen negative re specific tra	nuclear chror	nucleus	92	-
YPR111W	DBF20	0.5489	962	4	4	3.324	65.879	Ser/Thr kinas protein ami protein seri	cytoplasm	cytoplasm	5	-
YPR141C	KAR3	0.4975	2394	6	11	3.248	84.003	Minus-end-di meiosis*	microtubule spindle pole	nucleus/SPB	N/A	-
YPR159W	KRE6	0.6784	43	5	17	4.760	80.122	Protein requi cell wall org glucosidase	integral to m	vacuole	30	-

Supplementary Information, Table 2 SPB proteins examined for binding to the Cdc5 PBD. Number of potential PBD binding sites is indicated, along with western blots. Input (5% of extract) and PBD pulldown are shown (Input, Pulldown). Gene annotations are from Saccharamyces Genome Database (1) except where otherwise referenced.

References

(1) Hong, E.L., *et al.* "Saccharomyces Genome Database", http://www.yeastgenome.org. October 2006

(2) Ghaemmaghami, S. *et al.* Global analysis of protein expression in yeast. *Nature* **425**, 737-741 (2003)

(3) Huh, W.K. *et al.* Global analysis of protein localization in budding yeast. *Nature* **425**, 686-691 (2003)

(4) Periodic genes of the yeast *Saccharomyces cerevisiae*: A combined analysis of five cell cycle data sets. http://www.fhcrc.org/science/labs/breeden/cellcycle/

Systematic Name	Standard Name	# Potential Cdc6 PBD Binding Sites	Protein Abundance (2) (Molecules /Cell)	Molecular Weight (Da)	Description	GO Term - Biological Process	GO Term - Molecular Function	GO Term - Cellular Component	GFP localization (3)	Input, Pulldown
YAL016W	TPD3	6	16,900	70,906	Regulatory su	protein biosyn	protein phosp	cytoplasm*	cytoplasm,nucl	
YAL034W-A	MTW1	36	2,610	33,243	Essential con	regulation of e	guanyl-nucleo	bud	spindle pole	
YAL047C	SPC72	8	639	72,104	Component c	mitotic sister c	structural con	outer plaque	spindle pole	 
YAR019C	CDC15	19	238	110,283	Protein kinas	protein amino	protein kinase	bud neck*	ambiguous,spin	not seen
YBL034C	STU1	26	521	174,176	Component c	microtubule ni	structural con	spindle pole	ambiguous,spin	
YBL063W	KIP1	26	57	125,793	Kinesin-relate	microtubule ni	structural con	spindle pole	microtubule	
YBR107C	IML3	1	125	28,066	Protein with a	telomere mair	phosphate tra	mitochondric	nucleus,spindle	
YBR109C	CMD1	2	not visualized	16,135	Calmodulin; C	endocytosis*	protein bindin	cytoplasm*	bud neck,cell pe	not seen
YBR211C	AME1	4	1,630	37,461	Essential kine	attachment of	molecular fun	spindle pole	spindle pole	
YBR233W-A	DAD3	0	468	10,848	Essential pro	mitotic spindle	protein bindin	kinetochore*	spindle pole	
YCL029C	BIK1	3	300	51,092	Microtubule-s	mitotic spindle	microtubule b	spindle pole	spindle pole,mic	
YDL028C	MPS1	15	low signal	86,827	Dual-specifici	mitotic spindle	protein threor	spindle pole	bud neck	
YDR016C	DAD1	3	799	10,516	Essential pro	mitotic spindle	structural con	condensed n	spindle pole	
YDR130C	FIN1	0	not visualized	33,186	Basic protein	intermediate fi	molecular fun	nucleus*	cytoplasm,nucl	
YDR201W	SPC19	3	639	16,909	Component c	mitotic spindle	structural con	spindle pole	spindle pole	
YDR318W	MCM21	2	952	42,971	Protein involv	chromosome s	protein bindin	condensed n	nucleus,spindle	
YDR320C-A	DAD4	1	967	8,155	Essential pro	mitotic spindle	protein bindin	kinetochore*	spindle pole	
YDR356W	SPC110	7	279	111,781	Inner plaque	microtubule ni	structural con	central plaqu	spindle pole	 
YDR532C		5	377	44,674	Protein of unk	biological proc	molecular fun	spindle pole	ambiguous,spin	strain not available
YEL061C	CIN8	9	238	113,310	Kinesin motor	sporulation*	serine-type en	vacuole (sen	spindle pole,mic	
YER016W	BIM1	3	3,630	38,361	Microtubule-b	microtubule ni	structural con	spindle pole	microtubule	
YER018C	SPC25	1	3,280	25,244	Component c	chromosome s	structural con	condensed n	spindle pole	

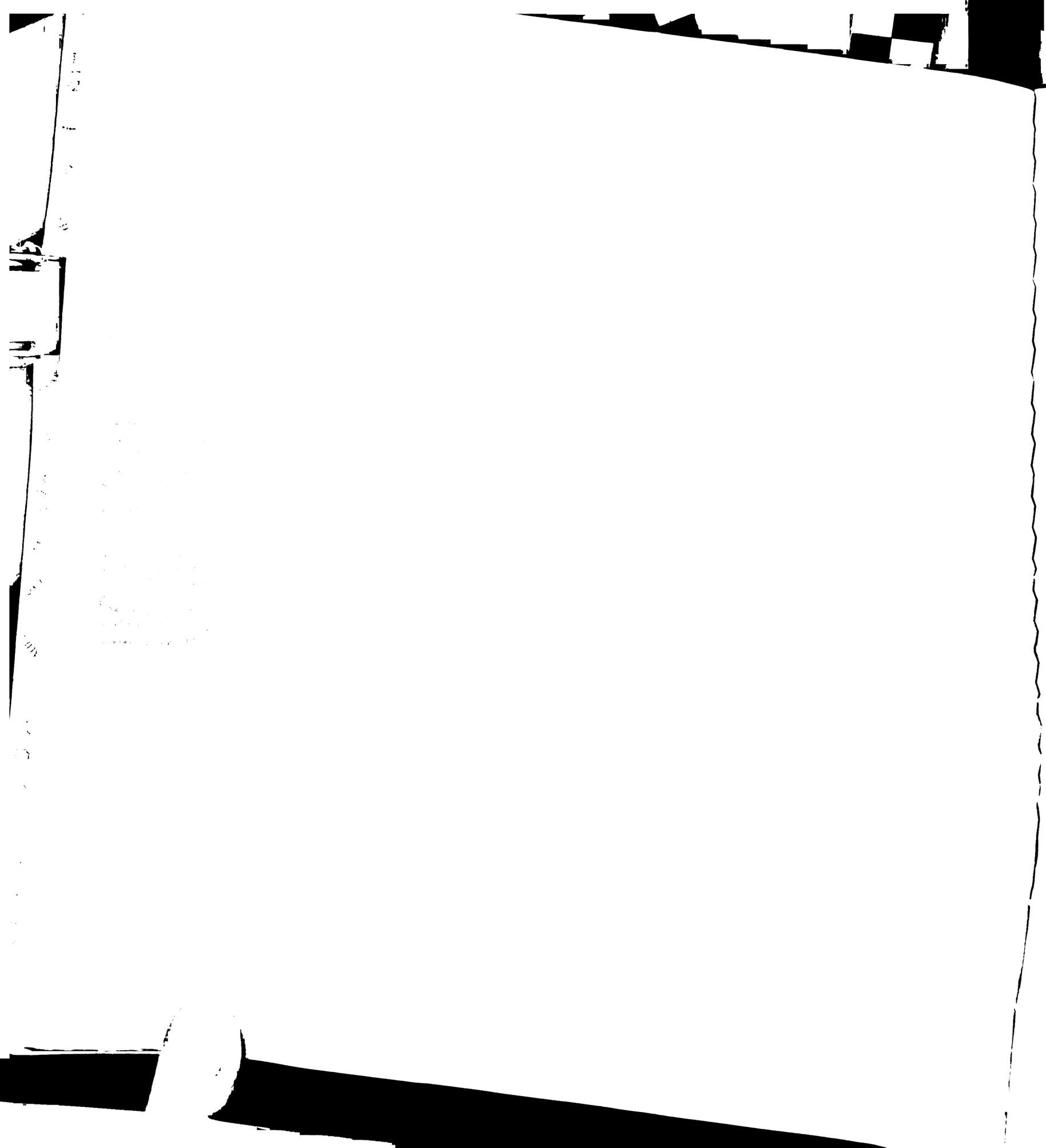

YFL037W	TUB2	5	not visualized	50,922	Beta-tubulin, mitotic sister c structural con spindle pole	none	strain not available	
YFR028C	CDC14	6	6,550	61,906	Protein phos protein amino phosphoprote nucleus*	nucleolus		
YGL061C	DUO1	5	996	27,473	Essential mit mitotic spindle structural con spindle pole	spindle pole		
YGL075C	MPS2	2	not visualized	44,585	Essential mei spindle pole b structural con nuclear enve	spindle pole		
YGL093W	SPC105	14	not visualized	104,825	Protein requir microtubule n structural con mitochondric	spindle pole	not seen	
YGL170C	SPO74	4	not visualized	47,700	Component c sporulation (s structural mol spindle pole	none	not seen	
YGR092W	DBF2	6	3,500	66,148	Ser/Thr kinas protein amino protein serine bud neck*	bud neck,cytopl		
YGR140W	CBF2	10	1,350	111,916	Essential kine chromosome : DNA bending condensed n	nucleus,spindle		
YGR179C	OKP1	6	2,690	47,349	Outer kinetoc chromosome : protein bindin condensed n	spindle pole		
YGR188C	BUB1	2	414	117,867	Protein kinas biological proc molecular fun cytoplasm	nucleus,spindle	not seen	
YHR172W	SPC97	9	2,230	96,824	Component c microtubule n structural con outer plaque	spindle pole		
YHR195W	NVJ1	7	1,900	38,421	Nuclear enve microautopha protein bindin nuclear enve	nucleus,spindle		
YIL106W	MOB1	1	5,020	35,882	Component c protein amino kinase regula bud neck*	cytoplasm,spinc		
YIL144W	TID3	11	1,160	80,487	Component c chromosome : structural con condensed n	spindle pole		
YIR010W	DSN1	7	1,310	65,692	Essential con chromosome : molecular fun kinetochore*	spindle pole		
YJL018W		19	4,510		Note: now mi biological proc molecular fun cytoplasm	spindle pole		
YJL019W	MPS3	19	not visualized	79,174	Essential inte biological proc molecular fun cytoplasm	none	not seen	
YJR053W	BFA1	5	1,380	66,086	Component c nucleotide-exc DNA binding* repairosome	spindle pole		
YJR089W	BIR1	20	not visualized	108,666	Protein involv chromosome : molecular fun mitochondric	nucleus,spindle	not seen	
YJR112W	NNF1	2	2,070	23,639	Essential con chromosome : molecular fun kinetochore*	spindle pole		
YJR135C	MCM22	3	1,030	27,587	Protein involv chromosome : protein bindin condensed n	nucleus,spindle		
YKL042W	SPC42	6	not visualized	42,271	Central plaqu microtubule n structural con central plaqu	spindle pole	not seen	
YKL049C	CSE4	5	not visualized	26,841	Centromere p mitotic sister c centromeric D kinetochore*	nucleus,spindle		
YKL052C	ASK1	7	2,840	32,056	Component c actin cytoskel molecular fun plasma mem	spindle pole		
YKL089W	MIF2	8	465	62,472	Kinetochore p chromosome : centromeric D nucleus*	spindle pole		
YKR037C	SPC34	5	echnical problem	34,077	Component c mitotic spindle structural con spindle pole	spindle pole		

YKR083C	DAD2	0	279	15,071	Essential pro	mitotic spindle	structural con	condensed n	spindle pole	
YLL003W	SFI1	11	low signal	112,978	Centrin (Cdc	G2/M transitio	molecular fun	half bridge o	spindle pole	
YLR045C	STU2	2	1,660	100,917	Microtubule-a	pyruvate meta	pyruvate deca	cytoplasm*	spindle pole	
YLR210W	CLB4	6	99	53,852	B-type cyclin	G2/M transitio	cyclin-depend	cytoplasm*	nucleus,spindle	
YLR212C	TUB4	12	7,200	52,627	Gamma-tubu	mitotic spindle	structural con	outer plaque	spindle pole	
YLR227C	ADY4	2	not visualized	57,832	Structural cor	sporulation	structural mol	spindle pole	none	not seen
YLR315W	NKP2	0	1,630	17,862	Non-essentia	biological proc	molecular fun	spindle pole	spindle pole	
YLR381W	CTF3	14	319	84,251	Outer kinetoc	chromosome s	protein bindin	condensed n	spindle pole	
YLR457C	NBP1	5	339	37,353	Component c	spindle pole b	molecular fun	nucleus*	spindle pole	
YML031W	NDC1	5	3,030	74,133	Nuclear enve	protein import	structural con	nuclear pore	nuclear periphe	
YML064C	TEM1	7	573	27,296	Gtp-binding p	regulation of e	protein bindin	spindle pole	punctate compc	
YML085C	TUB1	3	5,590	49,800	Alpha-tubulin	mitotic sister c	structural con	spindle pole	cytoplasm,punc	
YML124C	TUB3	4	12,300	49,694	Alpha-tubulin	mitotic sister c	structural con	spindle pole	cytoplasm,nucle	
YMR055C	BUB2	5	not visualized	35,027	Mitotic exit ne	regulation of e	GTPase activ	spindle pole	spindle pole	
YMR117C	SPC24	1	1,750	24,604	Component c	chromosome s	structural con	condensed n	spindle pole	
YMR198W	CIK1	1	99	69,069	CIK1 is impor	vesicle fusion	v-SNARE act	integral to G	microtubule	
YNL126W	SPC98	14	57	98,226	Component c	transport	transporter ac	mitochondric	punctate compc	slow growth - didn't screen
YNL172W	APC1	7	178	196,142	Largest subu	phosphatidylc	phosphatidyls	mitochondric	cytoplasm,nucle	
YNL188W	KAR1	2	not visualized	50,653	Essential pro	transport	molecular fun	nucleus	none	
YNL225C	CNM67	4	echnical problem	67,400	Component c	microtubule n	structural con	spindle pole	spindle pole	
YOL069W	NUF2	2	1,550	52,973	Component c	chromosome s	structural con	spindle pole	spindle pole	
YOL091W	SPO21	16	not visualized	69,876	Component c	meiosis*	structural mol	spindle pole	none	not seen
YOR014W	RTS1	2	300	85,334	B-type regula	biological proc	molecular fun	cellular com	cytoplasm,nucle	
YOR060C		3	1,690	29,557	Protein requir	biological proc	molecular fun	cytoplasm*	nucleus,spindle	
YOR073W	SGO1	19	low signal	66,706	Component c	mitotic sister c	molecular fun	nucleus*	nucleus,spindle	
YOR129C		14	768	102,249	Putative com	response to d	structural con	cytoplasm*	cytoplasm	

YOR177C	MPC54	5	low signal	54,358	Component c spore wall ass	structural mo	spindle pole	none	not seen
YOR195W	SLK19	12	314	95,380	Kinetochore-i meiosis*	molecular fun	condensed n	spindle pole	
YOR257W	CDC31	1	not visualized	18,751	Component c microtubule ni	structural con	nuclear pore	none	not seen
YOR373W	NUD1	15	892	94,103	Component c microtubule ni	structural con	spindle pole	spindle pole	
YPL018W	CTF19	3	1,250	42,782	Outer kinetoc chromosome :	protein bindin	nucleus*	ambiguous,spin	
YPL124W	SPC29	8	not visualized	29,280	Inner plaque	microtubule ni	structural con	central plaqu	spindle pole	
YPL155C	KIP2	2	656	78,377	Kinesin-relate	sporulation*	endopeptidas	mitochondric	spindle pole,mic	
YPL174C	NIP100	8	238	100,289	Large subunit	establishment	protein bindin	spindle pole	none	
YPL233W	NSL1	1	3,710	25,416	Essential con	chromosome	molecular fun	kinetochore*	spindle pole	
YPL253C	VIK1	4	not visualized	75,729	Protein that f	mitotic sister c	microtubule n	spindle pole	none	
YPL255W	BBP1	3	922	45,384	Protein requir	microtubule ni	structural con	spindle pole	spindle pole	
YPL269W	KAR9	7	656	74,244	Karyogamy p	nuclear migra	molecular fun	mating proje	ambiguous,spin	
YPR119W	CLB2	7	339	58,246	B-type cyclin	G2/M transitio	cyclin-depend	cytoplasm*	ambiguous,nucl	slow growth - didn't screen
YPR141C	KAR3	3	3,250	84,003	Minus-end-di	phospholipid t	acyltransferas	mitochondric	nucleus,spindle	
YPR174C		3	3,420	25,411	Protein of unk	biological proc	molecular fun	nuclear enve	nuclear periphe	

Appendix

Appendix 1: Plasmids

name	published as	old name	plasmid	Sequencing Status	sequencing info	Created by
AB1254		pRS1254	pRS426 GAL TAP			Erin O'Shea
DR1			pRS426-GALTAPCdc5	full	T431C(cdc5L20S), A1299G(silent), A2168G(silent)	Dave R. - Morgan lab
JP100			pRS426 cdc15-L99A (from SJ10)	full		Jennifer Paulson
JP101			pRS426 cdc15 HA-L99A (from SJ14)	full		Jennifer Paulson
JP102			pRS426 cdc15 HA-L99G (from SJ14)	full		Jennifer Paulson
JP103			pRS426 cdc15 HA3-L99G (from SJ21)	full		Jennifer Paulson
JP104			Ycplac111 GAL HA PLK K82M L130G			Jennifer Paulson
JP105			Ycplac111 GAL HA PLK K82M L130A			Jennifer Paulson
JP106			Ycplac111 GAL HA PLK L130G			Jennifer Paulson
JP107			Ycplac111 GAL HA PLK L130A			Jennifer Paulson
JP108			Ycplac111 GAL HA PLK W414F L130G			Jennifer Paulson
JP109			Ycplac111 GAL HA PLK W414F L130A			Jennifer Paulson
JP110			Ycplac111 GAL HA EGFP PLK L130G			Jennifer Paulson
JP111			Ycplac111 GAL HA EGFP PLK L130A			Jennifer Paulson
JP112			Ycplac111 GAL HA EGFPx3 PLK L130G			Jennifer Paulson
JP113			Ycplac111 GAL HA EGFPx3 PLK L130A			Jennifer Paulson
JP114			pRS426 cdc15 HA3 L99A (from SJ21)	region		Jennifer Paulson
JP115			PRS304 gal cdc15 HA L99A (from SJ26)	region		Jennifer Paulson
JP115			PRS304 gal cdc15 HA L99A (from SJ26)			Jennifer Paulson
JP116			pRS306 gal cdc15 myc12 L99G (from SJ35)	region		Jennifer Paulson
JP116			pRS306 gal cdc15 myc12 L99G (from SJ35)			Jennifer Paulson
JP117			pRS306 gal cdc15 myc12 L99A (from SJ35)	region		Jennifer Paulson
JP117			pRS306 gal cdc15 myc12 L99A (from SJ35)			Jennifer Paulson
JP118			pRS306 gal cdc15 6His L99G (from SJ39)	region		Jennifer Paulson
JP118			pRS306 gal cdc15 6His L99G (from SJ39)			Jennifer Paulson
JP119			pRS306 gal cdc15 6His L99A (from SJ39)	region		Jennifer Paulson
JP119			pRS306 gal cdc15 6His L99A (from SJ39)			Jennifer Paulson
JP120		SJ55-G1	YCplac111-HA3-DBF2(M254G)		A1598G(D533G) from parent	Jennifer Paulson
JP121		SJ55-G2	YCplac111-HA3-DBF2(M254G)		A1598G(D533G) from parent	Jennifer Paulson
JP122		SJ55A	YCplac111-HA3-DBF2(M254A)		A1598G(D533G) from parent	Jennifer Paulson
JP123		SJ57G	pRS426-HA3-DBF2(M254G)		A1598G(D533G) from	Jennifer

					parent	Paulson
JP124		SJ57A1	pRS426-HA3-DBF2(M254A)		A1598G(D533G) from parent	Jennifer Paulson
JP125		SJ57A2	pRS426-HA3-DBF2(M254A)		A1598G(D533G) from parent	Jennifer Paulson
JP126			PRS315 CDC5 L158G L157V (from p012)			Jennifer Paulson
JP127			PRS315 CDC5 L158G L157I (from p012)			Jennifer Paulson
JP160			pRS306/Dbf2		391-1612, 1644-2615 - C908T(H114Y) from genomic PCR - dbf2 coding from 569-2287	Jennifer Paulson
JP164		(DBF2 - 456,+427)	pRS316/Dbf2 cloned in as SacI/XhoI insert		398-1615, 1647-2611 - C908T(H114Y) from genomic PCR - dbf2 coding from 569-2287	Jennifer Paulson
JP168			pRS426/Dbf2		390-1612, 1756-2613 - C908T(H114Y) from genomic PCR - dbf2 coding from 569-2287	Jennifer Paulson
JP176		CV2	PRS315 CDC5 L158G C96V (from p012)		– not fully sequenced	Jennifer Paulson
JP177		Mob1-2a	pRS426-GALMob1TAP (genomic Mob1 cloned into pRS1254)	full	1-942	Jennifer Paulson
JP178		Mob1-5a	pRS426-GALMob1TAP (genomic Mob1 cloned into pRS1254)	full	1-942	Jennifer Paulson
JP179		DR1-A2	pRS426-GALTAPCdc5L158A	full	366-2487 (cdc5 coding from 373-2487) T431C(cdc5L20S), A1299G(sil), A2168G(sil)-all in parent	Jennifer Paulson
JP180		DR1-A3	pRS426-GALTAPCdc5L158A	full	339-2487 (cdc5 coding from 373-2487) T431C(cdc5L20S), A1299G(sil), A2168G(sil)-all in parent	Jennifer Paulson
JP181		DR1-G12	pRS426-GALTAPCdc5L158G	full	363-2487 (cdc5 coding from 373-2487) T431C(cdc5L20S), A1299G(sil), A2168G(sil)-all in parent	Jennifer Paulson
JP182		DR1-G13	pRS426-GALTAPCdc5L158G	full	363-2487 (cdc5 coding from 373-2487) T431C(cdc5L20S), A1299G(sil), A2168G(sil)-all in parent	Jennifer Paulson
JP183		p012L158Tb	pRS315-CDC5 L158T	full		Jennifer Paulson
JP184		p012C96V1	pRS315-CDC5 C96V	full		Jennifer Paulson
JP185		p012C96V1L158A1	pRS315-CDC5 C96V L158A	full		Jennifer Paulson
JP186		p012L158V1	pRS315-CDC5 L158V	full		Jennifer Paulson
JP187		p012L158V2	pRS315-CDC5 L158V	full		Jennifer Paulson
JP188		p012L15	pRS315-CDC5 L158S	245-796		Jennifer

		8S				Paulson
JP189		p012C96 V1L158V 2	pRS315-CDC5 C96V L158V	1-1760		Jennifer Paulson
JP190	pFastBac-CDC5		pFastBacHT A-CDC5			Dave R. - Morgan lab
JP191			pFastBacHT A-CDC5 C96V			Dave R. - Morgan lab
JP192		1	pFastBacHT A-CDC5 L158G	full		Jennifer Paulson
JP194		6B	pFastBacHT A-CDC5 C96V L158G	full		Jennifer Paulson
JP195		10A	pFastBacHT A-CDC5 C96V L158A	full		Jennifer Paulson
JP196		8A	pRS315-CDC5 C96V L158G	full		Jennifer Paulson
JP197		JP164-A1(gly)	pRS316-Dbf2M254G	region (C Zhang)	614-1049	Jennifer Paulson
JP199		JP164-A3(gly)	pRS316-Dbf2M254G	region (C Zhang)	614-1052	Jennifer Paulson
JP200		JP164-G1(ala)	pRS316-Dbf2M254A	region (C Zhang)		Jennifer Paulson
JP201		JP164-G2(ala) MA2	pRS316-Dbf2M254A	full (C Zhang)		Jennifer Paulson
JP202		JP172-SJ09 #3	PRS426-GAL-CDC15TAP	region	540-899, made by cloning from SJ09 to remove mutation in JP172	Jennifer Paulson
JP203		new 9C	pFastBacHT A-CDC5 L158A	full		Jennifer Paulson
JP204		new 9D	pFastBacHT A-CDC5 L158A	full		Jennifer Paulson
JP205		new 9E	pFastBacHT A-CDC5 L158A	full		Jennifer Paulson
JP206		9-14-04 1E	PRS426-GAL-CDC15TAP L99G	full		Jennifer Paulson
JP207		9-14-04 2C	PRS426-GAL-CDC15TAP L99A	full		Jennifer Paulson
JP208		AVMA1	pRS316-Dbf2 A253VM254A	region (C Zhang)		Jennifer Paulson
JP209		LIMA1	pRS316-Dbf2 L205IM254A	region (C Zhang)		Jennifer Paulson
JP210		CVMA3	pRS316-Dbf2 C203VM254A	full (C Zhang)		Jennifer Paulson
JP211		WHK-1	pFastBacHT A-CDC5 L158G,W517F,H641A, K643M	site	910-2232 (ends at 2118)	Jennifer Paulson
JP212	pSPC72	F2B3 2-7-06	pRS426-GAL-SPC72TAP (1-622)	full	T905A (I302N), T113C-silent	Jennifer Paulson
JP213		3A 1-12-06	pRS426-GAL-SPC72TAP 1-115	full		Jennifer Paulson
JP214		4A 1-13-06	pRS426-GAL-SPC72TAP 1-267	full		Jennifer Paulson
JP215		5B 1-13-06	pRS426-GAL-SPC72TAP 99-267	full		Jennifer Paulson
JP216		7A 1-17-06	pRS426-GAL-SPC72TAP 99-622	full	T905A (I302N), T113C-silent	Jennifer Paulson
JP217		8B 1-17-06	pRS426-GAL-SPC72TAP 231-622	full	T905A (I302N), T113C-silent	Jennifer Paulson
JP218		9B 1-13-06	pRS426-GAL-SPC72TAP 345-622	full	T1113C-silent	Jennifer Paulson
JP219		10B 1-12-06	pRS426-GAL-SPC72TAP 433-622	full		Jennifer Paulson
JP220		11A 1-12-06	pRS426-GAL-SPC72TAP 477-622	full		Jennifer Paulson
JP221		1B	pRS426-GAL-SPC72TAP S48A FspI	full	T905A (I302N),	Jennifer

					T113C-silent	Paulson
JP222		2A	pRS426-GAL-SPC72TAP S47AS48A FspI	full	T905A (I302N), T113C-silent	Jennifer Paulson
JP223		3A	pRS426-GAL-SPC72TAP S232A BanI	full	T905A (I302N), T113C-silent	Jennifer Paulson
JP224	pSPC72-AA	4A	pRS426-GAL-SPC72TAP S231AS232A BanI	full	T905A (I302N), T113C-silent	Jennifer Paulson
JP225		5B	pRS426-GAL-SPC72TAP T277A HindIII	full	T905A (I302N), T113C-silent	Jennifer Paulson
JP226		6A	pRS426-GAL-SPC72TAP S276AT277AS278A PvuII	full	T905A (I302N), T113C-silent	Jennifer Paulson
JP227		MS p40	pHA3-k.l.URA3			Matt Sullivan (DOM)
JP228			pRS426-GAL-SPC72TAP S187A S188A SacII		T905A (I302N), T113C-silent	Jennifer Paulson
JP229		2A 5-25-06	pRS426-GAL-SPC72TAP S188A PvuII	full	T905A (I302N), T113C-silent	Jennifer Paulson
JP230			pRS426-GAL-SPC72TAP S188A SnaBI		T905A (I302N), T113C-silent	Jennifer Paulson
JP231		4G 5-26-06	pRS426-GAL-SPC72TAP S245AS246A SacII	full	T905A (I302N), T113C-silent	Jennifer Paulson
JP232		5B 5-26-06	pRS426-GAL-SPC72TAP S245A AvaI	full	T905A (I302N), T113C-silent	Jennifer Paulson
JP233		7F 6-1-06	pRS426-GAL-SPC72TAP S348A S349A NheI	full	T905A (I302N), T113C-silent	Jennifer Paulson
JP234			pRS426-GAL-SPC72TAP S349A S350A EagI		T905A (I302N), T113C-silent	Jennifer Paulson
JP235		9A 5-25-06	pRS426-GAL-SPC72TAP S349A NheI	full	T905A (I302N), T113C-silent	Jennifer Paulson
JP236		10A 5-25-06	pRS426-GAL-SPC72TAP S350A EagI	full	T905A (I302N), T113C-silent	Jennifer Paulson
JP237			pRS426-GAL-SPC72TAP S496A S497A MfeI		T905A (I302N), T113C-silent	Jennifer Paulson
JP238		12C 5-25-06	pRS426-GAL-SPC72TAP S497A MfeI	full	T905A (I302N), T113C-silent	Jennifer Paulson
JP239			pRS426-GAL-SPC72TAP S545A S546A BclI		T905A (I302N), T113C-silent	Jennifer Paulson
JP240			pRS426-GAL-SPC72TAP S546A BclI		T905A (I302N), T113C-silent	Jennifer Paulson
JP241		1A 6-3-06	pRS426-GAL-SPC72TAP (1-347)	full	T905A (I302N), T113C-silent	Jennifer Paulson
JP242		2A 6-3-06	pRS426-GAL-SPC72TAP (1-413)	full	T905A (I302N), T113C-silent	Jennifer Paulson
JP243		3A 6-3-06	pRS426-GAL-SPC72TAP (1-468)	full	T905A (I302N), T113C-silent	Jennifer Paulson
JP244		4A 6-3-06	pRS426-GAL-SPC72TAP (1-477)	full	T905A (I302N), T113C-silent	Jennifer Paulson
JP245		5A 6-3-06	pRS426-GAL-SPC72TAP (1-578)	full	T905A (I302N), T113C-silent	Jennifer Paulson
JP246		7A 6-3-06	pRS426-GAL-SPC72TAP (99-347)	full	T905A (I302N), T113C-silent	Jennifer Paulson
JP247		8A 6-3-06	pRS426-GAL-SPC72TAP (99-413)	full	T905A (I302N), T113C-silent	Jennifer Paulson
JP248		9B 6-3-06	pRS426-GAL-SPC72TAP (99-468)	full	T905A (I302N), T113C-silent	Jennifer Paulson
JP249		10A 6-3-06	pRS426-GAL-SPC72TAP (99-477)	full	T905A (I302N), T113C-silent	Jennifer Paulson
JP250		11A 6-3-06	pRS426-GAL-SPC72TAP (99-578)	full	T905A (I302N), T113C-silent	Jennifer Paulson
JP251		13A 6-3-06	pRS426-GAL-SPC72TAP (152-347)	full	T905A (I302N), T113C-silent	Jennifer Paulson
JP252		14A 6-3-06	pRS426-GAL-SPC72TAP (152-413)	full	T905A (I302N), T113C-silent	Jennifer Paulson
JP253		15A 6-3-06	pRS426-GAL-SPC72TAP (152-468)	full	T905A (I302N), T113C-silent	Jennifer Paulson

JP254		16A 6-3-06	pRS426-GAL-SPC72TAP (152-477)	full	T905A (I302N), T113C-silent	Jennifer Paulson
JP255		17A 6-3-06	pRS426-GAL-SPC72TAP (152-578)	full	T905A (I302N), T113C-silent	Jennifer Paulson
JP256		18C 6-6-06	pRS426-GAL-SPC72TAP (152-622)	full	T905A (I302N), T113C-silent	Jennifer Paulson
JP257		19A 6-3-06	pRS426-GAL-SPC72TAP (468-622)	full	T905A (I302N), T113C-silent	Jennifer Paulson
JP258		1 6-25-06	pRS314-CDC5pr-CDC5 W517F H641A K643M	604-2118(end)	A911G, GG1550/1TT, A1797G, CA1921/2GC, AA1928/9TG	Jennifer Paulson
JP259		2 6-25-06	pRS314-CDC5pr-CDC5 W517F H641A K643M	604-2118(end)		Jennifer Paulson
JP260		315-WHK#1	pRS315-CDC5pr-CDC5 W517F H641A K643M	1-2118(end)		Jennifer Paulson
KL117	p315-cdc5-as1		cdc5-L158G PO12 parent			Kristi Lieberman
KL121	p306-cdc5-as1		cdc5-L158G PO34 parent			Kristi Lieberman
KL138			cdc-L158A PO12 parent			Kristi Lieberman
KL142			cdc5-L158A PO34 parent			Kristi Lieberman
KL145			pRS416 cdc15-L99A	full		Kristi Lieberman
KL150			pRS416 cdc15-L99G	full		Kristi Lieberman
KL155			cdc5-F211L PO12 parent			Kristi Lieberman
KL160+1			cdc5-F211L PO34 parent (not fully sequenced)			Kristi Lieberman
KL167+8			cdc5-L158G,F211L KL121 parent (not fully sequenced)			Kristi Lieberman
KL171			cdc5-L158A,F211L KL138 parent			Kristi Lieberman
KL178		p012-314	pRS314-CDC5	full		Kristi Lieberman
KL178-189			cdc5 inserts in pRS314 back bone - unsequenced			Kristi Lieberman
KL182		pKL138-314	pRS314-CDC5 L158A	1-389,641-2118(end)		Kristi Lieberman
KL202			Ycplac111 GAL			Kyung Lee
KL205			pRS306 CDC15 (use Bgl II for integration)			Kristi Lieberman
KL208			pRS306 cdc15-L99A			Kristi Lieberman
KL214			pRS306 cdc15-L99G			Kristi Lieberman
KL259			Ycplac111 GAL HA PLK K82M			Kyung Lee
KL261			Ycplac111 GAL HA PLK			Kyung Lee
KL408			Ycplac111 GAL HA PLK W414F			Kyung Lee
KL561			Ycplac111 GAL HA EGFP PLK			Kyung Lee
KL727			Ycplac111 GAL HA EGFPx3 PLK			Kyung Lee
KT127			pFA6a-link-yEGFP-Kan			Kurt Thorn Yeast 2004;21:661-670.
KT128			pFA6a-link-yEGFP-SpHIS5			Kurt Thorn Yeast 2004;21:661-670.
KT146			pFA6a-link-tdimer2-SpHIS5			Kurt Thorn Yeast

						2004;21:661-670.
KT176			pFA6a-link-tdimer2-CaURA3			Kurt Thorn Yeast 2004;21:661-670.
KT178			pFA6a-link-tdimer2-Kan			Kurt Thorn Yeast 2004;21:661-670.
KT209			pFA6a-link-yEGFP-CaURA3			Kurt Thorn Yeast 2004;21:661-670.
PO12	p315-CDC5		pCDC5 – 315 (CDC5 -456,+427)			Morgan lab
PO34	p306-CDC5		pHA3CDC5 – 306 (use HpaI for integration)			Morgan lab
see D.R	pGST-PBD		pGEX-PBD			Dave R. - Morgan lab
see D.R	pGST-PBD*		pGEX-PBD(W517F,H641A,K643M)			Dave R. - Morgan lab
SJ09			pRS416-CDC15 -406,+714 (genomic PvuII fragment)		has all mutations found in genomic sequence by Kristi on 6-29-00	Morgan lab
SJ10			pRS426 cdc15			Morgan lab
SJ14			pRS426 cdc15HA			Morgan lab
SJ21			pRS426 cdc15HA3			Morgan lab
SJ26			pRS304galcdc15HA			Morgan lab
SJ35			pRS306galcdc15myc12			Morgan lab
SJ39			pRS306galcdc15-6His			Morgan lab
SJ55			YCplac111-HA3-DBF2		?A1598G(D533G)	Morgan lab
SJ56			pRS406-HA3-DBF2		?A1598G(D533G)	Morgan lab
SJ57			pRS426-HA3-DBF2		A1598G(D533G)	Morgan lab

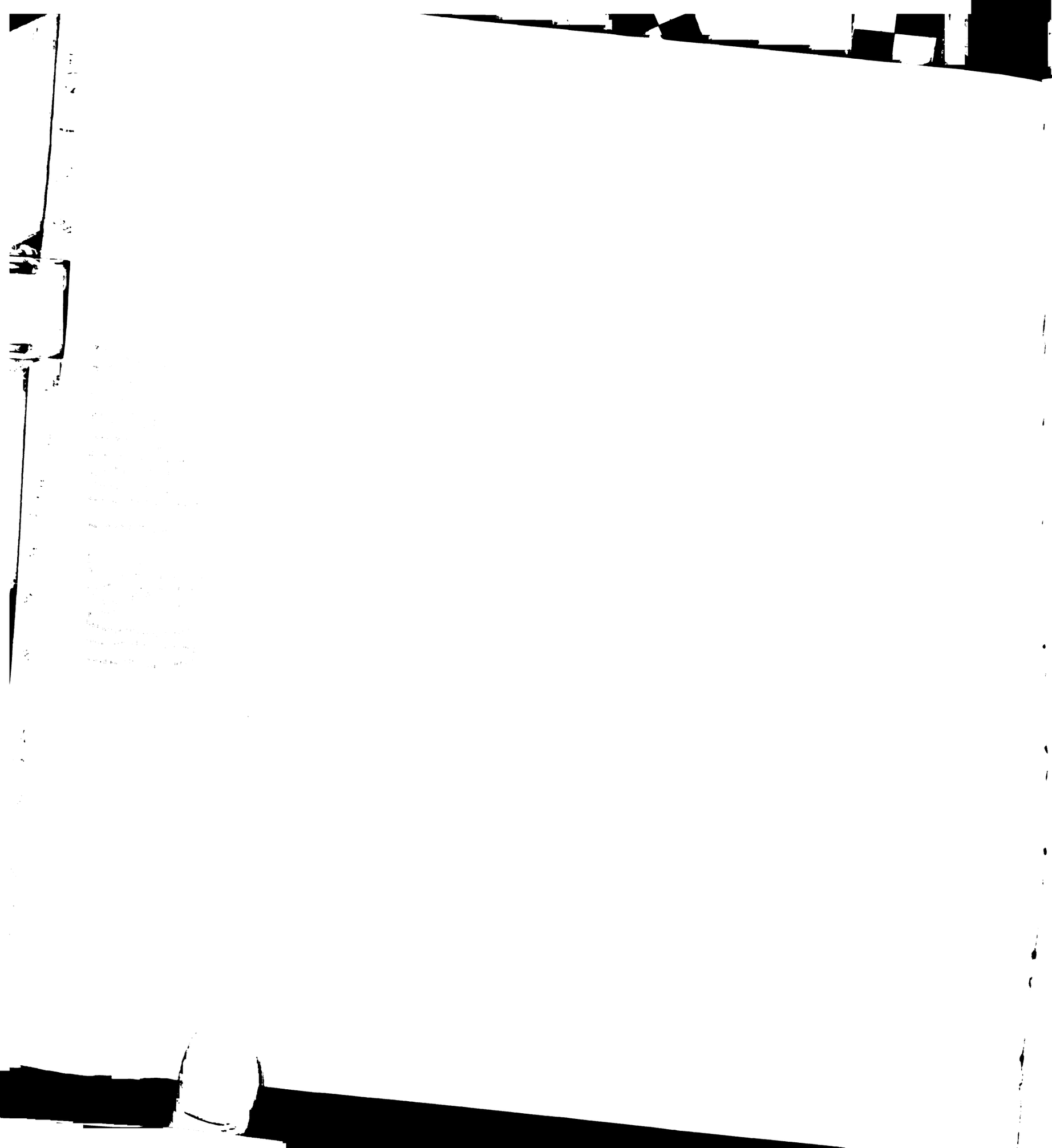

Appendix 2: Yeast strains

name	other name	lab	genotype
KLY1597		Kyung Lee	mata 969 cdc5::KanMX6 TUB1-GFP::LEU2 + Ycplac33-cdc5
KLY2372		Kyung Lee	mata W303 cdc5::KanMX6 TUB1-GFP::LEU2 + Ycplac33-cdc5
KLY1685		Kyung Lee	mata 969 cdc5::KanMX6 TUB1-GFP::LEU2 + Ycplac33-GAL1-EGFP-cdc5-1
KLY1687		Kyung Lee	mata 969 cdc5::KanMX6 TUB1-GFP::LEU2 + Ycplac33- GAL1-EGFP-PLK1
KLY969		Kyung Lee	mata leu2-3,112 trp1-289 ura3-5
AFS34		Morgan	
AFS35		Morgan	
604a		Morgan	
605alpha		Morgan	
AFS92		Morgan	W303(ura3-1, trp1-1, leu2-3,112, his3-11, ade2-1, can1-100), GAL+, bar1::hisG, MATa *Aaron Straight
SLJ443		Morgan	
JC34	SLJ296	Morgan	cdc5-1, bar-, mata
JC398		Morgan	W303, mat alpha, cdc5::URA4, his3::GALCDC5::HIS3, ura3::URA3::tetO, leu2::LEU2::tetRGFP
JAU05		Morgan	cdc28-as1 (F88G)
SLJ127		Morgan	cdc15-2
SLJ250		Morgan	cdc14-1
SLJ251		Morgan	dbf2-2
SLJ252		Morgan	
DOM274		Morgan	mat a, bar1D::hisg, trp1::256x LacO::TRP1, his3::Cup1-GFP-LacI::His3
DOM31		Morgan	mat alpha, cdc28-F88G
YM317		O'Shea	S288c, Gal overexpression strain Δhis3::pGAL10::GAL4; ura; leu; trp; prb1-1122; pep4-1
EY1261		O'Shea	mat alpha, can1Δ::MFA1pr-LEU2
KT621		K. Thorn	ykt621 = JLP32 TUB1-yECit::Hygro
KT622		K. Thorn	ykt622 = JLP38 TUB1-yECit::Hygro
KT624		K. Thorn	ykt624 = JLP01 TUB1-yECit::Hygro
KT626		K. Thorn	ykt626 = JYL69 TUB1-yECit::Hygro (MATa ura3-1 ADE2+ his3-11,15 leu2-3,112 trp1-1 can1-100)
JLP01		Shokat	AFS92 bkgd, CDC15-as1 (L99G) mat a
JLP02		Shokat	AFS92 bkgd, CDC15-as1 (L99G) mat a
JLP03		Shokat	AFS92 bkgd, CDC15-as1 (L99G) mat a
JLP04		Shokat	AFS92 bkgd, CDC15-as1 (L99G) mat a
JLP05		Shokat	SLF250 bkgd (cdc14-1), CDC15-as1 (L99G) mat a
JLP06		Shokat	SLF250 bkgd (cdc14-1), CDC15-as1 (L99G) mat a
JLP07		Shokat	SLF250 bkgd (cdc14-1), CDC15-as1 (L99G) mat a
JLP08		Shokat	SLF250 bkgd (cdc14-1), CDC15-as1 (L99G) mat a
JLP09		Shokat	SLF250 bkgd (cdc14-1), CDC15-as1 (L99G) mat a
JLP10		Shokat	SLF250 bkgd (cdc14-1), CDC15-as1 (L99G) mat a
JLP11		Shokat	SLF250 bkgd (cdc14-1), CDC15-as1 (L99G) mat a
JLP12		Shokat	SLF250 bkgd (cdc14-1), CDC15-as1 (L99G) mat a
JLP13		Shokat	SLF250 bkgd (cdc14-1), CDC15-as1 (L99G) mat a
JLP14		Shokat	SLF250 bkgd (cdc14-1), CDC15-as1 (L99G) mat a
JLP15		Shokat	AFS92 bkgd, CDC15-as2 (L99A) mat a

JLP16		Shokat	AFS92 bkgd, CDC15-as2 (L99A) mat a
JLP17		Shokat	AFS92 bkgd, CDC15-as2 (L99A) mat a
JLP18		Shokat	AFS92 bkgd, CDC15-as2 (L99A) mat a
JLP19		Shokat	AFS92 bkgd, CDC15-as2 (L99A) mat a
JLP20		Shokat	AFS92 bkgd, CDC15-as2 (L99A) mat a
JLP21		Shokat	AFS92 bkgd, CDC15-as2 (L99A) mat a
JLP22		Shokat	AFS92 bkgd, CDC15-as2 (L99A) mat a
JLP23		Shokat	MOB1-TAP::HIS, CDC15-as1 (gly) from popin #3
JLP24		Shokat	MOB1-TAP::HIS, CDC15-as1 (gly) from popin #3
JLP25		Shokat	MOB1-TAP::HIS, CDC15-as1 (gly) from popin #3
JLP26		Shokat	MOB1-TAP::HIS, CDC15-as1 (gly) from popin #6
JLP27		Shokat	MOB1-TAP::HIS, CDC15-as1 (gly) from popin #6
JLP28		Shokat	MOB1-TAP::HIS, CDC15-as1 (gly) from popin #6
JLP29		Shokat	MOB1-TAP::HIS, CDC15-as1 (gly) from popin #6
JLP30		Shokat	MOB1-TAP::HIS, CDC15-as1 (gly) from popin #6
JLP31		Shokat	(from JLP01) AFS92 bkgd, CDC15-as1 (L99G) mat alpha
JLP32		Shokat	AFS92 background, CDC5-as1 (L158G) mat a
			note: petite
JLP33		Shokat	AFS92 background, CDC5-as1 (L158G) mat a
JLP34		Shokat	AFS92 background, CDC5-as1 (L158G) mat a
JLP35		Shokat	AFS92 background, CDC5-as1 (L158G) mat a
JLP36		Shokat	AFS92 background, CDC5-as1 (L158G) mat a
JLP37		Shokat	AFS92 background, CDC5-as1 (L158G) mat a
JLP38		Shokat	AFS92 background, CDC5-as2 (L158A) mat a
JLP39		Shokat	mat alpha, can1Δ::MFA1pr-LEU2, CDC5-as1::k.lactis URA3
			note: Made by marker fusion PCR and recombination, CDC5 coding region fully sequenced in strain
JLP40		Shokat	Bfa1TAP background, CDC5-as1 mat a (pKL121 popinpopout) (Bfa1-121-B)
JLP41		Shokat	Bfa1TAP background, CDC5-as1 mat a (pKL121 popinpopout) (Bfa1-121-C)
JLP42		Shokat	Bfa1TAP background, CDC5-as1 mat a (pKL121 popinpopout) (Bfa1-121-D)
JLP43		Shokat	Scc1TAP background, CDC5-as1 mat a (pKL121 popinpopout) (Scc1-121-A)
JLP44		Shokat	Scc1TAP background, CDC5-as1 mat a (pKL121 popinpopout) (Scc1-121-B)
JLP45		Shokat	Scc1TAP background, CDC5-as1 mat a (pKL121 popinpopout) (Scc1-121-C)
JLP46		Shokat	Net1TAP background, CDC5-as1 mat a (pKL121 popinpopout) (Net1-121-A)
JLP47		Shokat	Net1TAP background, CDC5-as1 mat a (pKL121 popinpopout) (Net1-121-B)
JLP48		Shokat	Net1TAP background, CDC5-as1 mat a (pKL121 popinpopout) (Net1-121-C)
JLP49		Shokat	Cdc5TAP background, CDC5-as1 mat a (pKL121 popinpopout) (Cdc5-121-1)
JLP50		Shokat	Cdc5TAP background, CDC5-as1 mat a (pKL121 popinpopout) (Cdc5-121-1)
JLP51		Shokat	DOM274 background, CDC5-as1(L158G) mat a (pKL121 popinpopout)
JLP52		Shokat	DOM274 background, CDC5-as1(L158G) mat a (pKL121 popinpopout)
JLP53		Shokat	DOM274 background, CDC5-as1(L158G) mat a (pKL121 popinpopout)
JLP54-XXX		O'shea and Weissman Ghaemmaghami Nature 2003 425:737	TAP:::HIS3MX library strains arrayed in 96 well plates as identified in "TAP strains location number".
JLP55-XXX		Shokat	TAP:::HIS3MX, can1D::MFA1pr-LEU2, CDC5-as1::k.lactis URA3, MATa (JLP54xJLP39) (see "TAP strains location number")
JLP56		BY4741 - Brachmann	s288c background, MATa, designer deletions his3D1, leu2D0, met15D0, ura3D0 (TRP+) The library background strain!!

		Yeast 1998 14:115	
JLP57		26867 - Pan Molec Cell 2004 16:487	MATa/alpha, SPC72/spc72D::kanMX, CAN1/can1D::LEU2-MFA1pr-HIS3 magic marker strain, library background
JLP58		5556 - Winzeler Science 1999 285:901	MATa, kar3::kanMX, library background
JLP59		1023 - Winzeler Science 1999 285:901	MATa, kar9::kanMX, library background
JLP60		5125 - Winzeler Science 1999 285:901	MATa, dyn1::kanMX, library background
JLP61		10415 - Winzeler Science 1999 285:901	MATalpha, kin3::kanMX, library background
JLP62		11987 - Winzeler Science 1999 285:901	MATalpha, cnm67::kanMX, library background
JLP63		OShea/Weissman Huh Nature 2003 425:686	Mata, CDC5-GFP::HIS3MX
JLP64		OShea/Weissman Huh Nature 2003 425:687	Mata, SPC72-GFP::HIS3MX
JLP65		OShea/Weissman Ghaemmaghami Nature 2003 425:737	SAC7TAP:::HIS3MX library strain (YDR389W 3GS3/E1)
JLP66		OShea/Weissman Ghaemmaghami Nature 2003 425:737	CYK3TAP:::HIS3MX library strain (YDL117W 3GS4/B3)
JLP67		OShea/Weissman Ghaemmaghami Nature 2003 425:737	MCM2TAP:::HIS3MX library strain (YBC023C 2GS3/B7)
JLP68		Shokat	SAC7TAP:::HIS3MX, can1D::MFA1pr-LEU2, CDC5-as1::k.lactis URA3, MATa (libraryxJLP39)
JLP69		Shokat	CYK3TAP:::HIS3MX, can1D::MFA1pr-LEU2, CDC5-as1::k.lactis URA3, MATa (libraryxJLP39)
JLP70		Shokat	MCM2TAP:::HIS3MX, can1D::MFA1pr-LEU2, CDC5-as1::k.lactis URA3, MATa (libraryxJLP39)
JLP71		Shokat	MATa, CDC5-as1 by popin popout in JLP56
JLP72		Shokat	MATa, CDC5-as1 by popin popout in JLP56
JLP73		Shokat	Mata, CDC5-as1 CDC5-GFP::HIS3MX (popin popout in JLP63)
JLP74		Shokat	Mata, CDC5-as1 CDC5-GFP::HIS3MX (popin popout in JLP63)
JLP75		Shokat	Mata, CDC5-as1 SPC72-GFP::HIS3MX (popin popout in JLP64)
JLP76		Shokat	Mata, CDC5-as1 SPC72-GFP::HIS3MX (popin popout in JLP64)
JLP77		Shokat	Mata, CDC5-as1 SPC72-TAP::HIS3MX (popin popout in JLP54-2B10)
JLP78		Shokat	Mata, CDC5-as1 SPC72-TAP::HIS3MX (popin popout in JLP54-2B10)
JLP79	2B10/4C	Shokat	Mata, CDC5HA3::k.l.URA3, SPC72-TAP::HIS3MX (tagged in JLP54-2B10)

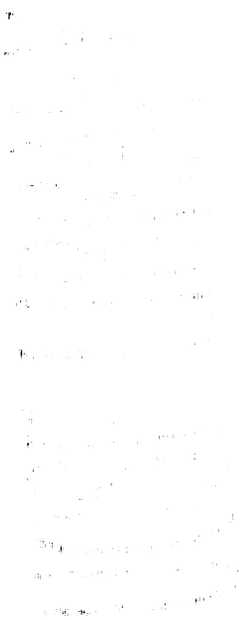

JLP80	77/4D	Shokat	Mata, CDC5-as1HA3::k.l.URA3, SPC72-TAP::HIS3MX (tagged in JLP77)
JLP81	2B10/1D	Shokat	Mata, NUD1HA3::k.l.URA3, SPC72-TAP::HIS3MX (tagged in JLP54-2B10)
JLP82	77/1-3A	Shokat	Mata, cdc5-as1 NUD1HA3::k.l.URA3, SPC72-TAP::HIS3MX (tagged in JLP77)
JLP83	2B10/2A	Shokat	Mata, KAR1HA3::k.l.URA3, SPC72-TAP::HIS3MX (tagged in JLP54-2B10)
JLP84	77/2B	Shokat	Mata, cdc5-as1 KAR1HA3::k.l.URA3, SPC72-TAP::HIS3MX (tagged in JLP77)
JLP85	2B10/6A	Shokat	Mata, CDC28HA3::k.l.URA3, SPC72-TAP::HIS3MX (tagged in JLP54-2B10)
JLP86	77/6A	Shokat	Mata, cdc5-as1 CDC28HA3::k.l.URA3, SPC72-TAP::HIS3MX (tagged in JLP77)
JLP87	2B10/5B	Shokat	Mata, KIN3HA3::k.l.URA3, SPC72-TAP::HIS3MX (tagged in JLP54-2B10)
JLP88	77/5B	Shokat	Mata, cdc5-as1 KIN3HA3::k.l.URA3, SPC72-TAP::HIS3MX (tagged in JLP77)

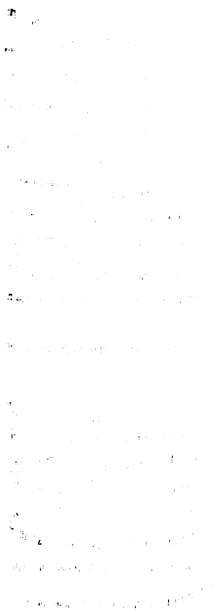

Appendix 3: Plate location of *cdc5-as1* TAP strain collection

location	ORF	gene name
1A01	YER165W	PAB1
1A02	YLR175W	CBF5
1A03	YPR024W	YME1
1A04	YGL137W	SEC27
1A05	YDR127W	ARO1
1A06	YGR218W	CRM1
1A07	YMR261C	TPS3
1A08	YGL201C	MCM6
1A09	YHL029C	
1A10	YNL197C	WHI3
1A11	YLR120C	YPS1
1A12	YBR200W	BEM1
1B01	YGL190C	CDC55
1B02	YDL178W	DLD2
1B03	YNL138W	SRV2
1B04	YKL195W	
1B05	YAL012W	CYS3
1B06	YER095W	RAD51
1B07	YNL007C	SIS1
1B08	YJR060W	CBF1
1B09	YHR098C	SFB3
1B10	YPR159W	KRE6
1B11	YNL154C	YCK2
1B12	YEL042W	GDA1
1C01	YDR498C	SEC20
1C02	YOL004W	SIN3
1C03	YHL030W	ECM29
1C04	YNL297C	MON2
1C05	YDR180W	SCC2
1C06	YJR092W	BUD4
1C07	YJL076W	NET1
1C08	YGL094C	PAN2
1C09	YBR059C	AKL1
1C10**	YHR154W	RTT107
1C11	YNL267W	PIK1
1C12	YML010W	SPT5
1D01	YNL236W	SIN4
1D02	YDR028C	REG1
1D03	YIL125W	KGD1
1D04	YPR019W	CDC54
1D05	YLR357W	RSC2
1D06	YLR045C	STU2
1D07	YIL038C	NOT3
1D08	YIL143C	SSL2

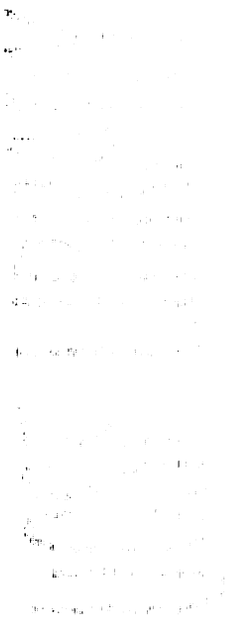

1D09	YPL153C	RAD53
1D10	YLR319C	BUD6
1D11	YMR277W	FCP1
1D12	YPR141C	KAR3
1E01	YBR212W	NGR1
1E02	YKL079W	SMY1
1E03	YEL007W	
1E04	YMR168C	CEP3
1E05	YOL148C	SPT20
1E06	YKL185W	ASH1
1E07	YJR053W	BFA1
1E08	YPR111W	DBF20
1E09	YBR274W	CHK1
1E10	YJL013C	MAD3
1E11	YDL101C	DUN1
1E12	YDL017W	CDC7
1F01	YIL123W	SIM1
1F02	YBL055C	
1F03	YKR092C	SRP40
1F04	YIL153W	RRD1
1F05	YJR043C	POL32
1F06	YOR026W	BUD3
1F07	YKL052C	ASK1
1F08	YDR170C	SEC7
1F09	YGL092W	NUP145
1F10	YER105C	NUP157
1F11	YMR301C	ATM1
1F12	YNL048W	ALG11
1G01	YNL180C	RHO5
1G02	YER155C	BEM2
1G03	YKR054C	DYN1
1G04	YER132C	PMD1
1G05	YNL172W	APC1
1G06	YBL034C	STU1
1G07	YNR031C	SSK2
1G08	YJL095W	BCK1
1G09	YAL024C	LTE1
1G10	YDR217C	RAD9
1G11	YBL007C	SLA1
1G12	YHR158C	KEL1
1H01**	YPL115C	BEM3
1H02	YLR383W	RHC18
1H03	YOL051W	GAL11
1H04	YHR102W	KIC1
1H05	YHR119W	SET1
1H06	YEL061C	CIN8
1H07	YJL084C	

1H08	YIL031W	ULP2
1H09**	YGR188C	BUB1
1H10	YAR019C	CDC15
1H11	YGR056W	RSC1
1H12	YHL007C	STE20
2A01	YDL220C	CDC13
2A02	YNL164C	IBD2
2A03	YGL180W	APG1
2A04	YOR058C	ASE1
2A05	YIL066C	RNR3
2A06	YDR369C	XRS2
2A07	YFL024C	EPL1
2A08**	YNL126W	SPC98
2A09	YGL216W	KIP3
2A10	YAL031C	FUN21
2A11	YOR014W	RTS1
2A12	YGL086W	MAD1
2B01	YCL039W	GID7
2B02	YMR001C	CDC5
2B03	YDR146C	SWI5
2B04	YPL155C	KIP2
2B05	YBR156C	SLI15
2B06	YMR032W	HOF1
2B07	YDR118W	APC4
2B08	YER173W	RAD24
2B09	YOL113W	SKM1
2B10	YAL047C	SPC72
2B11	YMR198W	CIK1
2B12	YDR144C	MKC7
2C01	YDL003W	MCD1
2C02	YPL179W	PPQ1
2C03	YDR004W	RAD57
2C04	YDR254W	CHL4
2C05	YPR065W	ROX1
2C06	YLR079W	SIC1
2C07	YBR107C	IML3
2C08	YDR424C	DYN2
2C09	YJR066W	TOR1
2C10	YLR310C	CDC25
2C11	YJR033C	RAV1
2C12	YGR014W	MSB2
2D01	YFR030W	MET10
2D02	YKL068W	NUP100
2D03	YMR273C	ZDS1
2D04	YGR143W	SKN1
2D05	YOR329C	SCD5
2D06	YIL140W	AXL2

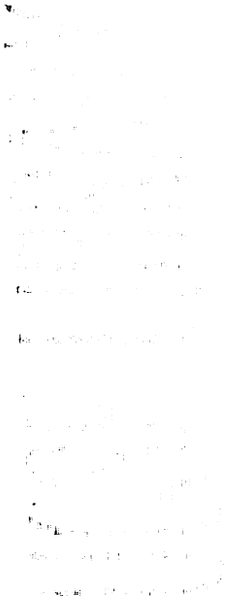

2D07	YOR008C	SLG1
2D08	YDR150W	NUM1
2D09	YFL033C	RIM15
2D10**	YGR098C	ESP1
2D11	YGR097W	ASK10
2D12	YJR035W	RAD26
2E01	YER032W	FIR1
2E02	YMR036C	MIH1
2E03	YDR277C	MTH1
2E04	YNL152W	
2E05	YNL058C	
2E06	YOL081W	IRA2
2E07	YIL030C	SSM4
2E08	YNL101W	AVT4
2E09	YCR069W	CPR4
2E10	YLR256W	HAP1
2E11	YMR190C	SGS1
2E12	YJR151C	DAN4
2F01	YGR070W	ROM1
2F02	YBL066C	SEF1
2F03	YBR108W	
2F04	YJL187C	SWE1
2F05*	YER125W	RSP5
2F06	YOR178C	GAC1
2F07	YFR022W	
2F08	YJL132W	
2F09	YNL012W	SPO1
2F10**	YLR273C	PIG1
2F11	YHR124W	NDT80
2F12*	YJL019W	MPS3
2G01	YGL116W	CDC20
2G02	YOR204W	DED1
2G03	YLR353W	BUD8
2G04	YBR045C	GIP1
2G05	YGL003C	CDH1
2G06	YNL166C	BNI5
2G07*	YLR303W	MET17
2G08	YER130C	
2G09	YNL188W	KAR1
2G10*	YJR125C	ENT3
2G11	YKL198C	PTK1
2G12	YHL022C	SPO11
2H01	YPR054W	SMK1
2H02	YOR113W	AZF1
2H03	YJR021C	REC107
2H04	YBR228W	SLX1
2H05	YER106W	MAM1

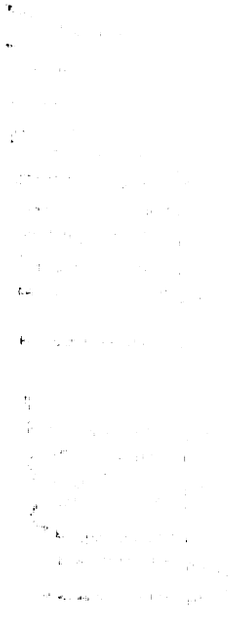

2H06	YHR014W	SPO13
2H07	YBR140C	IRA1
2H08	YDL194W	SNF3
2H09	YGL114W	
2H10	YOR348C	PUT4
2H11	YBR132C	AGP2
2H12	YDR192C	NUP42
3A01	YGR140W	CBF2
3A02	YNL172W	APC1
3A03	YBL034C	STU1
3A04	YLL003W	SFI1
3A05	YDL028C	MPS1
3A06	YOR073W	SGO1
3A07	YNL225C	CNM67
3A08	YOR177C	MPC54
3A09	YJR089W	BIR1
3A10	YGL093W	SPC105
3A11	YAL016W	TPD3
3A12	YLR045C	STU2
3B01	YHR172W	SPC97
3B02	YPR141C	KAR3
3B03	YBL063W	KIP1
3B04	YEL061C	CIN8
3B05	YGR188C	BUB1
3B06	YAR019C	CDC15
3B07	YDR356W	SPC110
3B08	YKR037C	SPC34
3B10	YJL019W	MPS3
3B11	YFR028C	CDC14
3B12	YML124C	TUB3
3C01	YML085C	TUB1
3C02	YOR129C	
3C03	YPL174C	NIP100
3C05	YNL126W	SPC98
3C06	YOR195W	SLK19
3C07	YOL091W	SPO21
3C08	YJR053W	BFA1
3C09	YGR092W	DBF2
3C10	YOR014W	RTS1
3C11	YLR381W	CTF3
3C12	YPL155C	KIP2
3D01	YIL144W	TID3
3D02	YFL037W	TUB2
3D03	YLR227C	ADY4
3D04	YIL106W	MOB1
3D06	YPL269W	KAR9
3D08	YMR198W	CIK1

3D09	YNL188W	KAR1
3D10	YGL170C	SPO74
3D11	YOL069W	NUF2
3D12	YGR179C	OKP1
3E01	YIR010W	DSN1
3E02	YKL089W	MIF2
3E03	YPR119W	CLB2
3E04	YKL042W	SPC42
3E05	YER016W	BIM1
3E06	YLR210W	CLB4
3E07	YMR055C	BUB2
3E08	YDR130C	FIN1
3E09	YBR211C	AME1
3E10	YCL029C	BIK1
3E11	YDR532C	
3E12	YPL124W	SPC29
3F01	YKL052C	ASK1
3F02	YAL034W-A	MTW1
3F03	YOR060C	
3F04	YPL018W	CTF19
3F05	YLR457C	NBP1
3F06	YER018C	SPC25
3F07	YPR174C	
3F08	YPL233W	NSL1
3F09	YMR117C	SPC24
3F10	YDR318W	MCM21
3F11	YGL061C	DUO1
3F12	YBR107C	IML3
3G01	YJR135C	MCM22
3G02	YJR112W	NNF1
3G03	YBR109C	CMD1
3G04	YLR315W	NKP2
3G05	YJL018W	
3G06	YDR201W	SPC19
3G07	YKR083C	DAD2
3G08	YKL049C	CSE4
3G09	YML031W	NDC1
3G10	YBR233W-A	DAD3
3G11	YDR016C	DAD1
3G12	YDR320C-A	DAD4
3H01	YHR195W	NVJ1
3H02	YPL255W	BBP1
3H03	YML064C	TEM1
3H04	YGL075C	MPS2
3H05	YOR257W	CDC31
3H06	YOR373W	NUD1
3H07	YPL253C	VIK1

3H08	YLR212C	TUB4
3H09	YNL272C	SEC2
*, ** - Strain not present		

Bibliography

Adames, N. R., Oberle, J. R., and Cooper, J. A. (2001). The surveillance mechanism of the spindle position checkpoint in yeast. J Cell Biol *153*, 159-168.

Adams, J. A. (2001). Kinetic and catalytic mechanisms of protein kinases. Chem Rev *101*, 2271-2290.

Alexandru, G., Uhlmann, F., Mechtler, K., Poupart, M. A., and Nasmyth, K. (2001). Phosphorylation of the cohesin subunit Scc1 by Polo/Cdc5 kinase regulates sister chromatid separation in yeast. Cell *105*, 459-472.

Alexandru, G., Zachariae, W., Schleiffer, A., and Nasmyth, K. (1999). Sister chromatid separation and chromosome re-duplication are regulated by different mechanisms in response to spindle damage. Embo Journal *18*, 2707-2721.

Andrews, P. D. (2005). Aurora kinases: shining lights on the therapeutic horizon? Oncogene *24*, 5005-5015.

Arnaud, L., Pines, J., and Nigg, E. A. (1998). GFP tagging reveals human Polo-like kinase 1 at the kinetochore/centromere region of mitotic chromosomes. Chromosoma *107*, 424-429.

Asakawa, K., Yoshida, S., Otake, F., and Toh-e, A. (2001). A novel functional domain of Cdc15 kinase is required for its interaction with Tem1 GTPase in Saccharomyces cerevisiae. Genetics *157*, 1437-1450.

Asano, S., Park, J. E., Sakchaisri, K., Yu, L. R., Song, S., Supavilai, P., Veenstra, T. D., and Lee, K. S. (2005). Concerted mechanism of Swe1/Wee1 regulation by multiple kinases in budding yeast. Embo J *24*, 2194-2204.

Azzam, R., Chen, S. L., Shou, W., Mah, A. S., Alexandru, G., Nasmyth, K., Annan, R. S., Carr, S. A., and Deshaies, R. J. (2004). Phosphorylation by cyclin B-Cdk underlies release of mitotic exit activator Cdc14 from the nucleolus. Science *305*, 516-519.

Bachant, J., Alcasabas, A., Blat, Y., Kleckner, N., and Elledge, S. J. (2002). The SUMO-1 isopeptidase Smt4 is linked to centromeric cohesion through SUMO-1 modification of DNA topoisomerase II. Mol Cell *9*, 1169-1182.

Balasubramanian, M. K., Bi, E., and Glotzer, M. (2004). Comparative analysis of cytokinesis in budding yeast, fission yeast and animal cells. Curr Biol *14*, R806-818.

Bardin, A. J., and Amon, A. (2001). Men and sin: what's the difference? Nat Rev Mol Cell Biol *2*, 815-826.

Bardin, A. J., Boselli, M. G., and Amon, A. (2003). Mitotic exit regulation through distinct domains within the protein kinase Cdc15. Mol Cell Biol *23*, 5018-5030.

Bardin, A. J., Visintin, R., and Amon, A. (2000). A mechanism for coupling exit from mitosis to partitioning of the nucleus. Cell *102*, 21-31.

Barr, F. A., Sillje, H. H., and Nigg, E. A. (2004). Polo-like kinases and the orchestration of cell division. Nat Rev Mol Cell Biol *5*, 429-440.

Bartholomew, C. R., Woo, S. H., Chung, Y. S., Jones, C., and Hardy, C. F. (2001). Cdc5 interacts with the Wee1 kinase in budding yeast. Mol Cell Biol *21*, 4949-4959.

Bishop, A. C., Buzko, O., and Shokat, K. M. (2001). Magic bullets for protein kinases. Trends Cell Biol *11*, 167-172.

Bishop, A. C., Kung, C. Y., Shah, K., Witucki, L., Shokat, K. M., and Liu, Y. (1999). Generation of monospecific nanomolar tyrosine kinase inhibitors via a chemical genetic approach. Journal of the American Chemical Society *121*, 627-631.

Bishop, A. C., Shah, K., Liu, Y., Witucki, L., Kung, C. Y., and Shokat, K. M. (1998). Design of allele-specific inhibitors to probe protein kinase signaling. Current Biology *8*, 257-266.

Bishop, A. C., Ubersax, J. A., Petsch, D. T., Matheos, D. P., Gray, N. S., Blethrow, J., Shimizu, E., Tsien, J. Z., Schultz, P. G., Rose, M. D., *et al.* (2000). A chemical switch for inhibitor-sensitive alleles of any protein kinase. Nature *407*, 395-401.

Bloecher, A., Venturi, G. M., and Tatchell, K. (2000). Anaphase spindle position is monitored by the BUB2 checkpoint. Nat Cell Biol *2*, 556-558.

Booher, R. N., Deshaies, R. J., and Kirschner, M. W. (1993). Properties of Saccharomyces cerevisiae wee1 and its differential regulation of p34CDC28 in response to G1 and G2 cyclins. Embo J *12*, 3417-3426.

Bothos, J., Tuttle, R. L., Ottey, M., Luca, F. C., and Halazonetis, T. D. (2005). Human LATS1 is a mitotic exit network kinase. Cancer Res *65*, 6568-6575.

Brar, G. A., Kiburz, B. M., Zhang, Y., Kim, J. E., White, F., and Amon, A. (2006). Rec8 phosphorylation and recombination promote the step-wise loss of cohesins in meiosis. Nature *441*, 532-536.

Byers, B., and Goetsch, L. (1974). Duplication of spindle plaques and integration of the yeast cell cycle. Cold Spring Harb Symp Quant Biol *38*, 123-131.

Byers, B., and Goetsch, L. (1975). Behavior of spindles and spindle plaques in the cell cycle and conjugation of Saccharomyces cerevisiae. J Bacteriol *124*, 511-523.

Chan, E. H., Nousiainen, M., Chalamalasetty, R. B., Schafer, A., Nigg, E. A., and Sillje, H. H. (2005). The Ste20-like kinase Mst2 activates the human large tumor suppressor kinase Lats1. Oncogene *24*, 2076-2086.

Charles, J. F., Jaspersen, S. L., Tinker-Kulberg, R. L., Hwang, L., Szidon, A., and Morgan, D. O. (1998). The Polo-related kinase Cdc5 activates and is destroyed by the mitotic cyclin destruction machinery in S. cerevisiae. Curr Biol *8*, 497-507.

Chen, X. P., Yin, H., and Huffaker, T. C. (1998). The yeast spindle pole body component Spc72p interacts with Stu2p and is required for proper microtubule assembly. J Cell Biol *141*, 1169-1179.

Cheng, K. Y., Lowe, E. D., Sinclair, J., Nigg, E. A., and Johnson, L. N. (2003). The crystal structure of the human polo-like kinase-1 polo box domain and its phospho-peptide complex. Embo J *22*, 5757-5768.

Cheng, L., Hunke, L., and Hardy, C. F. J. (1998). Cell cycle regulation of the Saccharomyces cerevisiae polo-like kinase cdc5p. Molecular and Cellular Biology *18*, 7360-7370.

Cogswell, J. P., Brown, C. E., Bisi, J. E., and Neill, S. D. (2000). Dominant-negative polo-like kinase 1 induces mitotic catastrophe independent of cdc25C function. Cell Growth Differ *11*, 615-623.

Cohen-Fix, O., Peters, J. M., Kirschner, M. W., and Koshland, D. (1996). Anaphase initiation in Saccharomyces cerevisiae is controlled by the APC-dependent degradation of the anaphase inhibitor Pds1p. Genes Dev *10*, 3081-3093.

Cohen, M. S., Zhang, C., Shokat, K. M., and Taunton, J. (2005). Structural bioinformatics-based design of selective, irreversible kinase inhibitors. Science *308*, 1318-1321.

Corbett, M., Xiong, Y., Boyne, J. R., Wright, D. J., Munro, E., and Price, C. (2006). IQGAP and mitotic exit network (MEN) proteins are required for cytokinesis and re-

polarization of the actin cytoskeleton in the budding yeast, Saccharomyces cerevisiae. Eur J Cell Biol *85*, 1201-1215.

D'Amours, D., and Amon, A. (2004). At the interface between signaling and executing anaphase--Cdc14 and the FEAR network. Genes Dev *18*, 2581-2595.

D'Aquino, K. E., Monje-Casas, F., Paulson, J., Reiser, V., Charles, G. M., Lai, L., Shokat, K. M., and Amon, A. (2005). The protein kinase Kin4 inhibits exit from mitosis in response to spindle position defects. Mol Cell *19*, 223-234.

Dephoure, N., Howson, R. W., Blethrow, J. D., Shokat, K. M., and O'Shea, E. K. (2005). Combining chemical genetics and proteomics to identify protein kinase substrates. Proc Natl Acad Sci U S A *102*, 17940-17945.

Eckerdt, F., Yuan, J., and Strebhardt, K. (2005). Polo-like kinases and oncogenesis. Oncogene *24*, 267-276.

Elez, R., Piiper, A., Giannini, C. D., Brendel, M., and Zeuzem, S. (2000). Polo-like kinase1, a new target for antisense tumor therapy. Biochem Biophys Res Commun *269*, 352-356.

Elia, A. E., Cantley, L. C., and Yaffe, M. B. (2003). Proteomic screen finds pSer/pThr-binding domain localizing Plk1 to mitotic substrates. Science *299*, 1228-1231.

Elia, A. E., Rellos, P., Haire, L. F., Chao, J. W., Ivins, F. J., Hoepker, K., Mohammad, D., Cantley, L. C., Smerdon, S. J., and Yaffe, M. B. (2003). The molecular basis for phosphodependent substrate targeting and regulation of Plks by the Polo-box domain. Cell *115*, 83-95.

Frenz, L. M., Lee, S. E., Fesquet, D., and Johnston, L. H. (2000). The budding yeast Dbf2 protein kinase localises to the centrosome and moves to the bud neck in late mitosis. Journal of Cell Science *113 Pt 19*, 3399-3408.

Geymonat, M., Spanos, A., Walker, P. A., Johnston, L. H., and Sedgwick, S. G. (2003). In vitro regulation of budding yeast Bfa1/Bub2 GAP activity by Cdc5. J Biol Chem *278*, 14591-14594.

Ghaemmaghami, S., Huh, W. K., Bower, K., Howson, R. W., Belle, A., Dephoure, N., O'Shea, E. K., and Weissman, J. S. (2003). Global analysis of protein expression in yeast. Nature *425*, 737-741.

Golsteyn, R. M., Mundt, K. E., Fry, A. M., and Nigg, E. A. (1995). Cell cycle regulation of the activity and subcellular localization of Plk1, a human protein kinase implicated in mitotic spindle function. J Cell Biol *129*, 1617-1628.

Gruneberg, U., Campbell, K., Simpson, C., Grindlay, J., and Schiebel, E. (2000). Nud1p links astral microtubule organization and the control of exit from mitosis. Embo J *19*, 6475-6488.

Guthrie, C., and Fink, G. R. (2002). Guide to yeast genetics and molecular and cell biology (San Diego, Calif.: Academic Press).

Hanke, J. H., Gardner, J. P., Dow, R. L., Changelian, P. S., Brissette, W. H., Weringer, E. J., Pollok, B. A., and Connelly, P. A. (1996). Discovery of a novel, potent, and Src family-selective tyrosine kinase inhibitor. Study of Lck- and FynT-dependent T cell activation. J Biol Chem *271*, 695-701.

Hergovich, A., Stegert, M. R., Schmitz, D., and Hemmings, B. A. (2006). NDR kinases regulate essential cell processes from yeast to humans. Nat Rev Mol Cell Biol *7*, 253-264.

Hirota, T., Morisaki, T., Nishiyama, Y., Marumoto, T., Tada, K., Hara, T., Masuko, N., Inagaki, M., Hatakeyama, K., and Saya, H. (2000). Zyxin, a regulator of actin filament assembly, targets the mitotic apparatus by interacting with h-warts/LATS1 tumor suppressor. J Cell Biol *149*, 1073-1086.

Ho, Y., Gruhler, A., Heilbut, A., Bader, G. D., Moore, L., Adams, S. L., Millar, A., Taylor, P., Bennett, K., Boutilier, K., *et al.* (2002). Systematic identification of protein complexes in Saccharomyces cerevisiae by mass spectrometry. Nature *415*, 180-183.

Hoepfner, D., Schaerer, F., Brachat, A., Wach, A., and Philippsen, P. (2002). Reorientation of mispositioned spindles in short astral microtubule mutant spc72Delta is dependent on spindle pole body outer plaque and Kar3 motor protein. Mol Biol Cell *13*, 1366-1380.

Hornig, N. C., and Uhlmann, F. (2004). Preferential cleavage of chromatin-bound cohesin after targeted phosphorylation by Polo-like kinase. Embo J *23*, 3144-3153.

Hu, F., Wang, Y., Liu, D., Li, Y., Qin, J., and Elledge, S. J. (2001). Regulation of the Bub2/Bfa1 GAP complex by Cdc5 and cell cycle checkpoints. Cell *107*, 655-665.

Huang, J., Wu, S., Barrera, J., Matthews, K., and Pan, D. (2005). The Hippo signaling pathway coordinately regulates cell proliferation and apoptosis by inactivating Yorkie, the Drosophila Homolog of YAP. Cell *122*, 421-434.

Huh, W. K., Falvo, J. V., Gerke, L. C., Carroll, A. S., Howson, R. W., Weissman, J. S., and O'Shea, E. K. (2003). Global analysis of protein localization in budding yeast. Nature *425*, 686-691.

Hwa Lim, H., Yeong, F. M., and Surana, U. (2003). Inactivation of mitotic kinase triggers translocation of MEN components to mother-daughter neck in yeast. Mol Biol Cell *14*, 4734-4743.

Jaspersen, S. L., Charles, J. F., and Morgan, D. O. (1999). Inhibitory phosphorylation of the APC regulator Hct1 is controlled by the kinase Cdc28 and the phosphatase Cdc14. Current Biology *9*, 227-236.

Jaspersen, S. L., Charles, J. F., Tinker-Kulberg, R. L., and Morgan, D. O. (1998). A late mitotic regulatory network controlling cyclin destruction in Saccharomyces cerevisiae. Molecular Biology of the Cell *9*, 2803-2817.

Jaspersen, S. L., and Morgan, D. O. (2000). Cdc14 activates cdc15 to promote mitotic exit in budding yeast. Current Biology *10*, 615-618.

Jaspersen, S. L., and Winey, M. (2004). The budding yeast spindle pole body: structure, duplication, and function. Annu Rev Cell Dev Biol *20*, 1-28.

Jiménez, J., Cid, V. J., Cenamor, R., Yuste, M., Molero, G., Nombela, C., and Sánchez, M. (1998). Morphogenesis beyond cytokinetic arrest in Saccharomyces cerevisiae. Journal of Cell Biology *143*, 1617-1634.

Kaiser, P., Sia, R. A., Bardes, E. G., Lew, D. J., and Reed, S. I. (1998). Cdc34 and the F-box protein Met30 are required for degradation of the Cdk-inhibitory kinase Swe1. Genes Dev *12*, 2587-2597.

Kitada, K., Johnson, A. L., Johnston, L. H., and Sugino, A. (1993). A Multicopy Suppressor Gene of the Saccharomyces-Cerevisiae G1 Cell Cycle Mutant Gene Dbf4 Encodes a Protein Kinase and Is Identified As Cdc5. Molecular and Cellular Biology *13*, 4445-4457.

Knight, Z. A., and Shokat, K. M. (2005). Features of selective kinase inhibitors. Chem Biol *12*, 621-637.

Knop, M., Pereira, G., Geissler, S., Grein, K., and Schiebel, E. (1997). The spindle pole body component Spc97p interacts with the gamma-tubulin of Saccharomyces cerevisiae and functions in microtubule organization and spindle pole body duplication. Embo J *16*, 1550-1564.

Knop, M., and Schiebel, E. (1997). Spc98p and Spc97p of the yeast gamma-tubulin complex mediate binding to the spindle pole body via their interaction with Spc110p. Embo J *16*, 6985-6995.

Knop, M., and Schiebel, E. (1998). Receptors determine the cellular localization of a gamma-tubulin complex and thereby the site of microtubule formation. Embo J *17*, 3952-3967.

Komarnitsky, S. I., Chiang, Y. C., Luca, F. C., Chen, J., Toyn, J. H., Winey, M., Johnston, L. H., and Denis, C. L. (1998). DBF2 protein kinase binds to and acts through the cell cycle-regulated MOB1 protein. Molecular and Cellular Biology *18*, 2100-2107.

Lane, H. A., and Nigg, E. A. (1996). Antibody microinjection reveals an essential role for human polo-like kinase 1 (Plk1) in the functional maturation of mitotic centrosomes. J Cell Biol *135*, 1701-1713.

Lee, K. S., Park, J. E., Asano, S., and Park, C. J. (2005). Yeast polo-like kinases: functionally conserved multitask mitotic regulators. Oncogene *24*, 217-229.

Lee, K. S., Yuan, Y. L., Kuriyama, R., and Erikson, R. L. (1995). Plk is an M-phase-specific protein kinase and interacts with a kinesin-like protein, CHO1/MKLP-1. Mol Cell Biol *15*, 7143-7151.

Lee, S. E., Frenz, L. M., Wells, N. J., Johnson, A. L., and Johnston, L. H. (2001). Order of function of the budding-yeast mitotic exit-network proteins Tem1, Cdc15, Mob1, Dbf2, and Cdc5. Current Biology *11*, 784-788.

Lee, S. E., Jensen, S., Frenz, L. M., Johnson, A. L., Fesquet, D., and Johnston, L. H. (2001). The Bub2-dependent mitotic pathway in yeast acts every cell cycle and regulates cytokinesis. J Cell Sci *114*, 2345-2354.

Leung, G. C., Hudson, J. W., Kozarova, A., Davidson, A., Dennis, J. W., and Sicheri, F. (2002). The Sak polo-box comprises a structural domain sufficient for mitotic subcellular localization. Nat Struct Biol *9*, 719-724.

Levin, D. E. (2005). Cell wall integrity signaling in Saccharomyces cerevisiae. Microbiol Mol Biol Rev *69*, 262-291.

Li, S. J., and Hochstrasser, M. (2000). The yeast ULP2 (SMT4) gene encodes a novel protease specific for the ubiquitin-like Smt3 protein. Mol Cell Biol *20*, 2367-2377.

Lippincott, J., and Li, R. (1998). Dual function of Cyk2, a cdc15/PSTPIP family protein, in regulating actomyosin ring dynamics and septin distribution. Journal of Cell Biology *143*, 1947-1960.

Lippincott, J., and Li, R. (1998). Sequential assembly of myosin II, an IQGAP-like protein, and filamentous actin to a ring structure involved in budding yeast cytokinesis. Journal of Cell Biology *140*, 355-366.

Lippincott, J., Shannon, K. B., Shou, W. Y., Deshaies, J., and Li, R. (2001). The Tem1 small GTPase controls actomyosin and septin dynamics during cytokinesis. Journal of Cell Science *114*, 1379-1386.

Liu, Y., Bishop, A., Witucki, L., Kraybill, B., Shimizu, E., Tsien, J., Ubersax, J., Blethrow, J., Morgan, D. O., and Shokat, K. M. (1999). Structural basis for selective inhibition of Src family kinases by PP1. Chemistry and Biology *6*, 671-678.

Liu, Y., Shah, K., Yang, F., Witucki, L., and Shokat, K. M. (1998). Engineering Src family protein kinases with unnatural nucleotide specificity. Chemistry & Biology *5*, 91-101.

Liu, Y., Shah, K., Yang, F., Witucki, L., and Shokat, K. M. (1998). A molecular gate which controls unnatural ATP analogue recognition by the tyrosine kinase v-Src. Bioorganic and Medicinal Chemistry *6*, 1219-1226.

Liu, Y., Shreder, K. R., Gai, W., Corral, S., Ferris, D. K., and Rosenblum, J. S. (2005). Wortmannin, a widely used phosphoinositide 3-kinase inhibitor, also potently inhibits mammalian polo-like kinase. Chem Biol *12*, 99-107.

Lowery, D. M., Lim, D., and Yaffe, M. B. (2005). Structure and function of Polo-like kinases. Oncogene *24*, 248-259.

Luca, F. C., Mody, M., Kurischko, C., Roof, D. M., Giddings, T. H., and Winey, M. (2001). Saccharomyces cerevisiae Mob1p is required for cytokinesis and mitotic exit. Mol Cell Biol *21*, 6972-6983.

Lupas, A., Van Dyke, M., and Stock, J. (1991). Predicting coiled coils from protein sequences. Science *252*, 1162-1164.

Mah, A. S., Jang, J., and Deshaies, R. J. (2001). Protein kinase Cdc15 activates the Dbf2-Mob1 kinase complex. Proc Natl Acad Sci U S A *98*, 7325-7330.

McMillan, J. N., Sia, R. A., Bardes, E. S., and Lew, D. J. (1999). Phosphorylation-independent inhibition of Cdc28p by the tyrosine kinase Swe1p in the morphogenesis checkpoint. Mol Cell Biol *19*, 5981-5990.

McMillan, J. N., Theesfeld, C. L., Harrison, J. C., Bardes, E. S., and Lew, D. J. (2002). Determinants of Swe1p degradation in Saccharomyces cerevisiae. Mol Biol Cell *13*, 3560-3575.

Menssen, R., Neutzer, A., and Seufert, W. (2001). Asymmetric spindle pole localization of yeast Cdc15 kinase links mitotic exit and cytokinesis. Current Biology *11*, 345-350.

Morandell, S., Stasyk, T., Grosstessner-Hain, K., Roitinger, E., Mechtler, K., Bonn, G. K., and Huber, L. A. (2006). Phosphoproteomics strategies for the functional analysis of signal transduction. Proteomics *6*, 4047-4056.

Morgan, D. O. (1997). Cyclin-dependent kinases: engines, clocks, and microprocessors. Annu Rev Cell Dev Biol *13*, 261-291.

Morgan, D. O. (1999). Regulation of the APC and the exit from mitosis. Nature Cell Biology *1*, E47-53.

Mortensen, E. M., Haas, W., Gygi, M., Gygi, S. P., and Kellogg, D. R. (2005). Cdc28-dependent regulation of the Cdc5/Polo kinase. Curr Biol *15*, 2033-2037.

Nakajima, H., Toyoshima-Morimoto, F., Taniguchi, E., and Nishida, E. (2003). Identification of a consensus motif for Plk (Polo-like kinase) phosphorylation reveals Myt1 as a Plk1 substrate. J Biol Chem *278*, 25277-25280.

O'Connell, M. J., Krien, M. J., and Hunter, T. (2003). Never say never. The NIMA-related protein kinases in mitotic control. Trends Cell Biol *13*, 221-228.

Obenauer, J. C., Cantley, L. C., and Yaffe, M. B. (2003). Scansite 2.0: Proteome-wide prediction of cell signaling interactions using short sequence motifs. Nucleic Acids Res *31*, 3635-3641.

Park, J. E., Park, C. J., Sakchaisri, K., Karpova, T., Asano, S., McNally, J., Sunwoo, Y., Leem, S. H., and Lee, K. S. (2004). Novel functional dissection of the localization-specific roles of budding yeast polo kinase Cdc5p. Mol Cell Biol *24*, 9873-9886.

Pawson, T. (2004). Specificity in signal transduction: from phosphotyrosine-SH2 domain interactions to complex cellular systems. Cell *116*, 191-203.

Pearson, C. G., and Bloom, K. (2004). Dynamic microtubules lead the way for spindle positioning. Nat Rev Mol Cell Biol *5*, 481-492.

Pereira, G., Grueneberg, U., Knop, M., and Schiebel, E. (1999). Interaction of the yeast gamma-tubulin complex-binding protein Spc72p with Kar1p is essential for microtubule function during karyogamy. Embo J *18*, 4180-4195.

Pereira, G., Höfken, T., Grindlay, J., Manson, C., and Schiebel, E. (2000). The Bub2p spindle checkpoint links nuclear migration with mitotic exit. Molecular Cell *6*, 1-10.

Pereira, G., Manson, C., Grindlay, J., and Schiebel, E. (2002). Regulation of the Bfa1p-Bub2p complex at spindle pole bodies by the cell cycle phosphatase Cdc14p. J Cell Biol *157*, 367-379.

Pereira, G., and Schiebel, E. (2005). Kin4 kinase delays mitotic exit in response to spindle alignment defects. Mol Cell *19*, 209-221.

Pruyne, D., Legesse-Miller, A., Gao, L., Dong, Y., and Bretscher, A. (2004). Mechanisms of polarized growth and organelle segregation in yeast. Annu Rev Cell Dev Biol *20*, 559-591.

Roegiers, F., and Jan, Y. N. (2004). Asymmetric cell division. Curr Opin Cell Biol *16*, 195-205.

Sakchaisri, K., Asano, S., Yu, L. R., Shulewitz, M. J., Park, C. J., Park, J. E., Cho, Y. W., Veenstra, T. D., Thorner, J., and Lee, K. S. (2004). Coupling morphogenesis to mitotic entry. Proc Natl Acad Sci U S A *101*, 4124-4129.

Seong, Y. S., Kamijo, K., Lee, J. S., Fernandez, E., Kuriyama, R., Miki, T., and Lee, K. S. (2002). A spindle checkpoint arrest and a cytokinesis failure by the dominant-negative polo-box domain of Plk1 in U-2 OS cells. J Biol Chem *277*, 32282-32293.

Shah, K., Liu, Y., Deirmengian, C., and Shokat, K. M. (1997). Engineering unnatural nucleotide specificity for Rous sarcoma virus tyrosine kinase to uniquely label its direct substrates. Proceedings of the National Academy of Sciences of the United States of America *94*, 3565-3570.

Shannon, K. B., and Li, R. (1999). The multiple roles of Cyk1p in the assembly and function of the actomyosin ring in budding yeast. Molecular Biology of the Cell *10*, 283-296.

Shirayama, M., Zachariae, W., Ciosk, R., and Nasmyth, K. (1998). The Polo-like kinase Cdc5p and the WD-repeat protein Cdc20p/fizzy are regulators and substrates of the anaphase promoting complex in Saccharomyces cerevisiae. Embo Journal *17*, 1336-1349.

Shou, W., Azzam, R., Chen, S. L., Huddleston, M. J., Baskerville, C., Charbonneau, H., Annan, R. S., Carr, S. A., and Deshaies, R. J. (2002). Cdc5 influences phosphorylation of Net1 and disassembly of the RENT complex. BMC Mol Biol *3*, 3.

Shou, W., Seol, J. H., Shevchenko, A., Baskerville, C., Moazed, D., Chen, Z. W., Jang, J., Charbonneau, H., and Deshaies, R. J. (1999). Exit from mitosis is triggered by Tem1-dependent release of the protein phosphatase Cdc14 from nucleolar RENT complex. Cell *97*, 233-244.

Shulewitz, M. J., Inouye, C. J., and Thorner, J. (1999). Hsl7 localizes to a septin ring and serves as an adapter in a regulatory pathway that relieves tyrosine phosphorylation of Cdc28 protein kinase in Saccharomyces cerevisiae. Mol Cell Biol *19*, 7123-7137.

Sia, R. A., Bardes, E. S., and Lew, D. J. (1998). Control of Swe1p degradation by the morphogenesis checkpoint. Embo J *17*, 6678-6688.

Smith, M. R., Wilson, M. L., Hamanaka, R., Chase, D., Kung, H., Longo, D. L., and Ferris, D. K. (1997). Malignant transformation of mammalian cells initiated by constitutive expression of the polo-like kinase. Biochemical and Biophysical Research Communications *234*, 397-405.

Song, S., Grenfell, T. Z., Garfield, S., Erikson, R. L., and Lee, K. S. (2000). Essential function of the polo box of Cdc5 in subcellular localization and induction of cytokinetic structures. Molecular and Cellular Biology *20*, 286-298.

Song, S. G., and Lee, K. S. (2001). A novel function of Saccharomyces cerevisiae Cdc5 in cytokinesis. Journal of Cell Biology *152*, 451-469.

Soues, S., and Adams, I. R. (1998). SPC72: a spindle pole component required for spindle orientation in the yeast Saccharomyces cerevisiae. J Cell Sci *111 (Pt 18)*, 2809-2818.

Spankuch-Schmitt, B., Bereiter-Hahn, J., Kaufmann, M., and Strebhardt, K. (2002). Effect of RNA silencing of polo-like kinase-1 (PLK1) on apoptosis and spindle formation in human cancer cells. J Natl Cancer Inst *94*, 1863-1877.

Spankuch-Schmitt, B., Wolf, G., Solbach, C., Loibl, S., Knecht, R., Stegmuller, M., von Minckwitz, G., Kaufmann, M., and Strebhardt, K. (2002). Downregulation of human polo-like kinase activity by antisense oligonucleotides induces growth inhibition in cancer cells. Oncogene *21*, 3162-3171.

Spankuch, B., Matthess, Y., Knecht, R., Zimmer, B., Kaufmann, M., and Strebhardt, K. (2004). Cancer inhibition in nude mice after systemic application of U6 promoter-driven short hairpin RNAs against PLK1. J Natl Cancer Inst *96*, 862-872.

St John, M. A., Tao, W., Fei, X., Fukumoto, R., Carcangiu, M. L., Brownstein, D. G., Parlow, A. F., McGrath, J., and Xu, T. (1999). Mice deficient of Lats1 develop soft-tissue sarcomas, ovarian tumours and pituitary dysfunction. Nat Genet *21*, 182-186.

Stegmeier, F., Visintin, R., and Amon, A. (2002). Separase, polo kinase, the kinetochore protein Slk19, and Spo12 function in a network that controls Cdc14 localization during early anaphase. Cell *108*, 207-220.

Sullivan, M., and Uhlmann, F. (2003). A non-proteolytic function of separase links the onset of anaphase to mitotic exit. Nat Cell Biol *5*, 249-254.

Sunkel, C. E., and Glover, D. M. (1988). polo, a mitotic mutant of Drosophila displaying abnormal spindle poles. J Cell Sci *89 (Pt 1)*, 25-38.

Tolliday, N., VerPlank, L., and Li, R. (2002). Rho1 directs formin-mediated actin ring assembly during budding yeast cytokinesis. Curr Biol *12*, 1864-1870.

Toyn, J. H., Araki, H., Sugino, A., and Johnston, L. H. (1991). The cell-cycle-regulated budding yeast gene DBF2, encoding a putative protein kinase, has a homologue that is not under cell-cycle control. Gene *104*, 63-70.

Ubersax, J. A., Woodbury, E. L., Quang, P. N., Paraz, M., Blethrow, J. D., Shah, K., Shokat, K. M., and Morgan, D. O. (2003). Targets of the cyclin-dependent kinase Cdk1. Nature *425*, 859-864.

Uhlmann, F., Wernic, D., Poupart, M. A., Koonin, E. V., and Nasmyth, K. (2000). Cleavage of cohesin by the CD clan protease separin triggers anaphase in yeast. Cell *103*, 375-386.

Vallen, E. A., Caviston, J., and Bi, E. (2000). Roles of Hof1p, Bni1p, Bnr1p, and myo1p in cytokinesis in Saccharomyces cerevisiae. Molecular Biology of the Cell *11*, 593-611.

Visintin, R., and Amon, A. (2001). Regulation of the mitotic exit protein kinases Cdc15 and Dbf2. Mol Biol Cell *12*, 2961-2974.

Visintin, R., Craig, K., Hwang, E. S., Prinz, S., Tyers, M., and Amon, A. (1998). The phosphatase Cdc14 triggers mitotic exit by reversal of Cdk-dependent phosphorylation. Molecular Cell *2*, 709-718.

Visintin, R., Hwang, E. S., and Amon, A. (1999). Cfi1 prevents premature exit from mitosis by anchoring Cdc14 phosphatase in the nucleolus. Nature *398*, 818-823.

Visintin, R., Stegmeier, F., and Amon, A. (2003). The role of the polo kinase Cdc5 in controlling Cdc14 localization. Mol Biol Cell *14*, 4486-4498.

Witucki, L. A., Huang, X., Shah, K., Liu, Y., Kyin, S., Eck, M. J., and Shokat, K. M. (2002). Mutant tyrosine kinases with unnatural nucleotide specificity retain the structure and phospho-acceptor specificity of the wild-type enzyme. Chem Biol *9*, 25-33.

Xu, S., Huang, H. K., Kaiser, P., Latterich, M., and Hunter, T. (2000). Phosphorylation and spindle pole body localization of the Cdc15p mitotic regulatory protein kinase in budding yeast. Current Biology *10*, 329-332.

Yaffe, M. B., Leparc, G. G., Lai, J., Obata, T., Volinia, S., and Cantley, L. C. (2001). A motif-based profile scanning approach for genome-wide prediction of signaling pathways. Nat Biotechnol *19*, 348-353.

Yang, X., Li, D. M., Chen, W., and Xu, T. (2001). Human homologue of Drosophila lats, LATS1, negatively regulate growth by inducing G(2)/M arrest or apoptosis. Oncogene *20*, 6516-6523.

Yoshida, S., Asakawa, K., and Toh-e, A. (2002). Mitotic exit network controls the localization of Cdc14 to the spindle pole body in Saccharomyces cerevisiae. Curr Biol *12*, 944-950.

Yoshida, S., Kono, K., Lowery, D. M., Bartolini, S., Yaffe, M. B., Ohya, Y., and Pellman, D. (2006). Polo-like kinase Cdc5 controls the local activation of Rho1 to promote cytokinesis. Science *313*, 108-111.

Yoshida, S., and Toh-e, A. (2002). Budding yeast Cdc5 phosphorylates Net1 and assists Cdc14 release from the nucleolus. Biochem Biophys Res Commun *294*, 687-691.

Zhang, C., Kenski, D. M., Paulson, J. L., Bonshtien, A., Sessa, G., Cross, J. V., Templeton, D. J., and Shokat, K. M. (2005). A second-site suppressor strategy for chemical genetic analysis of diverse protein kinases. Nat Methods *2*, 435-441.

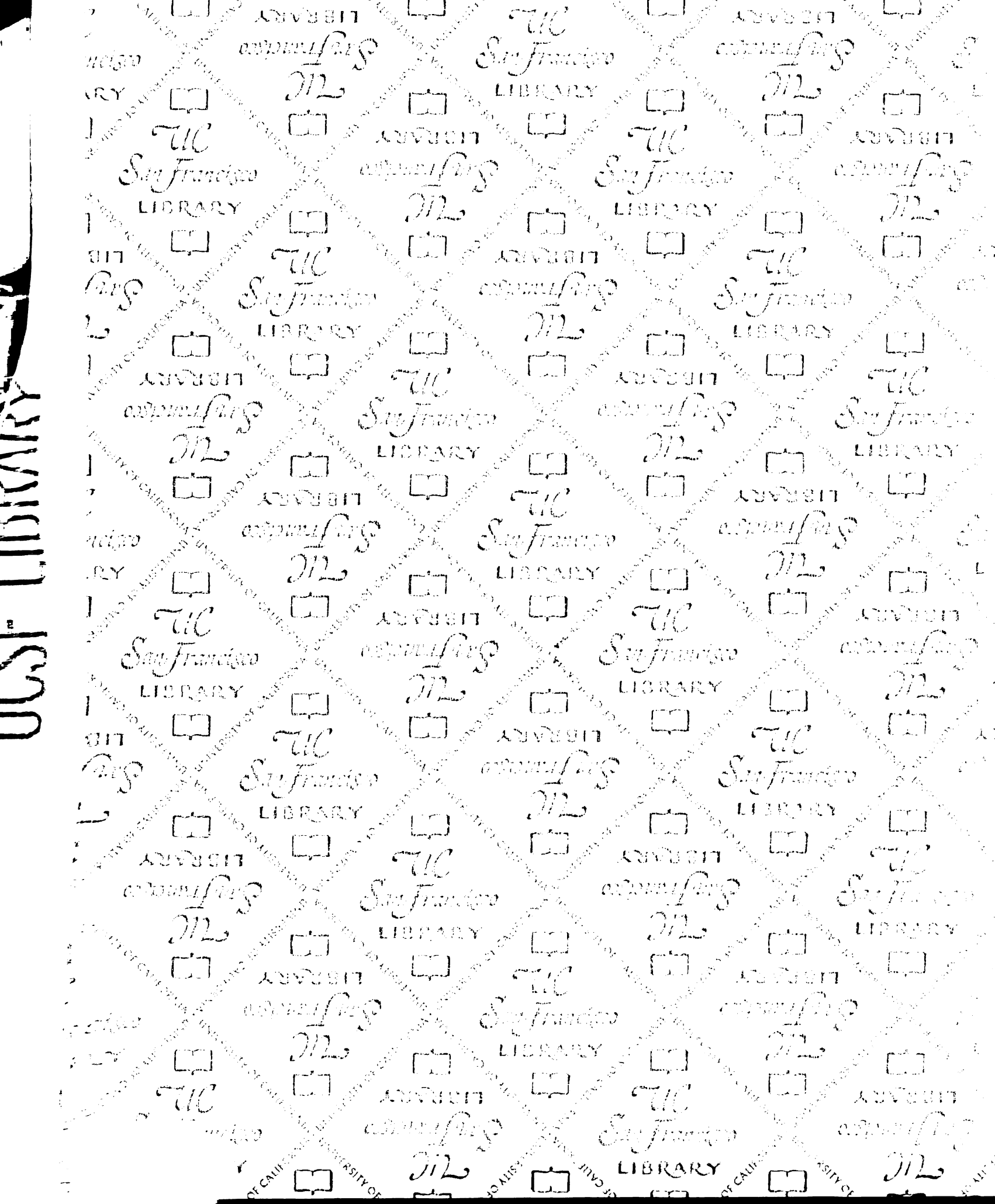
UC San Francisco LIBRARY